Republic of Iraq

Ministry of Higher Education and

Scientific Research

University of Babylon /College of Science

Chemistry Department

Theoretical Study of New Corticosteroids Derivatives Based on Betamethasone Drug

A Thesis

Submitted to the Council of the College of Science at the University of Babylon as Partial Fulfilments of the requirements for the Degree of Master of Science in Chemistry

By

Ferdoss Sami Abdel AL-Ameer AL-Rubiay

B.Sc.1997-1998

Supervised by

Prof. Dr. Abbas Abid Ali Drea

2022 A.D **1443 A.H**

بسم الله الرحمن الرحيم

﴿ رَبِّ أَوْزِعْنِي أَنْ أَشْكُرَ نِعْمَتَكَ الَّتِي أَنْعَمْتَ عَلَيَّ وَعَلَى

وَالِدَيَّ وَأَنْ أَعْمَلَ صَالِحاً تَرْضَاهُ وَأَدْخِلْنِي بِرَحْمَتِكَ فِي عِبَادِكَ

الصَّالِحِينَ ﴾

صدق الله العلي العظيم
سورة النمل
الآية 19

Certification

I certify that this thesis was prepared under my supervision at the Department of Chemistry, College of Science, University of Babylon, as partial fulfilment of requirements for the degree of Master in Science OF Chemistry, and that this work has never been published anywhere.

According I recommend this study for discussion.

Supervisor:

Signature:

Name: Dr. Abbas Abid Ali Drea

Title: Professor

Data:

In the view of the available recommendation , I forward this thesis for debate by the examining committee.

Head of chemistry Department:

Signature:

Name: Dr. Saadun Abdulla Auwda

Title: Professor

Address: Babylon University, College of Science, Chemistry Department

Data:

Declaration

I(Ferdoss Sami Abdel Ameer) Who conducted this study entitled " **Theoretical Study of New Corticosteroids Derivatives Based on Betamethasone Drug"**and submitted it a partial fulfilment of the requirements for Master degree of Chemistry, College of Science, Babylon University. The study was carried out under the supervision of Prof. Dr. Abbas Abed Ali Drea at the Department of Chemistry, College of Science ,Babylon University. I confirm that the work presented in this thesis has not been previously submitted for a thesis, Doctor or Diploma, Master at any higher education institution. Also, I declare that all information in this document has been obtained in accordance with the academic rules and ethical conducts. I also declare that , as required by these rules and conducts. I have fully cited and documented all methods, figures and results that are not original to this work, or any information that is not derived from this work; I confirm that this has been indicated in this thesis

Ferdoss Sami Abdel AL-Ameer

2022

Dedication

To: Great teacher and Leader, Our messenger Mohammed and his Family.

To: The candle that was light to light my way, to the tender heart.

----- **My father**

To: Whom that planted me in life as a seed and watered me from her blood drop by drop. ----- **My mother**

To: My support and my companions, to I see my joy in their eyes.

---- **My brothers and my sisters**

To: The apple of my eyes and the joy of my life.

---------- **My dear daughter**

Acknowledgments

I extend my thanks and gratitude to my respected professor, Dr. Abbas Abed Ali Drea, for his advice and academic guidance throughout the period of this work. I thank God Almighty because I completed the research under his supervision. The builder had a great impact on development my research capabilities through writing research in a precise methodology under his supervision.

I extend my sincere thanks to the University of Babylon ,the College of Science and the Department of Chemistry for granting me this Degree.

I extend my thanks and gratitude to my Family, my brothers, my sisters, my dear daughter, for their support and bear with me the study period over the past two years.

I Would like to express my special thanks and gratitude to my respected professors for their great help me during the research period: Dr. Liqaa Hussain AL-jelawy, Dr. Mohanad Moussa AL-Hachamii, Dr. Mahmoud Hussain Hadwan AL-Kaffaji .

LIST OF CONTENTS

LIST OF FIGURS

LIST OF TABLES

LIST OF SCHEMES

LIST OF ABBRAVATIONS

ADEO	(10S,13S)-10,13-dimethyl-1,6,7,8,10,12,13,14,15,16-decahydro-3H-cyclopenta[a]phenanthrene-3,17(2H)-dione
AMPT	2-oxo-2-((10S,13S)-10,13,16-trimethyl-3-oxo-2,3,6,7,8,10,12,13,14,15-decahydro-1H-cyclopenta[a]phenanthren-17-yl)ethyl acetate
AEMP	2-oxo-2-((6aS,8aS,8bS,9aR)-6a,8a,9a-trimethyl-4-oxo-1,2,4,5,6,6a,8,8a,9a,10,10a,10b-dodecahydro-8bH-naphtho[2',1':4,5]indeno[1,2-b]oxiren-8b-yl)ethyl acetate
AHMP	2-((10S,13S,17R)-17-hydroxy-10,13,16-trimethyl-3-oxo-2,3,6,7,8,10,12,13,14,17-decahydro-1H-cyclopenta[a]phenanthren-17-yl)-2-oxoethyl acetate
AHMD	2-((10S,13S,16S,17R)-17-hydroxy-10,13,16-trimethyl-3-oxo-2,3,6,7,8,10,12,13,14,15,16,17-dodecahydro-1H-cyclopenta[a]phenanthren-17-yl)-2-oxoethyl acetate
AHEM	2-((4aS,4bS,5aS,6aS,7R,8S)-7-hydroxy-4a,6a,8-trimethyl-2-oxo-2,3,4,4a,5a,6,6a,7,8,9,9a,9b,10,11-tetradecahydrocyclopenta[1,2]phenanthro[4,4a-b]oxiren-7-yl)-2-oxoethyl acetate
AFHTDPO (Betamethasone.NH_2)	(13S,16S)-17-amino-9-fluoro-11-hydroxy-17-(2-hydroxyacetyl)-10,13,16-trimethyl-6,7,8,9,10,11,12,13,14,15,16,17-dodecahydro-3H-cyclopenta[a]phenanthren-3-one
Betamethasone molecule	(13S,16S)-9-fluoro-11,17-dihydroxy-17-(2-hydroxyacetyl)-10,13,16-trimethyl-6,7,8,9,10,11,12,13,14,15,16,17-dodecahydro-3H-cyclopenta[a]phenanthren-3-one
CKMP	((10S,16R,Z)-17-(1-chloro-2-oxoethylidene)-10,13-dimethyl-3-oxo-2,3,6,7,8,10,12,13,14,15,16,17-dodecahydro-1H-cyclopenta[a]phenanthren-16-yl)methylium
DHEM	(4aS,4bS,5aS,6aS,7R,8S)-7-hydroxy-7-(2-hydroxyacetyl)-4a,6a,8-trimethyl-5a,6,6a,7,8,9,9a,9b,10,11-decahydrocyclopenta[1,2]phenanthro[4,4a-b]oxiren-2(4aH)-one
ELDO	(10R,13S)-3-ethoxy-10,13-dimethyl-1,2,7,8,9,10,11,12,13,14,15,16-dodecahydro-17H-cyclopenta[a]phenanthren-17-one
EMDO	(10R,13S,16R)-3-ethoxy-10,13,16-trimethyl-1,2,7,8,10,12,13,14,15,16-decahydro-17H-cyclopenta[a]phenanthren-17-one
EFHTDPO(Betamethasone. NH	(13S,16S)-17-(ethylamino)-9-fluoro-11-hydroxy-17-(2-hydroxyacetyl)-10,13,16-trimethyl-

CH_2CH_3)	6,7,8,9,10,11,12,13,14,15,16,17-dodecahydro-3H-cyclopenta[a]phenanthren-3-one
ELISA	enzyme-linked immunosorbent assays
FHCPCC (Betamethasone.COOH)	(13S,16S)-9-fluoro-11-hydroxy-17-(2-hydroxyacetyl)-10,13,16-trimethyl-3-oxo-6,7,8,9,10,11,12,13,14,15,16,17-dodecahydro-3H-cyclopenta[a]phenanthrene-17-carboxylic acid
FHACPC (Betamethasone.CONH2)	(13S,16S)-9-fluoro-11-hydroxy-17-(2-hydroxyacetyl)-10,13,16-trimethyl-3-oxo-6,7,8,9,10,11,12,13,14,15,16,17-dodecahydro-3H-cyclopenta[a]phenanthren-17-yl carbamate
HAEO	9-hydroxy-1,6,7,8,9,10,11,12,13,14,15,16-dodecahydro-3H-cyclopenta[a]phenanthrene-3,17(2H)-dione
HCoV-OC43	human coronavirus-Organ Culture 43
HCoV-229E	human coronaviruses-229E
HCoV-HKU1	human coronaviruses-Hong Kong University 1
HCoV-NL63	human coronaviruses-NetherLand 63
LDA	local density approximation
MERS	Middle East Respiratory Syndrome
SARS	Severe Acute Respiratory Syndrome
WHO	World Health Organization

LIST OF SYMBLS

Symbol	Symbol Explanation
AM1	Austin Model 1
PM3	Parameterization Model, Version 3
PM6	Parameterization Model, Version 6
CNDO	Complete Neglect Differential Overlap
MNDO	Modified Neglect of Diatomic Overlap
INDO	Intermediate Neglect of Differential Overlap
NDDO	Neglect Differential Diatomic Overlap
MINDO3	Modified Intermediate Neglect Differential Overlap
RM1	Recife Model 1
HOMO	Highest Occupied Molecular Orbital
LUMO	Lowest Unoccupied Molecular Orbital
E_b	Energy Barrier
E_g	Energy Gap
ESP	Electrostatic Potential
I.R	Infrared Spectrum
U.V	Ultra Violet
VIS	Visible
STO	Slater Type Orbital´s
HF	Hartree-Fock
UHF	Unrestricted Hartree–Fock
RHF	Restricted Hartree–Fock
ROHF	Restricted Open-Shell Hartree–Fock
ZPE	Zero-point Energy
ΔH	Enthalpy Reaction Chang
Ts	Transition State
Ψ	Wave Function
$\hat{H}$	Hamiltonian Operator
$\hat{f}$	Fock Operator
kcal	Kilocalories
Mol.	Mole
PES	Potential Energy Surface
a.u.	Atomic Unite
e.v.	Electron Volte
$\boldsymbol{\upsilon}^{HF}$	HF Potential
$\hat{h}$	Core Hamiltonian
$\hat{J}_b$	Coulomb Operator
$\hat{K}_b$	Exchange Operator
X_a, X_b	Spin Orbital
N, l, m	Quantum Numbers

r , Θ,Φ	Spherical Coordinates
Å	Angstrom
α	Spin Function(UP)
β	Spin Function(DOWN)
$Y_{l,m}$	Spherical Harmonic
φ^{μ}	Basis Functions
$C_{\mu i}$	The Molecular Orbital Expansion Coefficients
Θ	Angle
°	Degree
ζ	Orbital Exponents
∇^2	Laplacian Operators

Summary:

Theoretical study of Betamethasone drug has been carried by using different computation methods such as Semi-empirical method(PM3) and density functional theory(B_3LYP) at basis set(3-21G and 6-31G). Packed programs such as Gaussian 09 program and Hyperchem 8.02 program have been used to achieve the required theoretical computations.

The characterization of estimation study has been done through geometrical optimization structure for all chemical species at aground state. At the same time, all respective properties such as the special orientation of atoms in the molecule, the bond parameters(bond length and bond angles), the chemical reactivity, potential energy surface, molecular orbitals (HOMO and LUMO), electrostatic potential and zero-point energy have been determined to get on a clear view about chemical modulation.

Molecular spectrum such as electronic transitions and vibration frequencies of Betamethasone has been estimated, later comparative with practical spectrum. The mass spectrum of Betamethasone has been studied practically to get on the actual chemical structure of the drug moiety.

The suggestion of transition states for rate determinate step(slow step) of chemical reactions has been tested through computations of the first negative imaginary frequency and zero-point energy to discover the transition state which gives the actual path step for the selected chemical reactions. At the same time the thermodynamic values and energy barrier value of each reaction step been calculated to employ Hess's law of thermochemistry for all chemical reactions.

The suggestion of four new derivatives of Betamethasone has been done through substituted functional groups into the reactive site of drug moiety such as -NH_2, -$NHCH_2CH_3$, -COOH, and -$CONH_2$. Comparative between original

moiety and its derivatives through transition state of rate-determining step, chemical reaction formation, chemical reactivity and global index parameters. From the obtained results, it was found that.

The total energy and energy-gap of the Betamethasone drug is equal to -1331.653 kCal/mol, and 0.079 eV, respectively. The major bond length is O5-H30 bond which is represented the lowest stability than other chemical bonds and more chemical reactivity with a dissociation energy value equal to 33.35 kCal/mol. Sequential reaction steps of Betamethasone formation have been done through enthalpy of formation equal to -452.406 kCal/mol.

Four suggested derivatives of Betamethasone that had been suggested by the theoretical investigation are AFHTDPO (Betamethasone-NH_2), EFHTDPO (Betamethasone-$NHCH_2CH_3$), FHCPCC (Betamethasone-COOH), and FHACPC (Betamethasone-$CONH_2$).

Two of the new suggested derivatives, were AFHTDPO (Betamethasone.NH_2), EFHTDPO(Betamethasone.$NHCH_2CH_3$) were more chemical effective than the Betamethasone molecule according to the theoretical calculation while FHCPCC(Betamethasone. COOH), FHACPC(Betamethasone.$CONH_2$) are less chemical effective. Both AFHTDPO (Betamethasone.NH_2), EFHTDPO(Betamethasone.$NHCH_2CH_3$) can be used as an Antidrug toward coronavirus or any other viruses after they are prepared and application tests.

1- Introduction

1-1 viruses

A virus is a sub microscopic infectious agent that replicates only inside the living cells of an organism[1]. Viruses infect all life forms, from animals and plants to microorganisms, including bacteria and archaea[2]. Scientific opinions differ on whether viruses are a form of life or organic structures that interact with living organisms[3]. They have been described as (organisms at the edge of life)[4], since they resemble organisms in that they possess genes, evolve by natural selection[5], and reproduce by creating multiple copies of themselves through self-assembly. Although they have genes, they do not have a cellular structure, which is often seen as the basic unit of life.

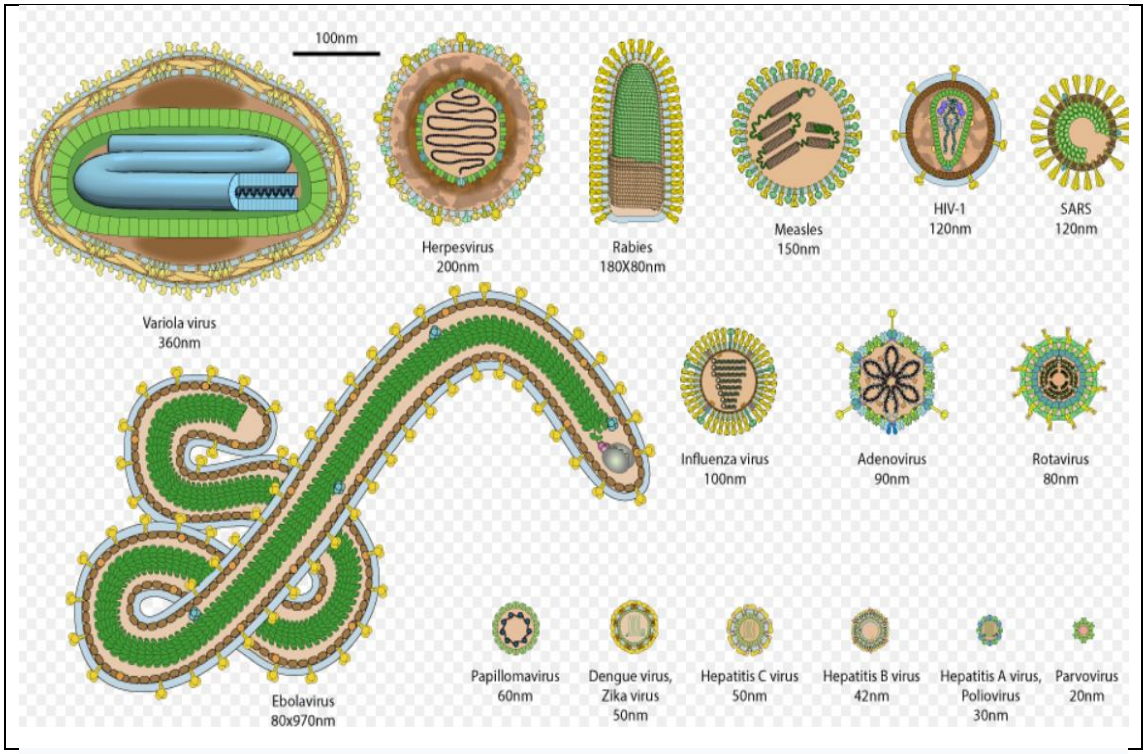

Figure (1-1). Virions of some of the most common human viruses with their relative size [5].

1-2 Coronaviruses

Viruses are microscopic parasitic particles that are unable to multiply on their own. They can infect and multiply in the host cell if they enter it[6] Coronaviruses are a broad group of viruses that can infect both animals and humans and cause diseases for them [7]. Coronavirus disease 2019 (shortened "COVID19") is a new respiratory illness produced by a novel coronavirus that was initially discovered in Wuhan, China, in December 2019[8]. The world health organization (WHO) authentically called this infectious illness Novel Coronavirus-Infected Pneumonia (NCIP) and the virus had been named 2019 novel coronavirus (2019-nCoV)[9]. CoVs are members of the Corona virinae subfamily of the Corona viridae family of the order Nido virales. There are four genera in this subfamily: Alpha coronavirus, Beta coronavirus, Gamma coronavirus, and Delta coronavirus. CoVs have (65–125 nm in diameter) and a 30 kb single-stranded positive-sense RNA (+ssRNA) genome with a 5′-cap structure[5′-methylated head] and a 3′-poly-A [3′-polyadenylated] tail[10], [11]. The disease was originally categorized as a zoonotic disease since the infection can be passed from human to human and animal to human[12]. It spreads from person to person via droplets, faeces, and direct touch, with an incubation period of 2-14 days [13]. Although seven coronaviruses can cause illness in humans throughout the world, the four most prevalent human coronaviruses are human coronavirus-Organ Culture 43(HCoV-OC43), human coronaviruses-229E (HCoV-229E), human coronaviruses-Hong Kong University 1 (HCoV-HKU1) and human coronaviruses-NetherLand 63 (HCoV-NL63)[14]. They typically cause respiratory infections ranging from the common cold to more serious diseases like Middle East Respiratory Syndrome (MERS), Severe Acute Respiratory Syndrome (SARS), and the most discovered recently coronavirus (COVID-19) cause infectious disease[7]. Coronaviruses (CoVs) are a type of virus with prickly spikes protruding from its surface. They have RNA viruses

that are enveloped, club-like spikes that protrude from their surface, and a unique replicating process[15]. Three novel human coronaviruses have appeared in the last 20 years: SARSCoV in 2002, Middle East respiratory disease (MERS)-CoV in 2012, and COVID-19's causal agent, SARS-CoV-2 in 2019. and they're all thought to have come from bats[16]–[18]. COVID-19 has been labelled a public health emergency of international concern by the World Health Organization (WHO). On January 30, 2020, (PHEIC)[19].

1-2-1 Symptoms of covid-19

After an incubation period of around 5-2 days, COVID-19 infection symptoms arise [12]. From the commencement of COVID-19 symptoms until death, the time ranged from 6 to 41 days, with a median of 14 days [20]. The length of time depends on the patient's age and the state of his or her immune system. When comparing patients above the age of 70 to those under the age of 70, it was shorter. Fever, cough, and exhaustion are the most prevalent symptoms of COVID-19 infection, but other symptoms include sputum production, haemoptysis, headache, dyspnea, diarrhoea and lymphopenia [20]–[23]. It's worth noting that the symptoms of COVID-19 and previous beta coronaviruses are similar, including fever, dry cough, dyspnea, and bilateral ground-glass opacities on chest CT scans [24]. yet, COVID-19 displayed certain unparalleled clinical characteristics, such as the targeting of the lower airway, as evidenced by upper respiratory tract symptoms such as sneezing, rhinorrhoea and sore throat[25], [26].

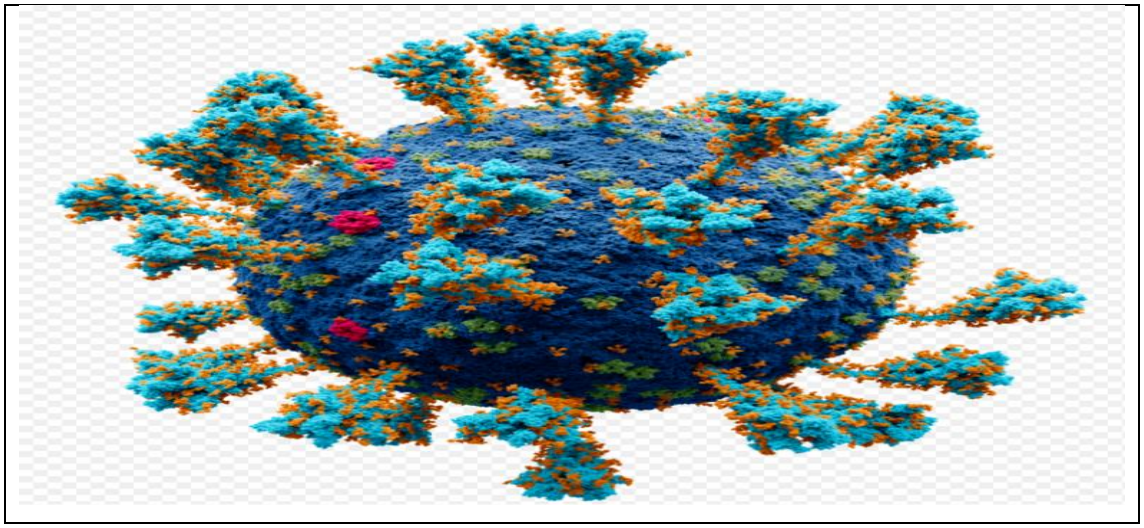

Figure(1-2). Shape of covid-19 [6].

1-2-2 Treatment of COVID -19

There are currently very few approved therapies for human coronavirus such as Pfizer tablet, but a variety of medical countermeasures, such as direct-acting antivirals (DAAs). Host-targeted antivirals, and immunomodulatory are being prescribed off-label for COVID-19 in an attempt to reduce disease severity based on previous observational studies for other coronaviruses [27] and interest by symptomatic therapy like monitoring vital signs, maintaining oxygen saturation and blood pressure, and treating complications like secondary infections or organ failure[28]. Furthermore, numerous medications are now being examined in randomized control studies to determine efficacy[29], [30] with over 300 trials related to COVID-19 being registered[31]. The medications now being tested are thought to target different stages of the virus's life cycle. The treatment's three goals are as follows:

1- To administer an early antiviral treatment that will be more effective during the first 7–14 days of infection, when the infection is highest in the upper and lower respiratory tract.

2- To treatment the cytokine storm to avoid the onset of ARDS and prevent unnecessary the need for mechanical ventilation, which has a 50% mortality rate.

3- To lower the risk of serious thromboembolic events[32]. Many corticosteroids, such as cortisone, hydrocortisone, prednisolone, methylprednisolone, betamethasone, and dexamethasone, are used to treat numerous viral illnesses (Gagyor *et al*., 2019; Sullivan *et al*., 2016; Thaera *et al*., 2010), but betamethasone and dexamethasone as more effective inhibitors of SARS CoV-2 Mpro[33].

Ascorbic acid (vitamin C), zinc , vitamin D[33]–[35] and N-acetylcysteine[36], [37] have all been proposed as COVID-19 preventative or treatment options due to their ability to impact immunological response and reactive oxygen and nitrogen species, as well as their availability as over-the-counter drugs.

1-2-3 Laboratory Diagnosis

Clinical specimens include nasal secretions, sputum, blood and bronchoalveolar lavage (BAL) taken from suspected patients. For laboratory diagnosis, the samples are submitted to specialized COVID-19 serological and molecular testing. Serological studies that identify specific COVID-19 proteins use enzyme-linked immunosorbent assays (ELISA) or Western blots. Real-time PCR (RT-PCR) or Northern blot hybridization targeting specific COVID-19 genes are used in molecular methods[38]. The presence of viral antigens in clinical specimens is determined utilizing a direct immunological fluorescence test (IFA).

1-3 Glucocorticoids

Glucocorticoids are cholesterol derivatives steroid hormones synthesized and secreted by the adrenal gland in response to stress and belong to the corticosteroids family[39].Glucocorticoids are corticosteroids that bind to the glucocorticoid receptor[40] found in nearly every vertebrate animal cell[41] and that are required for mammals to operate normally[42]. Glucocorticoids (GCs) are steroid hormones that are commonly utilized to treat inflammation and autoimmune disorders. As a result, they're utilized in medicine to treat disorders including allergies, asthma, autoimmune diseases, and sepsis that are caused by an overactive immune system.They have anti-inflammatory properties throughout all tissues and regulate metabolism in muscle, fat, liver, and bone and play a role in water and electrolyte balance [42], the immunological response(anti-inflammatory) growth, cardiovascular function mood and cognitive functioning , reproduction and development [43]. The term "glucocorticoid" is derived from its role in glucose metabolism regulation, synthesis in the adrenal cortex, and steroidal structure[44]. Dr. Philip Hench first proposed glucocorticoid therapy for the treatment of rheumatoid arthritis in the 1940s [45]. Since then, glucocorticoids have been widely used to treat inflammatory diseases such as asthma, allergic rhinitis, ulcerative colitis, and a variety of other dermatological, ophthalmic, neurological, and autoimmune conditions[45] .

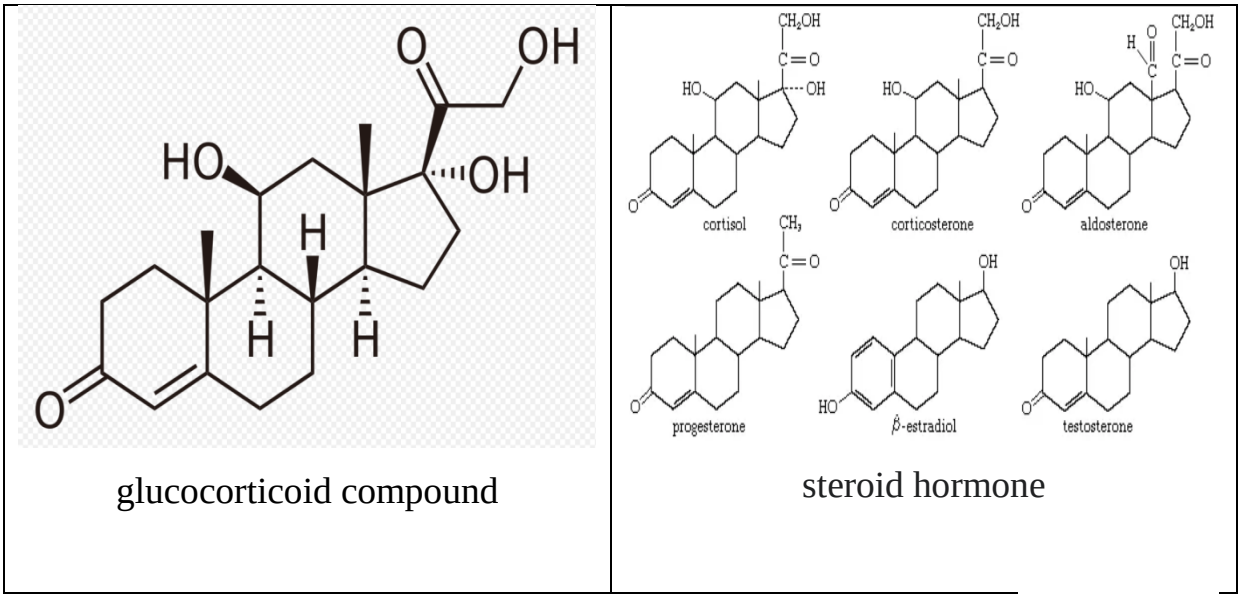

Figure(1-3). Chemical structure of glucocorticoid compounds (cortisol) and steroid hormone [39].

1-4 Betamethasone Drug

Betamethasone is a fluorinated glucocorticoid that is synthesized (GC) by using the starting material 9-α-hydroxyandrost-4-ene-3,17-one (9-α-OH-AD). Some of this compound's esters and salts are commonly employed as anti-inflammatory, immunosuppressive, and antiproliferative medicines, as well as in the dermatological treatment of various skin conditions[46], [47]. It has the ability to treatment into many different diseases including Rheumatic disorders such as rheumatoid arthritis and systemic lupus erythematosus, skin diseases such as dermatitis and psoriasis, allergic conditions such as asthma and angioedema, preterm labour to speed the development of the baby's lungs, Crohn's disease, and cancers such as leukaemia. It can be taken orally, injected into a muscle, or given topically to the skin in the form of a cream, liquid or lotion ,It's also a crucial intermediate in the production of pharmaceuticals like clobetasol and diflorasone. The glucocorticoid class of drugs includes betamethasone ,It is a stereoisomer of dexamethasone, with only the spatial arrangement of the methyl group at position 16 changing between the two molecules.

Betamethasone was first patented in 1955 and approved for medical use in the United States in 1961[47]. The production of steroid medicines and hormones is based on a combination of microbial technologies and chemical synthesis[48] . The α-9,11-halohydrin functionality in steroids, which is required for their biological activity, can be generated by dehydration the α-11-hydroxysteroid. the starting material used to betamethasone synthesis is 9-α-hydroxyandrost-4-ene-3,17-one (9-α-OH-AD)[49], [50]. The indirect 16-methylation with CH_3Br, the introduction of the 17-side chain with 2-chlorovinyl ethyl ether, and microorganism fermentation for the 1,2-dehydrogenation are all important to the success of the betamethasone synthesis[51].

corticosteroids like betamethasone can function through nongenomic and genomic pathways The genomic pathway is slower and happens when glucocorticoids activate glucocorticoid receptors and initiate downstream effects that enhance transcription of anti-inflammatory genes such as phosphoenolpyruvate carboxykinase (PEPCK), IL-1 receptor antagonist, and tyrosine aminotransferase (TAT). The non-genomic route, on the other hand, can elicit a faster response by modulating T-cell, platelet, and monocyte activity through utilize of membrane-bound receptors and second messengers. [52]. Corticosteroids bind to the glucocorticoid receptor, which inhibits pro-inflammatory signals while increasing anti-inflammatory signals[53]. The fundamental action of betamethasone drug occurs through binding to specific intracellular glucocorticoid receptors and subsequently binds to DNA to modify gene expression. The synthesis of certain anti-inflammatory proteins is induced while the synthesis of certain inflammatory mediators is inhibited.

Betamethasone metabolism produces six metabolites, and among the metabolic processes are 6-β hydroxylation, 11-β-hydroxyl oxidation, and reduction of the C-20 carbonyl group followed by removal of the side chain[54].

Betaderm, Betaloan Suik, Betaflam, Betnesol, Celestoderm, Celestone Soluspan, Dermacinrx Therazole Pak, Diprolene, Diprosalic are some of the brand names for Betamethasone drug. the generic name is betamethasone which has the chemical formula $C_{22}H_{29}FO_5$, molecular weight equal to 392.4611. Figure(1-4) shows molecular structure of Betamethasone.

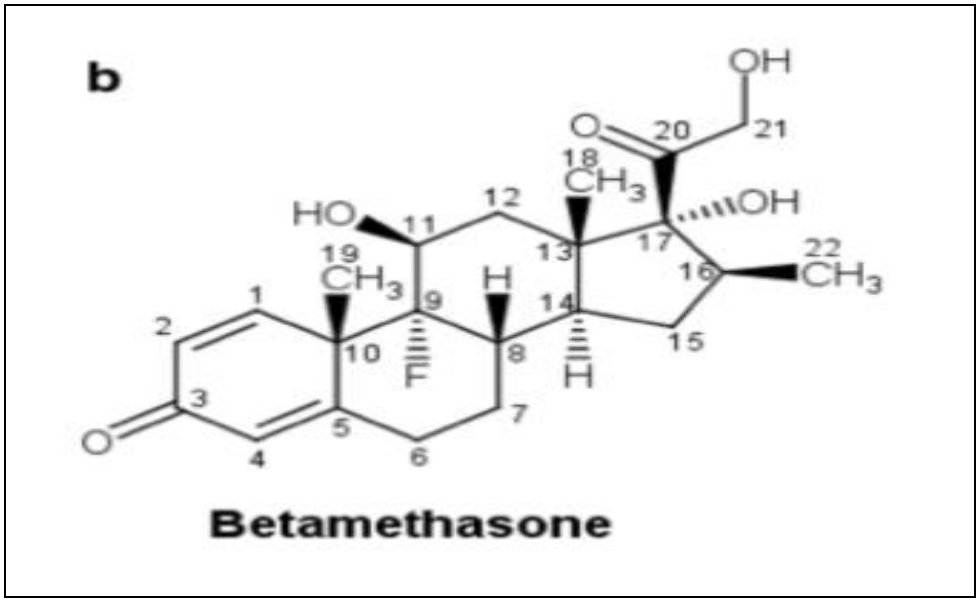

Figure (1-4). The molecular structure of Betamethasone

1-5 Molecular modelling of drugs

Computational programs are used to achieve molecular simulation of medications to reduce the cost and time of drug design. It plays an important role in drug development and discovery [55]. Over the last several decades, significant progress has been made in computer science, molecular biology, mathematics, biochemistry, biophysics, pharmacokinetics, and pharmacodynamics, aided by the rapid growth of reasonable drug design, which has been used in the discovery of novel medications [56]. A new drug's synthesis is a difficult process. Pharmaceutical and biotechnology companies must spend a significant amount of money to model a single medication that can cure a disease or alleviate the effects of another. Most pharmaceutical and biotechnology companies say it is costly and takes 12 to 15 years to

complete[57], [58]. Both molecular structures and physicochemical properties have piqued the interest of medicinal chemists as a modern drug research and development technique for completing structure-activity relationships in the development of drug designs and modelling. The chemical structure of the drug molecule affects its structural and physicochemical properties [59], [60].

To obtain candidate drugs with good pharmacological activities, chemists typically hold one part of a structural unit unchanged and optimize the structures of compounds, as well as explore the structure-activity relationship by adding or modifying various types of the functional group. Functional classes have a big influence on drug-like properties. The functional classes in the database of globally approved medicines, which include -F, -CHO, -CF_3, -NH_2, -OH, -CN, -NO_2, -SH, -COOR, -$CONH_2$, -COOH, -CONHOH, -PO_3H, -SO_3H, -SO_2NH_2, -AsO_3H[61]. To conduct a thorough examination of the frequency of functional groups in approved drugs and their relationship to drug-like properties, The frequency of occurrence of 16 types of functional groups among the 6891 drugs was counted. The most popular functional group in all databases is a hydroxyl group (OH), which has the highest incidence level in all databases. Furthermore, the functional groups -COOR or -COOH are the second most common. The substituent -F has a higher occurrence frequency in CNS products, but a lower occurrence frequency in the other drug sub-databases, which is considered to be helpful to drug production [62]–[64]. In anti-infective and anti-cancer drugs, the level of functional groups -NH_2 is higher than in the other sub-databases. The most uncommon functional group in all databases is -SH, which has the lowest incidence level in any drug category. Furthermore, the functional groups -CONHOH, -CHO, and -SO_3H are extremely rare in approved medicines[65] .

1-6 Computational chemistry

Computational chemistry is a branch of chemistry that incorporates elements of mathematics, physics, and computer science to explain the behaviour of atoms and molecules. Theoretical studies have grown in importance in recent years, taking a leading role in science, especially in the fields of pharmaceutical research and chemistry. Computational chemistry is a branch of chemistry that merges theoretical chemistry and computer science to assist scientists in clearer grasping the problem at hand, as well as solving problems in the lab

The main advantage of computational chemistry is that its conclusions are often in close agreement with those of experiments, and it can accurately anticipate and explain chemical phenomena as well as properties of compounds that have yet to be synthesized.

There is a list of atomic and molecular properties that may be examined using basic modern computational chemistry programs such as HyperChem, Gaussian, GAMESS, and others. Programs are based on the computational framework, such as atomic and molecular energies, molecular geometries (bond lengths, bond angles, and torsions), absorption intensities, charge distributions and molecular orbital energies(HOMO and LUMO), reaction barriers, vibrational frequencies, energies and geometries of transition states [66][67].

Solving the molecular Schrödinger equation is an essential goal of quantum computational chemistry projects.

A fundamental premise of quantum mechanics, is fully defined by the mathematical function for coordinates and spins of many particles known as state or the wave function Ψ, which contains all information about the system that can be known. During the operation of the linear Hermitian operators, the information can be acquired from the wave function[68].

Molecular mechanics, molecular dynamics, and electronic structure techniques are among the approaches used in computational chemistry. Classical mechanics is used in molecular mechanics to predict characteristics. Quantum mechanics is used in electronic structure computations. Semi-empirical method, density functional theory and ab initio are used to describe the properties of ground-states and excited states in molecules, as well as stationary states and those that develop with time. Every theory has different levels of precision and computing cost that can be achieved[69].

1-6-1 Molecular Mechanics(MM)

The energy of a molecule is calculated using a simple algebraic equation rather than total electron density or wave function in Molecular Mechanical (MM) techniques. This method is based on four factors:

1-The information that can be used to calculate the constants parameterize.

2-The energy expression's functional form.

3- The user's ability to be applying the technique in a manner consistent with the strengths and weaknesses in it[70].

4- The method used for optimizing the constants from that piece of information.

The theory of molecular mechanics is based on a model of a molecule as a collection of atoms held together by bonds. The energy can be determined from a collection of atoms and bonds (from a given molecule), and the geometry can be changed until the lowest energy is obtained, which corresponds to the molecule's ideal geometry[71]. The most common uses Calculate the geometries (energies) of tiny to medium-sized (no polymeric) molecules, as well as the geometry and energy of polymers, using molecular mechanics. Compute the energy and geometry of transition states (rare), improve organic synthesis, and then when molecules move, they produce a potential energy function that can be

used to compute molecular dynamics. The use of MM saves time on the computer when compared to quantum mechanical methods [72].

1-6-2 Hartree- Fock theory

Quantum chemistry is attempting to solve the Schrödinger equation, as represented in eq. (1-1), to accurately determine the properties of atomic and molecular systems resulting from the directly compute of wave functions for a large number of diatomic and polyatomic molecules using the Self Consistent Field (SCF) method[73].

$$\hat{H}\Psi = E\Psi - - - - - - (1-1)$$

Here: $\hat{H}$ is the Hamiltonian operator, Ψ is the wave function and E is the corresponding to the energy value

Hartree-Fock theory is a close approximation to Hamiltonian theory, and it serves as a foundation for more complex theories. It's also known as a mean-field theory because each electron is designed to move through a medium potential field generated by many other electrons in the system. The HF equations can be stated as follows, using the anti-symmetrized Hartree product $|X_a\rangle$ as an initial approximation to the wave function:

$$f|\chi_a\rangle = \varepsilon_a|\chi_a\rangle - - - - - (1-2)$$

In eq.$\boldsymbol{f}$ represented the Fock operator, Fock operator contains one an electron Hamiltonian operator as well as the efficiency of the one-electron potential.

$\boldsymbol{\upsilon}^{HF}$ represents the HF potential.

$$\hat{f}(1) = \hat{h}(1) + v^{HF}(1) = -\sum_{i=1}^{N}\frac{1}{2}\nabla_i^2 - \sum_{i=1}^{N}\sum_{A=1}^{M}\frac{z_A}{r_{iA}} + \sum_b \hat{j}_b(1) - \hat{k}_b(1) - - - (1-3)$$

Where: $\hat{h}$ represents the core Hamiltonian that includes all one –electron.

$\hat{j}_b$ is coulomb operator and exchange operator given by, $\hat{K}_b$both of which the two-electron terms, in eq.(1-4)and (1-5) respectively.

$$\hat{j}_b = \int dx_2 \mid \chi_b(2) \mid^2 r_{12}^{-1} - - - - - - - - (1-4)$$

$$\hat{k}_b(1)\chi_a(1) = \mid \int dx_2 \, \chi_b^*(2) r_{12}^{-1} \chi_a(2) \mid \chi_b(1) - - - - - - - - (1-5)$$

The numbers 1 and 2 relate to the location coordinates of electrons 1 and 2,r_{12} is the distance between the two electrons, k_b does not have the same straightforward classical explanation as $\hat{j}_b$, thus it must be described by its effect on the spin-orbital,X_a. There are many accurate solutions to the HF equations, but the ground state wave function according to the variation principle[69], represents the solution with the least energy available.

If the system contains any unpaired electrons, various types of HF might be chosen. Restricted open-shell Hartree–Fock (ROHF) or Unrestricted Hartree–Fock (UHF) can be employed for open-shell systems[74], [75]. Restricted Hartree–Fock (RHF) restricts an occupied orbital to be twice occupied and is being used for the closed-shell system (atomic or molecular).

1-6-2-1 Restricted open-shell Hartree – Fock method

Roothaan proposed the restricted open-shell Hartree–Fock (ROHF) approach roughly 50 years ago, based on spin density eigenvalues that are mathematically restrictive The ROHF method is a common tool used by quantum chemists to examine molecules with unpaired electrons and singly and doubly occupied

molecular orbitals. The lack of a single effective Fock operator is a major defect in this model [76], [77] and Figure (1-5) shows a graphic diagram of ROHF.

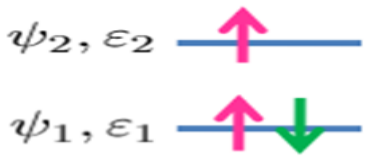

Figure (1-5). A graphic diagram of ROHF[77]

1-6-2-2 Restricted Hartree –Fock (closed shell)

For quantum chemists, the Restricted Hartree–Fock (RHF) methodology is the primary technique for treating closed-shell molecules[78]. "In RHF, each pair of electrons has the same spatial orbital, but each one has its spin, one up and one down. Because the double electrons are constrained to the same spatial orbital, this sort of wave function is known as a spin restricted wave function, resulting in the restricted Hartree–Fock method[75].

1-6-2-3 Unrestricted Hartree –Fock (UHF)

UHF theory was developed by John Pople and is used in the majority of ab initio programs. The most widely used molecular orbital methods for open-shell molecules with different numbers of electrons for each spin.UHF theory employs multiple molecular orbitals for alpha and Beta electrons. UHF is more favored over ROHF because it is easier to develop the post-Hartree Fock procedures and yields unique functions, where several Fock operators can produce the same end wave function[67]. Figure (1-6) shows a graphical diagram of UHF.

Figure (1-6). A graphical diagram of UHF

1-6-3 Density Functional theory (DFT)

The quantum mechanical modelling method is the density functional theory (DFT) that has been used in chemistry and physics to investigate the electronic structure of a variety of body systems, including atoms and molecules and also condensed phases. The features of a many-electron system can be determined using functions that are spatially dependent on electron density in this theory. As a result, the term "density functional theory" was coined from the use of an electron density functional. Because of the nature of the DFT approach, it includes some of the electron correlation[79], [80].

The needed form of the functional, which maps the electron density to the electronic wave function, is unknown from any system other than the free electron gas, which is a major problem in the DFT. To create the functional needed, various approximations will be applied. The functional in the local density approximation (LDA) is based on the density value in the coordinates where the function is assessed. Although the LDA is frequently used and successful in solid-state physics, it is a poor approximation for molecular calculations[81].

One significant advantage of DFT calculations is that they are faster and more accurate than ab initio approaches. With the same computing cost as HF techniques, DFT also contains components of electron correlation. This means that the DFT method is a particularly efficient approach to perform advanced computations on a system and can tackle systems more correctly and it is very big for post-HF approaches.

The disadvantages of DFT methods include that they cannot be improved systematically like wave function-based approaches, making it impossible to quantify the error associated with the computation without using experimental data or other kinds of calculations. The use of the DFT method to characterize

intermolecular interactions has its drawbacks, especially those involving dispersion forces or systems in which dispersion forces compete with other interactions (biomolecules)[82].

1-6-4 Semi-empirical method

Michael Polanyi and Henry Eyring [83] were the first to use the "semi-empirical" term in theoretical chemistry for their effort to together chemical kinetics, thermodynamics, quantum mechanics with each other, and also the theory of the binding electrons valence.

In quantum chemistry, semi-empirical methods are commonly used to study the structure, chemical reaction, stability and spectroscopy of molecules (big and complex molecules)[84].

Semi-empirical ways describe molecules by using the obvious interactions between electrons and nuclei. They are founded on the three fundamental principles.

1-There are explicit electron-nuclear and electron-electron interactions.

2-Electrons and nuclei are differentiated from one another.

3-interactions determine the distribution of space of nuclei, electrons and their energies.

Semi-empirical calculations are quicker than ab initio calculations, primarily because the number of integrals to be dealt with is substantially reduced by ignoring some and approximating others with experimental quantities or values from high-level DFT or ab initio calculations[85]. The advantages offered in energy calculations lead to semi-empirical methods that are 100 to 1000 times faster in general than ab initio HF or DFT ways of identical predictive quality, as well as the capacity to characterize bond breaking and bond-building reactions. Semi-empirical is a highly good calculation in a description of organic chemists, specifically those that gives the lowest energy geometries, which are also used to describe inorganic materials [86].

1-6-5 Ab-initio method

The computations have been given the label ab initio way (from the first principle) for apprise execution of the Hartree-Fock theory. This title has been given to computations that are procured directly from theoretical principles of quantum mechanics, electron masses and charges, atomic nuclei, and values of essential physical fixed, such as Planck's constant or the speed of light ($h= 6.626x10^{-34}$ J.s) , ($C=2.998 \ x10^{8}$ m/s), respectively, without the empirical data being included. These computations cover a semi- comprehensive mathematical treatment of the Hartree-Fock theory, which is inherent to the theoretical model. For complex algebraic formulae, exhaustive calculations of this sort can result in a potentially large number of integrations and differentiation[79], [87].

Solving the Schrodinger equation is required for ab initio calculations. The ab initio method was used to compute energies, molecular geometries, vibrational frequencies, spectroscopy, electron affinities, ionization potentials, and other parameters which link with electron distribution such as dipole moments.

Ab-initio ways should only be used on tiny systems. from among the disadvantage of ab-initio ways, The computational cost is high, and they always consume a massive amount of time, memory, and computer disk space [88], [89].

1-6-6 Basis set

In quantum chemistry, a basis set or basis function is a collection of functions that are merged to form molecular orbitals [90]. Gaussian type atomic functions as basis functions employ in Gaussian 09 and other ab initio electronic structure programs. “A basis set is a mathematical representation of a system's orbitals (which combine to approximate the whole electronic wave functions) that is

utilized in theoretical calculations. The fundamental functions should provide a complete set for a true representation of MOs". A typical MO can be defined as:

$$\emptyset_i = \sum_{\mu=1}^{N} C_{\mu i}\, \chi_\mu \; - - - - - - - - (1-6)$$

The MO expansion coefficients are denoted by $c_{\mu i}$. Normally, the basic functions, Xi... XN, are normalized functions. The coefficients of a linear combination of the basis functions in the basis set employed agree with these components. In this confined context, the operators are represented as matrices. When utilizing molecular computations, it's popular to employ a basis with a bounded number of atomic orbitals. The MOs are expanding by a set of atomic orbitals (AO) on created atoms.

The linear combination of atomic orbitals (LCAO) is a frequent name for this way. Bigger systems can quickly become unpractical. As a result, simpler functions Slater type orbitals (STO)[91] and Gaussian type orbitals (GTO) [92] are frequently utilized instead of AOs and they are regarded as the two most prevalent types of basis functions.

1-6-6-1 Basis sets of Minimal

Minimal basis sets, or single-zeta basis sets, are constructed using a single basis function for each core and valence orbitals in the system. The smallest basis set that utilizes very big molecules calculations in quantum mechanical computations appears as a kind of basis set. The STO-NG basis set is the minimum basis set. This N value is several primitive Gaussians are fitted to a single STO in a least-squares fashion to compose a single basis function.

"Extended basis sets are necessary for more precise outcomes. For example, through using three functions of Gaussian type[93], the basis set STO-3G is approximated of Slater orbitals.

1-6-6-2 Split Valence Basis sets

Expanding the basis set is a simple way to increase the number of basis functions employed per orbital. For more than one basis function of the variable orbital exponents to each valence orbital, split-valence basis sets have been used, but only for one basis function to each core orbital. for example, The valence double-zeta (VDZ) basis set, utilized two basis functions to each valence orbital, whereas the valence triple-zeta (VTZ) basis set utilized three. Pople and his co-workers[94][95] developed k-lmnG basis sets which is another example of them. The split-valence basis sets which commonly utilized are 3-21G, 6-31G, 6-21G, 6-311G, and 4-31G. The first number denotes how many primitives will be used in contracted core functions. The numbers next to the hyphen refer to the number of primitives used in valence functions, two numbers imply a valence-double (ζ) basis, while three numbers imply a valence-triple (ζ) basis. Table(1-1) shows the description of these basis sets.

Table(1-1). Description of split-valence Basis sets

Type of split valence orbital basis sets	Description
3-21G[94]	This notation denotes that the core 1s orbital is composed of three Gaussians, while the valence shell 2s and 2p orbitals are divided into two parts: the inner fraction is composed of two Gaussians, and the outer part is composed of one Gaussian.
6-31G[96]	This notation means that each core orbital is characterized by a single constriction of six GTO primitives, while the valence shell orbital is characterized by two contractions, one with three primitives and the other with one.
6-21G[94]	This notation denotes that the inner (1s) shell is made up of

	six Gaussian functions, as well as it has two valence shells 2s and 2p consisting of 2 and 1 Gaussian functions, respectively.
4-31G[97]	This notation denotes that each inner shell is represented by a single basis function that is the sum of four Gaussian functions and that each valence orbital is divided into inner and outer sections, each of which is defined by three and one Gaussian functions, respectively.
6-311G[98]	The core 1s orbital is composed of six Gaussians, while the valence shell 2s and 2p orbitals are divided into three parts: The contracted portion is the product of three Gaussians. 1 Gaussian is the more diffuse section.

1-6-6-3 Polarization and Diffuse Functions

To get improved results, the polarization functions must be introduced to the basis set[99]. Polarization functions are frequently more precise computed geometries and vibrational frequencies. The heavy elements functions desired higher angular momentum, such as d- and f-types. while helium and hydrogen atoms with p and d-types such as 6-31G. (d , p).

The flexibility of the basis set is increased by enabling the orbital form to alter. One or two plus signs appear in the diffuse functions. A single plus sign denotes the addition of diffuse functions to atoms other than hydrogen. The second plus sign indicates the diffuse functions are utilized for all atoms, such as 6-31+G* or 6-31++G*. The shape of the wave function far from the nucleus and which have greater electron density distributions on anions is illustrated by these diffuse functions[100].

Asterisks (*) or two asterisks (**) have been used to indicate polarization functions. A polarized basis set 6-31G*, for example, provides a basic set that adds d polarization functions to each non-hydrogen atom. while A 6-31G** basis set an add p functions to hydrogen's as well [99].

1-6-7 Geometry optimization

Geometry optimization is a technique for determining a molecule's lowest energy or more relaxing conformation. For all levels of calculation, the path is the same. Geometry optimization has to be the most necessary step in predicting the properties of a molecule using quantum mechanics calculations. A geometry optimized molecule represents the minimum structure of a potential energy surface, which is then used as a starting point for subsequent calculations such as single point, vibration, and so on.

Geometry optimization can also be used to forecast the molecule's equilibrium structure by locating minima on a potential energy surface (PES). A stationary point is a position on a PES where the forces are zero, and these are the spots that are typically found throughout an optimization. It's debatable whether these points constitute local or global minima, and perhaps even transition states. For geometry optimization, an input geometry is provided, and the calculation proceeds to move through the PES [101], [102].

1-6-7-2 Single point calculations

The fundamental molecular modelling computation is single point energy. Single point calculation (SPC) gives the static properties of a molecule, such as potential energy, electrostatic potential, derivatives of potential energy, molecular orbital energies, and molecular orbital coefficients for ground or excited states[103]. At a single fixed geometry, this algorithm simply calculates the energy, wave function, and other desired parameters. It's usually done first when studying a new molecule to determine the nature of its wave function. as well as, repeatedly it's also done next the geometry optimization.

1-6-7-3 Potential Energy Surface

Potential energy surface (PES) has an essential role in study of molecular structures and the analysed of reaction kinetics. In computational chemistry, the potential energy surface is a key concept. The PES is a relationship (mathematical or graphical) between the energy of a molecule (or a group of molecules) and its molecular structure[104]. The reactivity, structure, properties of the substance(like dipole moment, polarizability, etc.).The spectra of the molecules can be easily described in terms of the potential energy surfaces. In the Exceptions much simple states, the potential energy surface cannot be determined from the experiment. Computational chemistry has developed many ways for determing the potential energy surface. When the Born–Oppenheimer approximation is invoked in the solving of the Schrodinger equation for the molecular system, the potential energy surface emerges naturally [105][106]. For the diatomic molecule, PES is plotted in two dimensions as shown in Figure(1-7).

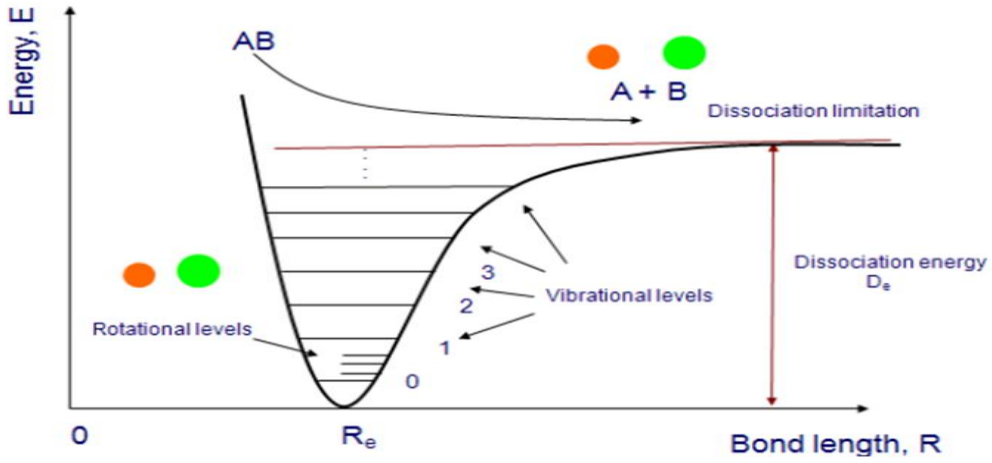

Figure (1-7). Potential Energy Curve for a Diatomic Molecule[107].

Whereas :

De: is the dissociation energy for AB molecule.

Re: is the equalization distance between two atoms.

There are a few particular dots on the PES that should be noted, which represent the minimum (local and global) and saddle point[108], which are

acted stationary dots on the PES. The minimum with a very lowest energy is the global energy minimum. The local minima corresponding is to the molecule's structure stabilization. A saddle point is the highest energy point along the path of minimum energy. This dot sometimes is defined as the transition state[109].

1-6-7-4 Transition state(TS)

The transition state is used to calculate transition state energy and for the optimization of reaction intermediate geometries[109]. The initial step in computationally modelling chemical reactions is due to the presence of a Molecular Potential Energy Surface that contains stationary dots along with the chemical reaction path reactant and product complexes are the endpoints of the chemical reaction path. the energy of the minima on the molecular potential energy surface, Furthermore, those structures agree with stable reactive intermediates. At the potential energy surface, the reactants and products have lesser energy positions separated by a greater energy region. when the transmission of energy from reactants to transition state products, the maximum energy is along a minimal energy pathway. The reactants, products, and transition state's minimal energy has been calculated. Rate constants and equilibrium constants are among the kinetic and thermodynamic parameters that can be estimated[110] . Because the reactant and the final product are observed, information about the reaction process by the minimal energy path of a reaction is often easier to identify a minimum structure than it is to optimize to a transition state, because minimization always prefers a structure with lower energy. When the saddle point is closed in transition-state discovery, the total energy increases or decreases[111], [112].

1-7 Global index Chemical Reactivity

Chemical reactivity is a good indication to describe the local reactivity in molecules [113].In terms of electronegativity (X), chemical potential (μ) [114], ionization potential energy (IE) [115], electron affinity (EA) [116], electrophilicity index (ω),reactivity characteristics like hardness(η) and softness(**σ**) [117]. The energy of HOMO is frequently linked to the molecules' ability to donate electrons, whereas the energy of LUMO is linked to the molecules' ability to accept electrons. As a result, a high HOMO value suggests a strong inclination to donate electrons to a suitable acceptor molecule with a low unoccupied molecular orbital energy. Similarly, a low LUMO value implies a strong proclivity for accepting electrons from the metal surface[66] . bandgap energy is regarded as an evaluative parameter very important for determining the molecular electrical transport properties which interpret the biological activity of chemical compounds due to changes in total dipole moment and changes in partial charge[118]. The E_{gap} (LUMO-HOMO) value is very important for determining the hard and soft molecules and therefore, The molecules which having large energy gaps or small energy gaps are defined as hard and soft molecules respectively, also the soft molecules are more polarizable than hard molecules because they require small energy for an excitation [119]. Therefore soft molecules have lower kinetic stability [118] . Through dependent on Koopmans theorem the highest occupied molecular orbital (HOMO) and the Lowest Unoccupied Molecular Orbital (LUMO) energy are utilized to estimate the IP and EA [120].where

$IP = - E_{HOMO}$ ----------(1-7)

$EA = - E_{LUMO}$ ----------(1-8)

Therefore, the chemical potential(μ),electronegativity(X), chemical hardness(η),chemical softness(S) and electrophilicity index(ω) were calculated according to the following equations[121], [122].

$\mu \approx -X = -(IP+EA)/2$ ---------(1-9)

$\eta = (IP-EA)/2$ ----------(1-10)

$S = 1/2\eta$ ----------(1-11)

$\omega = \mu^2/2\eta$ ----------(1-12)

$\Delta N = -\mu/\eta$ ----------(1-14)

where

IP= ionization potential

EA= electron affinity

μ= chemical potential

X= electronegativity

η= chemical Hardness

S= chemical softness

ω= electrophilicity index

ΔN = Additional electronic charge

1-8 Literature Survey

Fadhel O. E., *et al*., 2012, Estimation study of transition state and synthesis is carried, to synthesise the Barbituric Acid with their derivatives of 1, 3, 4-Thiadiazole. various computation methods of Quantum mechanics to estimate the real transition state using semi-empirical computation methods. Energetic parameters have been calculated such as zero-point energy, the first imaginary frequency and total binding energy to suggest the real transition state of chemical reaction [123].

L. Shao *et al*. in 2013, described the biosynthesis route of gentamicin and other aminoglycosides starting with the addition of D-xylohexose to paromamine (N-acetyl-D-glucosamine added to 2-DOS) and then subjecting it to a series of enzyme modifications that led to the biosynthesis of the final gentamicin[124] .
Belaidi, *et al*., in 2013, used the Gaussian 09 and HyperChem programs at ab initio and DFT methods to study the geometries, bond angle, bond length, charge densities, the heat of formation, bandgap energy of HOMO and LUMO molecular orbitals and Physico-chemical properties of thiazole and some of its derivatives. as well as , they were found that the results of calculations agree with experimental values[125].

R. Singh *et al*. in 2014, synthesised a new Schiff base of a molecule (S-benzyldithiocarbazate) and used H-NMR and FT-IR spectroscopic data to determine its structure. They have been determined the optimized structural parameters (bond angle and bond length), vibration frequencies, band gap energy and other properties for S-benzyl b-N-(4-NN biscynodiethyl amino phenyl methylene)dithiocarbazate by using semi-empirical computational methods (PM3 and AM1) and they found a good agreement between the theoretical and experimental values[126].

Ebtihal K. K., *et al*., 2015, Theoretically, metal complexes of the new tridentate Schiff base are proposed and synthesized as ligand type (NNO) obtained from Isatine. New Schiff base ligand [(E)-3-[(Z)-3-(2-aminoethyl imino)-1, 5-dimethyl-2-phenyl-2, 3-dihydro-1H-pyrazol-4-ylimino] indolin-2-one]. Transition metal ions such as Co(II), Ni(II), and Cu have been used to prepare the chelate complexes of three ligands. The results suggest that the geometrical structures of Co(II), Ni(II), and Cu(II) complexes are octahedral. The spectrum method, conductivity, and magnetic behaver investigations are used to identify compounds [127].

Halla T. M., *et al*., 2016, Computational methods are utilized to study a new Parkinson's disease treatment. Using PM3 semi-empirical calculations and DFT based on STO-3G, nine chemical compounds have been proposed. Chemically changed derivatives of active drugs are used to make new medications, which ignore undesirable drug features such as low solubility, low selectivity, instability, and excessive toxicity. All of the suggestions are made to prevent adverse effects and improve absorption distribution in living tissues [128].

Mansoorinasab, *et al*., In 2017, Using quantum mechanics, studied the processes of gentamicin drug interaction with COOH & COCl functionalized carbon nanotubes, as well as the energetic features of the chemical species. They discovered that the contact of a nanotube with gentamicin via COCl has a lower energy barrier than the interaction via COOH, and that the contribution via the NH pathway is larger. They also discovered that the presence of nanotubes reduces the stability of gentamicin[129].

Lekaa H. K., *et al*., in 2018, studied the Chemical reactivity of a new suggested Chemotherapy agent . This study involved Our new suggested chemotherapy agent is diaminobis((methylthio)oxy)platinum(VI)chloride (DMOP) complex.

The agent has been described to be an effective anticancer therapy. Suggested transition states formation of DMOP (II) complex(square planer) with purine bases(guanine and adenine) are studied by DFT/B3LYP method. They found an energy gap 0.02632 kCal.Mol^{-1} is a small value of indicators of high chemical reactivity for DMOP complex. The reaction is most probable of the complex with guanine bases than adenine bases by total energy value equal to -792.613 kcal mol^{-1} [130].

Dhevaraj ., *et al*., 2019, preparation a series of multi-heterocyclic anti-bacterial drugs 3-(4-(tetrazol-1-yl)phenyl)-5-phenyl-1H-pyrazoles are synthesized using the reaction with (E)-1-(4-(1H-tetrazol-1-yl)phenyl)-3-arylprop-2-en-1-one and hydrazine hydrate in the presence of weak acidic catalyst like acetic acid. The structures of synthesized compounds were confirmed by various spectral studies. Biological activity was measured antibacterial studies with MTT assay methods. The parameters such as optimized geometry, electronic properties and hyperpolarizability of the tetrazole containing pyrazoles have been calculated using density functional theory (DFT) with the application of hybrid functional "B3LYP". In fact, a good agreement between the calculating mode with the experimental one was attained using at the B3LYP/6-311G theoretical level. Therefore, used The dual heterocyclic system showed enhanced biological activity as compared to the isolated pyrazole compounds. As a result of these, the tetrazole moiety is accountable for an increase in biological activity in the whole molecular system[131].

Süleymanoğlu ., *et al*., 2020, Preparation New Schiff base derivatives with thiophene, 1- (4-(((5-phenylthiophene-2-yl) methylene) amino) phenyl) ethan-1-one (I) and 1-(4)-((benzo [b] thiophene-2-ylmethylene) amino) phenyl) ethan-1-

one (II), were synthesized and characterized by FTIR and NMR (1 H- and 13C NMR) spectroscopic methods. The structural parameters and spectral data of Schiff base derivatives were obtained by DFT/B3LYP/6- 311þþG(d,p) method and theoretical spectral data were compared with the experimental ones. Both compounds were tested for their antibacterial and antifungal properties against to the selected 15 bacteria and 4 fungi isolates, which could be threat to the public health, by microdilution broth assay with alamar blue. In vitro antimicrobial activity was determined by using the Minimum Inhibitory Concentration (MIC) values. Results show that, both compounds have high antibacterial activities against Enterococcus faecalis, Streptococcus agalactiae, Shigella flexneri isolates and the MIC values obtained for compounds I and II are 1250/2500, 1250/2500, 1250/ 312 mg/ml, respectively[132].

1-9 Aims of the Present Work

The main aims of the present work are to investigate new derivatives of Betamethasone drugs against Coronavirus. These aims are listed as follows.

1. Characterisation of the affected structural properties for Betamethasone drug.
2. Investigation of the effect of new substituted functional groups on chemical structure-activity of Betamethasone drug.
3. Estimation the reaction steps pathway of formation for the Betamethasone drug.
4. Investigation the optimized geometrical transition states of Betamethasone drug for slow rate determinate step of reaction formation.
5. Suggestion new derivatives, molecular models, for Betamethasone drug as new suggested drugs of Coronavirus.
6. Estimation the reaction steps pathway of formation for all suggested new derivatives of the Betamethasone drug.
7. Investigation the optimized geometrical transition states for all suggested new derivatives of Betamethasone drug through slow rate determinate step of reaction formation.
8. Procuration a comparative about the chemical activity, reactivity and global Index parameters of new suggested optimized model derivatives structures with the original moiety of Betamethasone drug.

2-1 Instruments and Package programs

2-1-1 Computers

Computational studies have been carried out by using various computers according to their specification to increase efficiency and minimize the required time for calculations.

Table (2-1).Types of computers and it's properties

Computer	Type	Processer	RAM	System type
Laptop	TOSHIBA- CORE i5 (5^{th} Gen)	Intel[R] Core[TM] i5-3320M CPU@2.60GH_Z	4.00 GB [3.90 GB usable]	64-bit operating system,x64-based processor Hard
Laptop	HP Pavilion-CORE i7 (9^{th} Gen)	Intel®Core™i7-9750H CUP@ 2.60GH_Z 2.59 GH_Z	16.0 GB(15.8 GB usable)	64-bit operating system, x64-based processor Hard
Desktop	Windows 10 Home single language	Intel®Core™i7-9750H CUP@ 2.60GH_Z 2.59 GH_Z	16.0 GB(15.8 GB usable)	64-bit operating system, x64-based processor Hard

2-1-2 Spectral Analytical Instruments

Instruments that have been used in molecular spectroscopy proving the chemical structure of betamethasone are listed in Table (2-2), according to their characteristics, workplace and origin. Betamethasone drug has been imported from China as 50 grams container made by company Energy chemical with 99% purity. Chemical formula $C_{22}H_{29}FO_5$.CAS (378-44-9).Molecular weight equal to 392.46 g/L. LOT NO(GD180321).

Table (2-2). Instruments of spectral Analysis for molecular spectroscopy

NO.	Instrument	specification	Origin	Work place
1	FT-IR Spectrophotometer	Bruker/ Equinox 55/Tensor 27	Germany	Iran
2	UV-visible Spectrophotometer	Perkin Elmer/ Lambda 850	United states	Iran
3	Mass Spectrophotometer	Agilent Technologies/ 5975C	United states	Iran

2-1-3 Packaged Software Programs

Package programs have been used to achieve the required data for the modulation study of Betamethasone. Table (2-3) shows the packaged programs and their specifications.

Table(2-3). Programs characteristics in this study

Programs	Version	Origin
Gaussian 09	7.0.0.0	Walling USA
Gauss view 05	5.0.8	Semichem USA
Hyperchem 08	8.0.2	Gainesville, Florida, USA.

2-2 Programme of Calculations

2-2-1 Gaussian program

Gaussian 09 is a commercial computational chemistry software produced by Gaussian, Inc. It is a resource by many authors, considered standard for molecular modelling for computational chemistry. The programs include all necessary major methods of molecular modelling. There are three various major levels of computations such as semi-empirical method, density functional theory (DFT) and ab-initio. Various requirements of molecular modelling can be carried out such as energies, geometries, vibrational frequencies, excited states, transition states, reaction paths and a set of properties based on different

uncorrelated and correlated wave's functions[133]. Chemical engineers, chemists, physicists, biochemists, and others utilize the Gaussian programme for researches in confirming and growing areas of the chemicals field[134]. Experimentally hard or hopeless such as short-lived intermediates and transition structures, as well as comparison with experimental data, such as X-ray crystallography technique[135].

2-2-2 Gauss View 05

Gauss 05 [133] has a full-featured graphical user interface called the Gauss view, with the aid of Gauss view, one can prepare input for subjugation Gaussians and see the output that Gaussian produces in graphic form. The first step in generating a Gaussian input file is to construct the required molecule. Gauss view is used to draw a molecular structure by calculating bond angles, bond lengths and dihedral angles for the molecule. Gauss view includes a fantastic molecular builder. Atoms, groups, rings, amino acids, and nucleosides can all be used to construct molecules. The Gaussian view shows several different Gaussian computed values, as shown below Molecular stereochemistry structure[136], [137] .

- The structures of optimized molecular.
- The electron density from any computed density.
- Electrostatic potential surfaces of molecular.
- Charges of atomics and dipoles moments.
- Calculation of IR, UV, NMR spectra.
- The Molecular. Orbitals (MO).

2-2-3 Hyperchem 8.02

Version 8.0.2 of HyperChem is a chemical calculational programme. It is the integrated graphic interface, calculational and visualization package. It has seen much use on Personal Computers. Density functional theory(DFT), semi-empirical, Ab initio and MM methods are all involved in HyperChem. Geometry optimization, vibrational frequencies, transition states, electronically excited states, and MD, QM/MM, and MC simulations have all been done using these methods. The program has included the drawing mode, thus the backbone drawing first, after that the hydrogen atoms spontaneously added. Because this sketcher does not determine the bond lengths or bond angles, the MM optimization was employed before doing the time-consuming computations [138]. Various rendering modes are present in the graphic interface. It is used to show molecular surfaces and vibrational mode animations. The electronic and vibrational spectra, as well as their intensities, are illustrated.

The calculation results are displayed on the screen by default, but they are not stored on the disk. The user can direct that all results from a particular session be written to a log file. The MM force fields are included in the program, which includes MM^{+}, BIO^{+}, OPLS, and AMBER. The semi-empirical methods include (extended Huckel, CNDO, INDO, ZINDO, MINDO/3, MNDO, PM3, PM6 and AM1). As well as, the ab initio calculations. Several common basis sets are used[139].

2-2-4 ChemDraw

ChemDraw is one of the most widely used chemical drawing programs. A comprehensive set of standard tools for sketching 2D chemical structures is included in the drawing software. Some more aspects are quite useful for chemists. One of these advantages is its ability to anticipate the NMR spectrum. Chemical structures can be used to generate IUPAC names. A structure can be created by systematic typing of a chemical name. Chemical compounds'

physical properties, such as melting point and boiling point, can also be calculated.

2-3 Calculation Methods

Different calculation methods have been approved out to calculate the energetic properties, scheme (2-1) shows path of computation into the Gaussian programme run the chemical system, it's necessary to give us real significant results [140]. Scheme (2-2) shows path of the computation into Hyperchem programme run the chemical system.

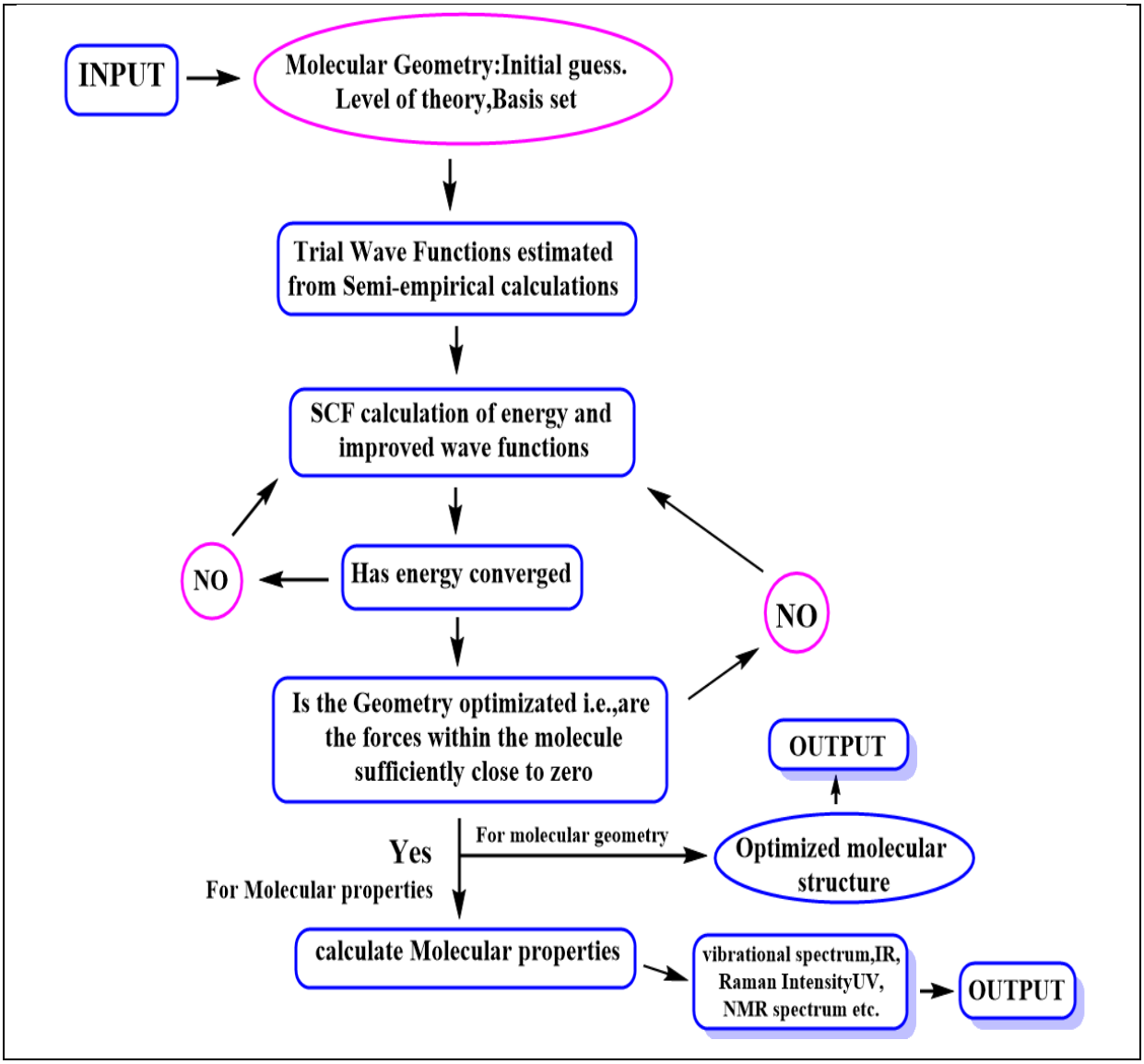

Scheme (2-1). Flow chart runs for Gaussian Programme[140].

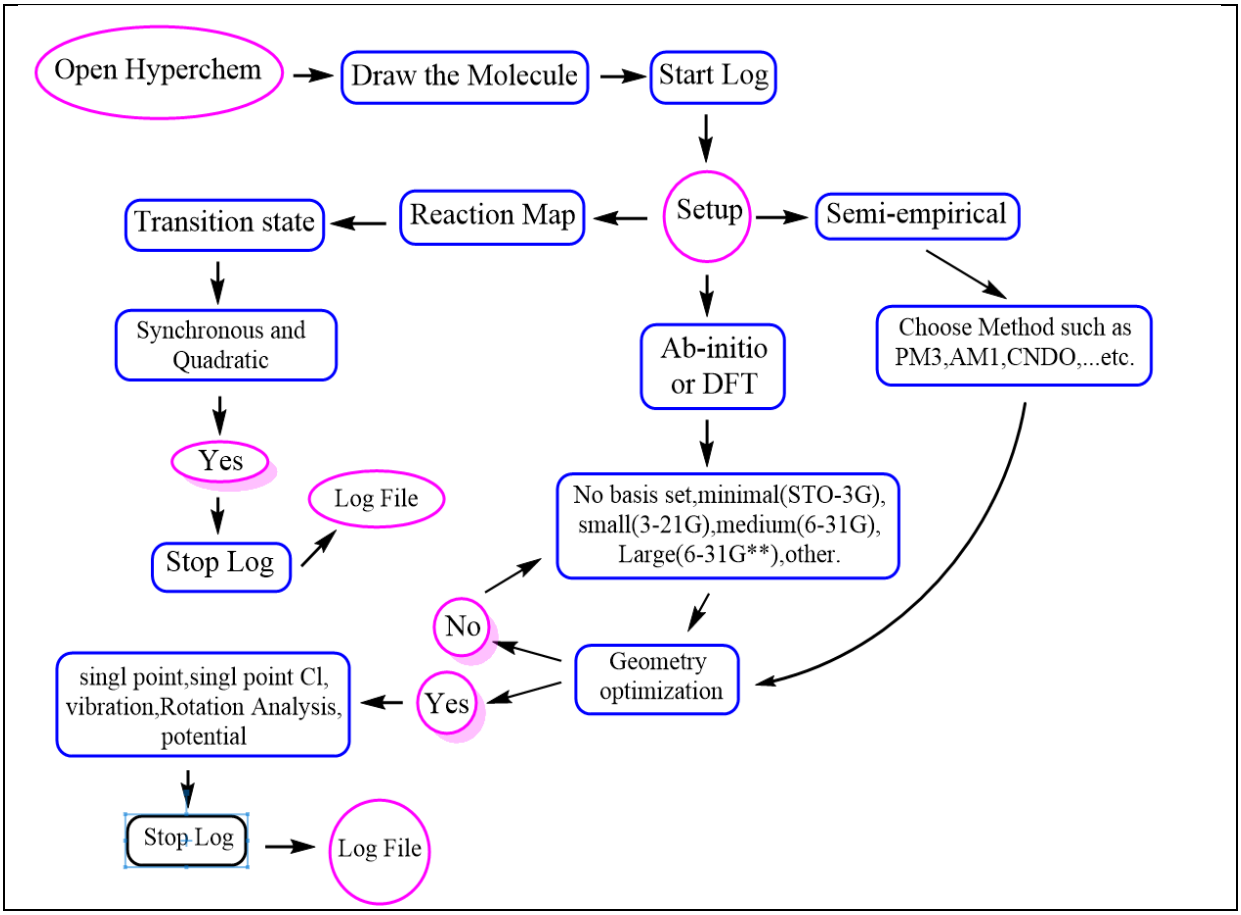

Scheme (2-2). Flow chart run for Hyperchem Programme.

2-3-1 Building of molecular structure

The Gaussian view 05 tools were used to build and exhibit a molecular structure that sketches into two-dimensional structures (2D). Converting a three-dimensional structure (3D) utilizing model building and presenting a molecular structure in a sketch region by selecting atoms from the periodic table and selecting a structure from the toolbar[109] .

In Hyperchem program, to construct the molecules, program tools were employed. After Hyperchem window was opened, the molecules were drawn using the drawing tools. Using the model builder, a two-dimensional representation of a molecule was drawn and then converted to a three-dimensional structure. Molecules have been shown in a variety of shapes (symbols, numerals) utilizing the display list and labels selection. By selecting Rendering from the display menu, the molecules were rendered in the form of

balls, cylinders, and tubes[111], [141] .Scheme (2-3) shows drawing the chemical structure of Betamethasone molecule.

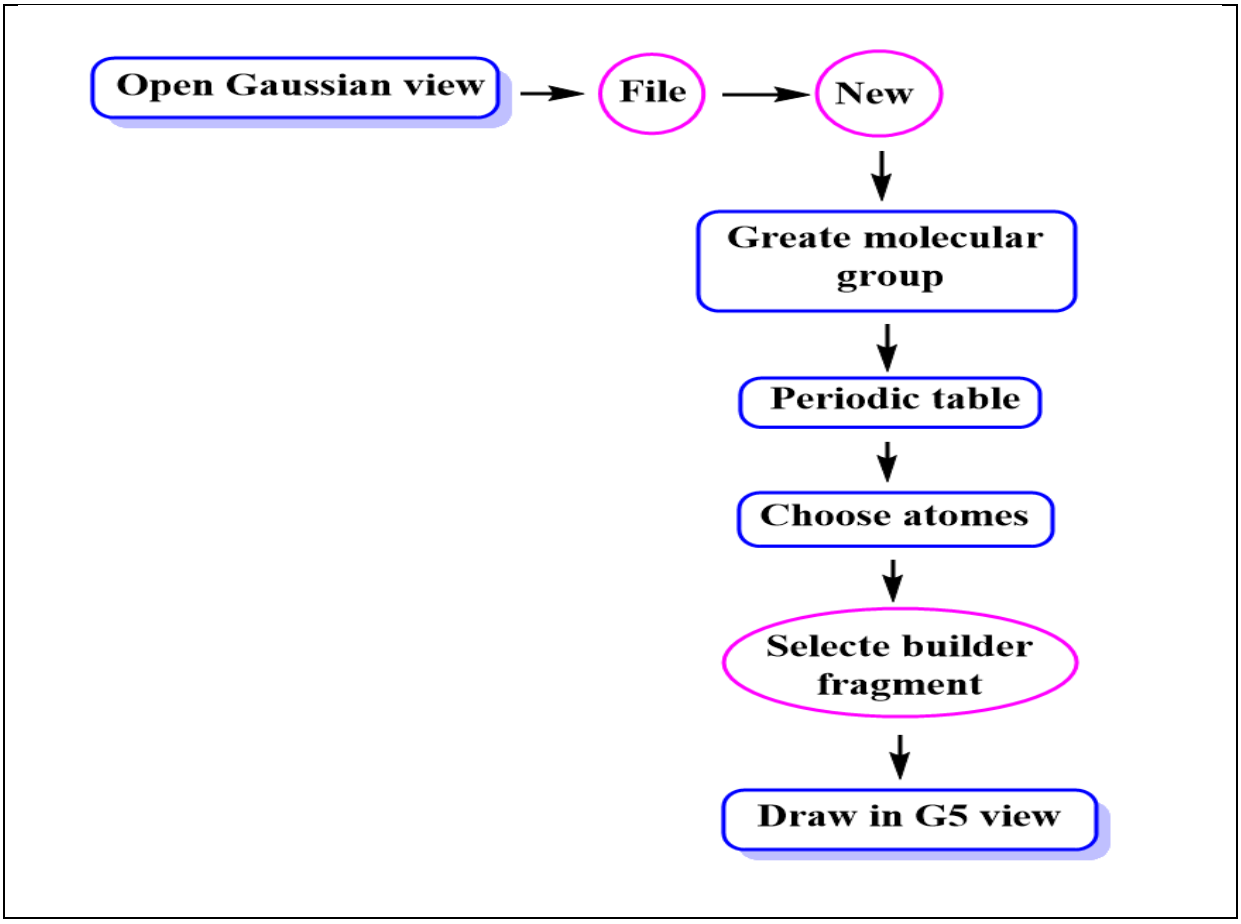

Scheme (2-3). Drawing chemical structure of betamethasone molecule[142].

2-3-2 Geometry Optimization

Geometry optimization is a technique for determining a molecule's lowest energy or most relaxing conformation. For all levels of calculation, the route is the same. Geometry optimization is the most crucial phase in predicting the properties of a molecule using quantum mechanics(QM) calculations, that a geometry optimized molecule represents the lowest structure of a potential energy surface, which is then utilized as a beginning point for sequential calculations. Different parameters such as total energy, atomic charges, dipole moment, heat of formation and binding energy, vibration, and others are

calculated using geometry optimization [101], [143]. The following path of geometry optimization in Gaussian 09 programme is shown in scheme(2-4).

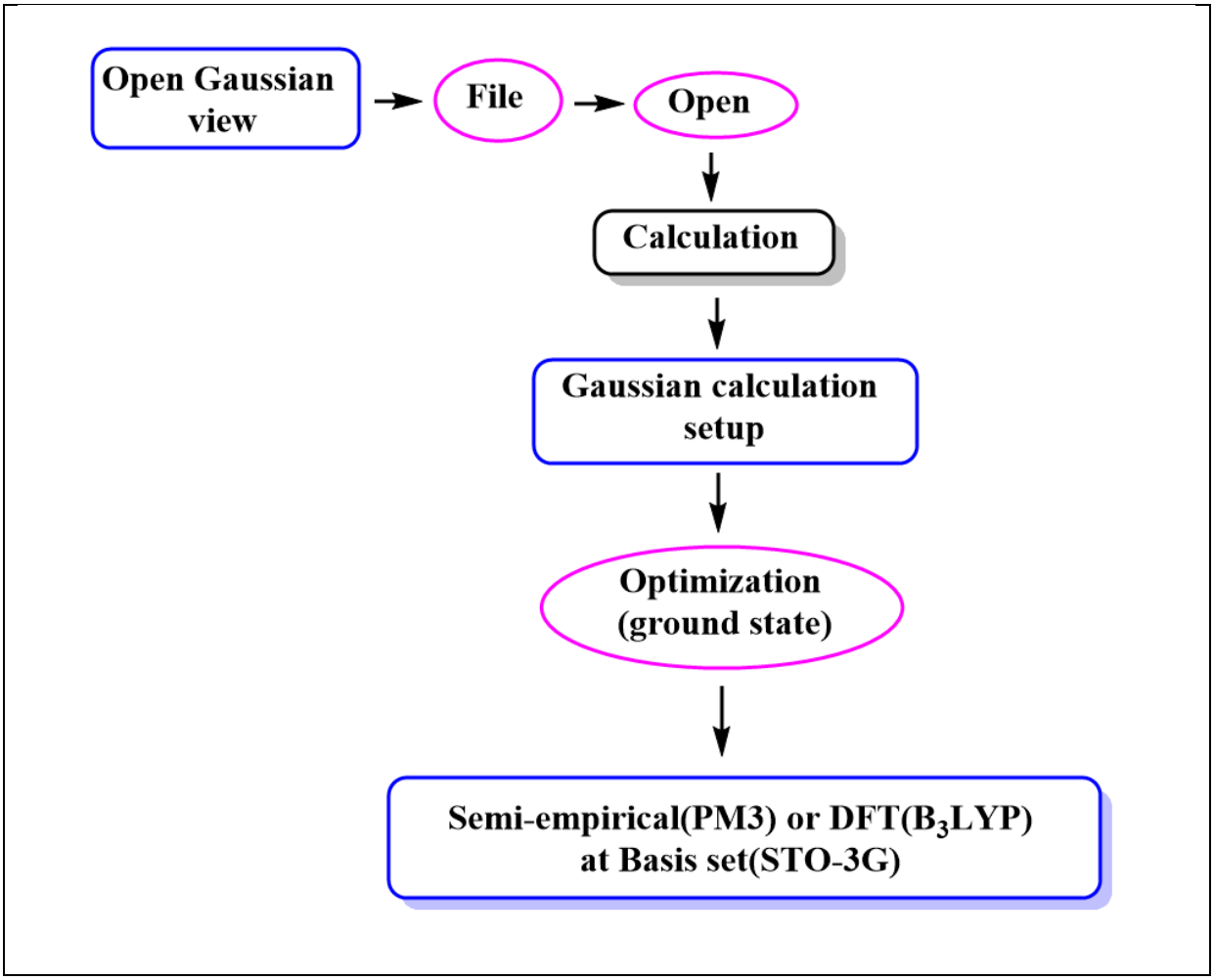

Scheme (2-4). Pathway of geometry optimization in Gaussian programme[142].

To compute the properties or physical characteristics of the molecule, it must have acquired the best structure of this molecule. In other words, determining the molecule's coordinates with the lowest attainable energy potential [141], [144]. The molecules have been completed after the construction and displaying process. The basis set minimal (STO-3G) has been utilized in the density functional computations, and the semi-empirical calculations PM3, CNDO, and other methods have been chosen from the setup menu, and the geometry optimization has been selected from the computing menu. next to the

completion of the calculations, the file was saved with the supplied name by selecting start Log from the file menu, which had been formatted before the computations and then selecting stop log. Then save the calculation results as an external file. The time it takes to compute the geometry optimized of the Betamethasone molecule using semi-empirical (PM3) and DFT(B3LYP) methods at different basis sets (3-21G and 6-31G). The Run time of geometry optimized for Betamethasone molecule in Gaussian programme is shown in Table (2-4).

Table(2-4). The Run time of geometry optimized for Betamethasone molecule in Gaussian programme.

Geometry optimization	Density function theory[B_3LYP]		Semi-empirical method[PM_3]
	3-21G	6-31G	
Run time	5hr:20 min:17.0sec	4hr:37min:31.0 sec.	00 hr:4 min:55 sec.

2-3-3 Single point calculation(SPC)

Single-point computations provided the stationary properties of molecules such as potential energy, electrostatic potential and molecular orbital energies for stable and excited states, as well as fundamental vibrational frequency computations, intensities of an electronic UV-visible spectrum, and bond properties (length, angle and order). The molecular structure's influence on single point computations is reflected in stationary point coordinates on the potential energy surface [143]. Single-point computations were performed directly after that the geometry optimization computations for the molecule were completed by selecting a single point from the Compute menu.

2-3-4 Configuration Interaction computation of wave function

Configuration interaction of wave function is the linear combination of Slater determinants, and it is an approach to improve the Hartree- Fock theory by including a description of correlated motions of an electron. The diagonalization of the Hamiltonian in the presumed subspace of determinants is used to determine differential linear coefficients. In Hyper-Chem, two types of Configuration interaction calculations have been carried out: odd excited and microstates. UV spectra have been created using semi-empirical and ab initio calculations using the singly excited CI. but the semi-empirical methods have just used the microstate CI to improve the wave function and energy values, including the electronic correlation. by the dependent on the electron configurations, There are limited states in the CI calculation that has been used. First, For DFT, semi-empirical, and ab initio ways closed-shell singlet ground states were utilized. Second, for the semi-empirical methods, half electron filled and excited singlet states were used. Third, the half electron filled, doublet, and triplet open-shell ground states have been utilised for the semi-empirical ways only[145].

After the geometry optimization computations were completed, the CI computations were conducted. from the calculation menu was selected single point CI computations were and after that from options dialogue box CI (3*3) Microstate has been chosen.

2-3-5 Potential energy of bonds

The dissociation energy of any bond can be computed by stretching the bond to its maximum length and calculating the difference between the bond's length stability and the maximum length potential. When the bonds' potential energy calculations were finished, they were plotted in a one-dimensional potential energy plot among energy and bond length if two atoms were chosen and if three atoms are chosen, the needed energy can be computed for the angles, and the same may be done for torsion angles energy with four atoms. In calculation, the PM3 method was picked, and then potential was selected from the computing menu.

2-3-6 Spectroscopic Investigation

The spectroscopic analysis provides structural information that may be compared to practical spectral data to ensure that details of our calculations are near to proposed chemical structures.

2-3-6-1 IR-Spectroscopy

The purpose of vibrational analysis study is to hand a general understanding of the stability of geometrized chemical structures and their reactivity to the environment surrounding or electromagnetic radiation interaction. Chemical species' bonds vibrate as soon as they are created, and they continue to vibrate within time. With the chemical bonded deployment on the symmetry axis of the structures and their identity, six diffracted kinds of vibration occur[146]. Hooke's law describes the movement of a vibrating spring as well as the relations among atom masses (m1, m2), bond force constant (f), and wavenumber (v), that appears in eq.(2-1)[147]:

$$v = \frac{1}{2\pi c}\sqrt{\frac{k}{\mu}} \qquad \text{---(2-1)}$$

Where:

ν: is the wavenumber in cm^{-1}.

c:is the speed of light in $cm.sec^{-1}$.

K: is the force constant of the bond in gm/cm^2.

μ:is the masses of the atoms [m1,m2] in gm.

2-3-6-2 UV-VIS spectroscopy

UV-Vis spectroscopy is a technique for determining a sample's absorption intensity and wavelength. In general, UV spectroscopy is used to study molecules and inorganic compounds in solution. UV and visible light photons have quite enough energy to cause outer electrons to excite or move to higher energy states. Bonding (low energy), anti-bonding (high energy), and non-bonding molecular orbitals are generated by the overlap of atomic orbitals. Transitions of electrons from bonding to anti-bonding molecular orbitals are usually connected with energy absorption[148].

2-3-6-3 Mass spectroscopy

Mass spectrometry is an analytical method for determining the mass-to-charge ratio (m/z) of one or more molecules in a sample. These measurements are frequently used to determine the exact molecular weight of components of the sample. Mass spectrometers are commonly used to identify unknown chemicals by determining their molecular weight, quantifying known compounds, and determining the structure and chemical characteristics of molecules.

The generation of gas-phase ions of the compound is the initial step in the mass spectrometric study of compounds, for example by electron ionization:

$$M + e^- \rightarrow M^{\bullet+} + 2e^- \quad \text{----(2-2)}$$

After that, the molecular ion is normally subjected to fragmentations. Because it is a radical action with an odd number of electrons, it can fragment to give either a molecule and a new radical action or a radical and an ion with an even number of electrons. such as in the following equations[149] .

$$M^{\bullet+} \rightarrow EE^{+} + R^{\bullet} \text{ ----(2-3)}$$

Even Ion Radical

$$M^{\bullet+} \rightarrow OE^{\bullet+} + N \text{ -----(2-4)}$$

Odd Ion-Molecule

2-3-7 Molecular orbitals View and Molecular electrostatic potential

The interaction of the energy of a system with the positive point charge can be defined as the Molecular Electrostatic Potential (MEP). The plot provides information about the activity of the molecules in real reactions with nucleophiles or electrophiles. Electrostatic potential (ESP) is important for finding possible sites of reaction in molecules. The negative regions of ESP have been illustrated in red colour, whereas The positive regions of ESP have been represented in green colour[150].

The molecular properties plot was used to show electrostatic potential, total charge density (which defines the likelihood of detecting electrons at a given place in space), and total spine density in 2D contours and 3D isosurfaces with ball and cylinder, tubes perspective. After the semi-empirical or DFT calculations were completed, and the Molecular Graphs plot was selected from the Compute menu.

The key orbitals involved in chemical stability are HOMO and LUMO[151], [152]. They were drawn in 2D and 3D using the same orbital option, and after

that, the energy gap (Egap) was calculated from the difference in energy between HOMO and LUMO as follows in eq.(2-5).

E_{gap} =LUMO – HOMO ----------(2-5)

2-3-8 Transition state search

A transition state search determined the maximum energy along the reaction pathway on the potential energy surface. It finds the first-order saddle point, which is a structure with one imaginary frequency that have one negative eigenvalue. To determine the energy barrier for the chemical reaction, a transition state computation must be performed. The transitional states of the structures were computed using the semi-empirical (CNDO) quantum mechanics method. After the geometry optimization has been completed for each structural reaction singly, the proposed transition states have the same work. The molecules and names of the reactant and product were first chosen from the selected menu, and then the number was chosen from the labels menu, which is found in the display menu. Then, from the setup menu, the reaction map was chosen to merge the same transition state and product. After that, the computing menu was used to pick the transition state, and the settings dialogue box for transition state search was used to select synchronous transit and quadratic. The start log in file menu has been selected before starting the transition state. Finally, after the calculations were performed, a stop log was chosen and the results were saved[153].

The activation energy (energy barrier) has been computed from the equation

$$E_b = E_{ts} - \sum E_r \quad \text{----(2-6)}$$

Where:

E_b = represented the energy barrier (Eb).

E_{ts} = represented the total energy for the transition state that has been taken from the log file of the transition state.

E_r = represented the summation of the total energy of reactants.

Table[2-5] was shown to the required time to calculate Betamethasone and its derivatives in the Gaussian programme.

Table (2-5). Geometry optimization structure of Betamethasone and its derivatives calculated at DFT(B_3LYP/6-31G)method

Compounds	Time [day: hr : min: sec]
Betamethasone	0 day:4 hr:37 min:31.0 sec.
AFHTDPO (Beta.NH_2)	1 day:22 hr:52 min:10.0 sec.
EFHTDPO(Beta.NHCH2CH3)	4 day:4 hr:17 min:54.0 sec.
FHCPCC(Beta. COOH)	2 day:22 hr:36 min: 33.0 sec.
FHACPC(Beta.$CONH_2$)	1 day:17 hr:44 min:51 sec.

2-3-9 Zero-point energy transition states

Zero-point energy has been calculated for transition states structures. The lowest energy value of a structure at the ground state is zero-point energy. It was computed as a preliminary step after the geometry optimization[154] . Zero-point energy(ZPE) is the non-thermic and kinetic power at zero degrees Kelvin, called Zero-point vibration, quantum oscillation, as well as newly dark energy.The DFT computations and semi-empirical calculations have been carried out by the ZPE. To compare the energies of all structures, the zero-point

vibrational energy was estimated after geometry optimization based on the plain vibration frequencies for all structures and proposed transition states[155].

Results and Discussion

3-1 Geometry optimization structure

Molecular structural properties of betamethasone drug were estimated using semi-empirical method (PM3) and density function theory (B3LYP)at basis sets (3-21G and 6-31G) as shown in Figure(3-1). The geometry-optimized structure of betamethasone is released a total energy equal to -1331.652742 a.u., since the orientated bonded atoms are labelled with number which represents the numerical order in geometry optimize structure [156], [157]. The atomic charge influence has a main role in application of quantum chemical calculations of molecular systems. Therefore molecular parameters such as dipole moment, electronic structure, polarizability and Mullikan atomic charge have been computed [158].

Figure(3-1) shows Mullikan charge distribution on atoms of Betamethasone, The hydrogen atoms have a positive charge, indicating that it is an acceptor atoms, while, the carbon; fluorine and oxygen atoms all have a significant negative charge, indicating that they are donor atoms.

At the same time the molecular orbitals (HOMO and LUMO)in three dimensions which appear in green and red colour respectively. Green colour represents the positive part of the wave function that would be attacked by a nucleophile, whereas red color represents the negative part of the wave function, which would be attacked by an electrophile[159]. The energy of HOMO is frequently linked to the molecules' ability to donate electrons, whereas the energy of LUMO is linked to the molecules' ability to accept electrons. As a result, a high HOMO value suggests a strong inclination to donate electrons to a suitable acceptor molecule with a low unoccupied molecular orbital energy. Similarly, a low LUMO value implies a strong proclivity for accepting electrons from the metal surface [66]. Electrophilic and nucleophilic attacks are also most likely to occur at atoms with large coefficients of corresponding atomic orbitals in HOMO and LUMO, respectively. This conduct

controls the Betamethasone molecule's chemical efficiency in the substitution reactions [160].

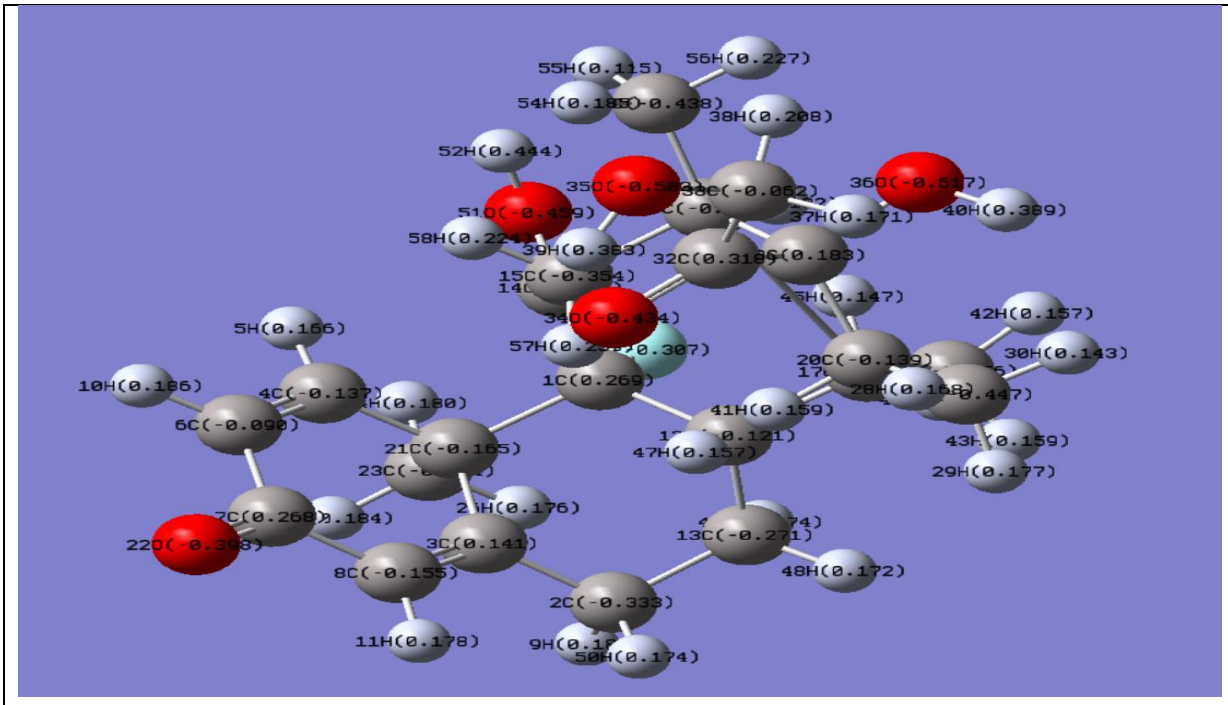

a-Mullikan charges distribution

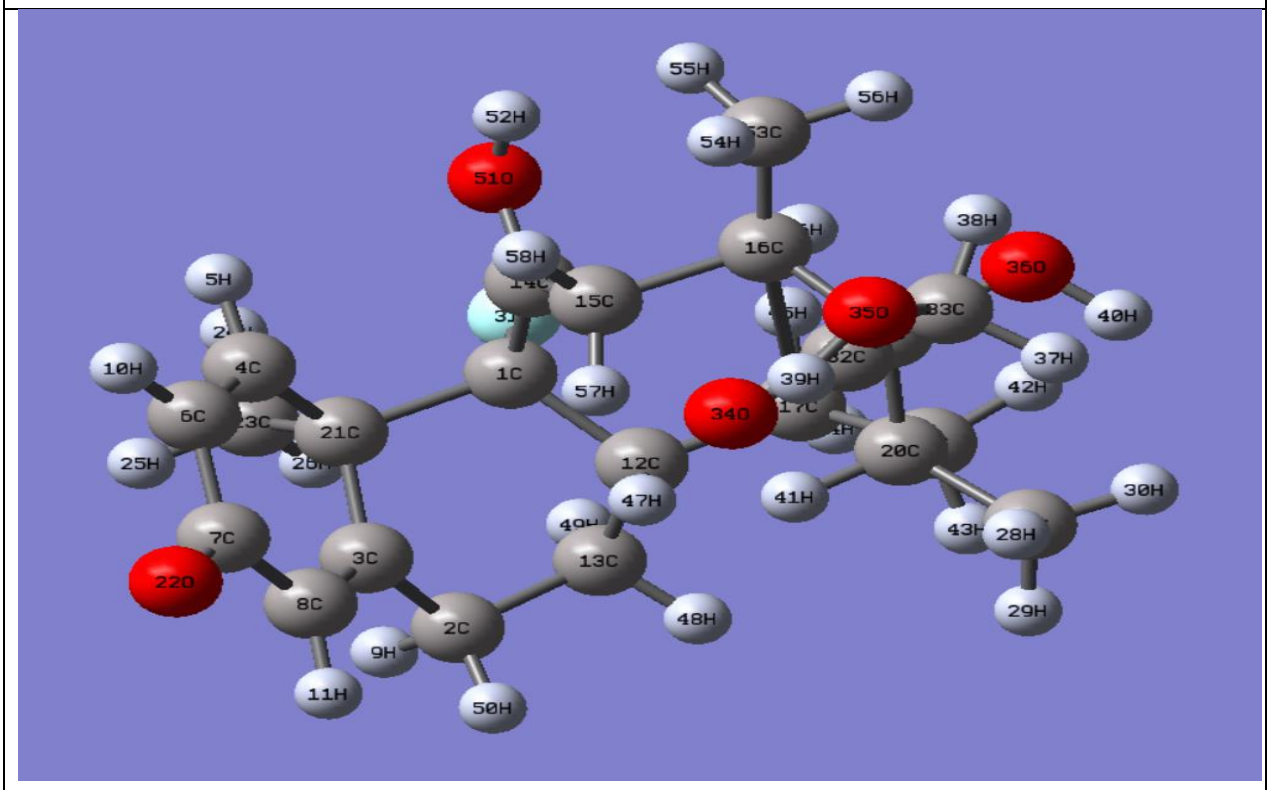

b-Geometry optimize

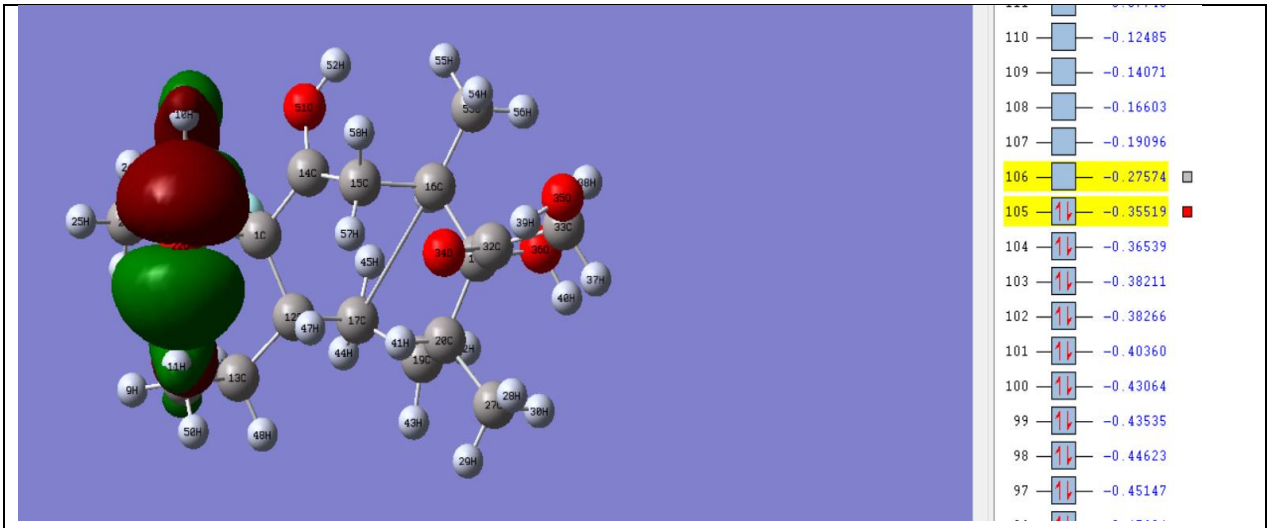

c-HOMO molecular orbital

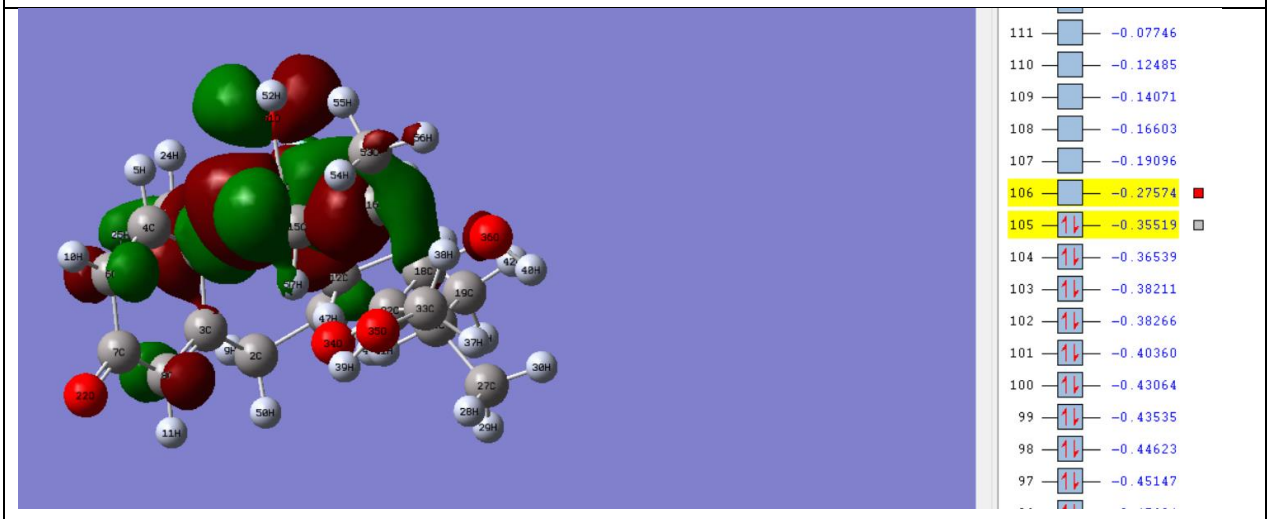

d-LUMO molecular orbital

Figure (3-1). Geometries optimized structure of betamethasone calculated by DFT (B_3LYP) method at Basis set (6-31G)

Band gap energy value is an important evaluative parameter for determination the molecular electrical transport properties. It is interpret the chemical reactivity and biological activity of chemical compounds due to changes in total dipole moment and changes in partial charge [118]. Table (3-1) shows the energetic properties of betamethasone, energy value of HOMO and LUMO orbitals are equal to -0.35519 and -0.27574 eV respectively. The energy gap of betamethasone compound is equal to 0.07945 eV. and that means lower electronic stability with higher chemical

reactivity[161]. Figure (3-2) shows Mulliken charges for the atoms of betamethasone molecule. The hydrogen atoms have a positive charge, while, the carbon; fluorine and oxygen atoms all have a significant negative charge.

Table (3-1). Energetic properties of betamethasone calculated by semi-empirical (PM3) and DFT(B3LYP) at basis sets(3-21G and 6-31G)

Energetic properties	DFT (B_3LYP) (3-21G)	DFT(B_3LYP) (6-31G)	Semi-empirical (PM_3)	Units
Total energy	-1324.772	-1331.652	-0.0737	a.u
RMS gradient	$1.3*10^{-6}$	$5.22*10^{-6}$	$4.92*10^{-6}$	a.u
Dipole moment	3.6073	6.6254	7.0428	Debye($kg.m^2$)
Energy of LUMO	-0.25580	-0.27574	-0.24376	e.V
Energy of HOMO	-0.34518	-0.35519	-0.48976	e.V
Energy gap	0.08938	0.07945	0.246	e.V
Time of calculation	5:20:17	4 :37:31	0:4:55	hr : min :sec

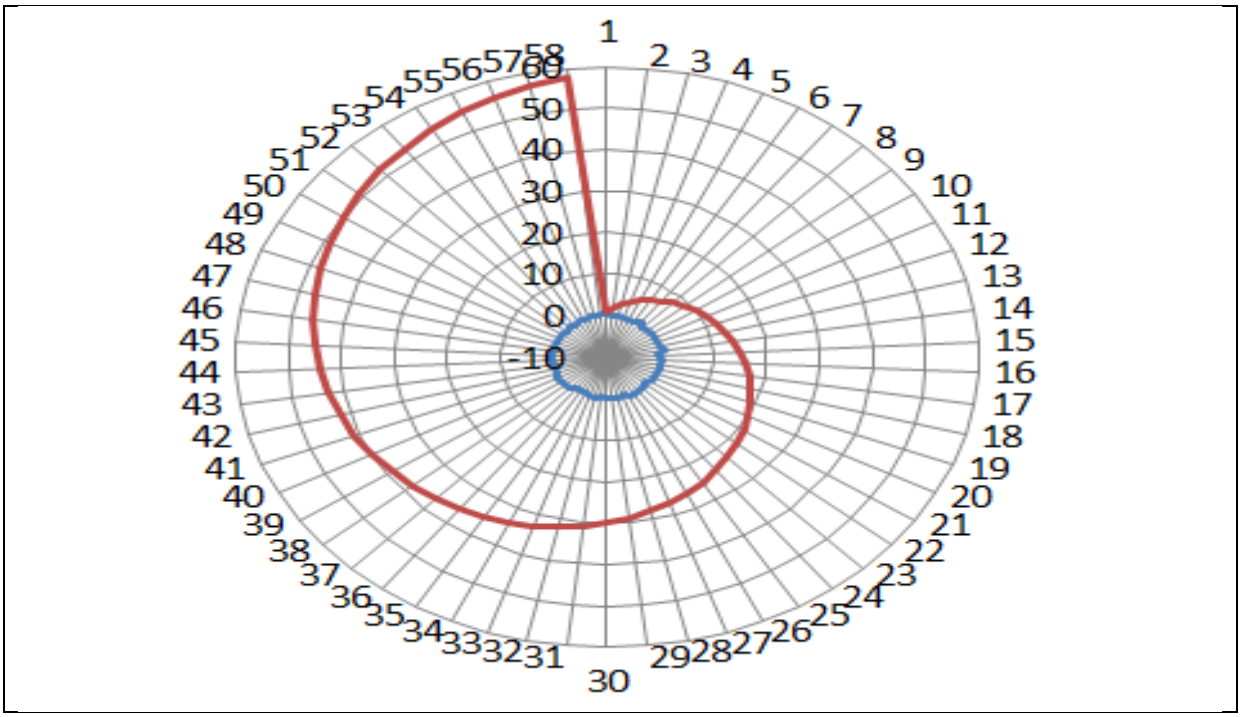

Figure(3-2). Mulliken charges for the atoms of betamethasone molecule calculated by DFT(B3LYP/6-31G) method

3-1-2 Estimation of chemical bonds

Structural properties such as bond lengths and bond angles of geometry optimized betamethasone compound have been estimated to determine the reactive chemical bonds of moiety, since the reactive bond is essential and very important in the chemical modulation of betamethasone moiety. Table(3-2) shows the chemical bonds of betamethasone. Bond lengths of betamethasone are ranged from 0.9 Å to 1.5 Å, while it was found that chemical bond R29 between carbon atom 16 and carbon atom 17 has a bond length equal to 2.7693 Å. This phenomenon gives an indication about this site is the lowest stability and its very reactive to chemical reaction than other chemical bonds. Other bonds such as R5, R10, R14, R24, R26, R30, R32, R37, and R44 have the same phenomena of length than other rest bonds. That's mean they found many active site on this molecule but the most probable site is R29. Figure (3-3) shows geometry optimization structure for Betamethasone.

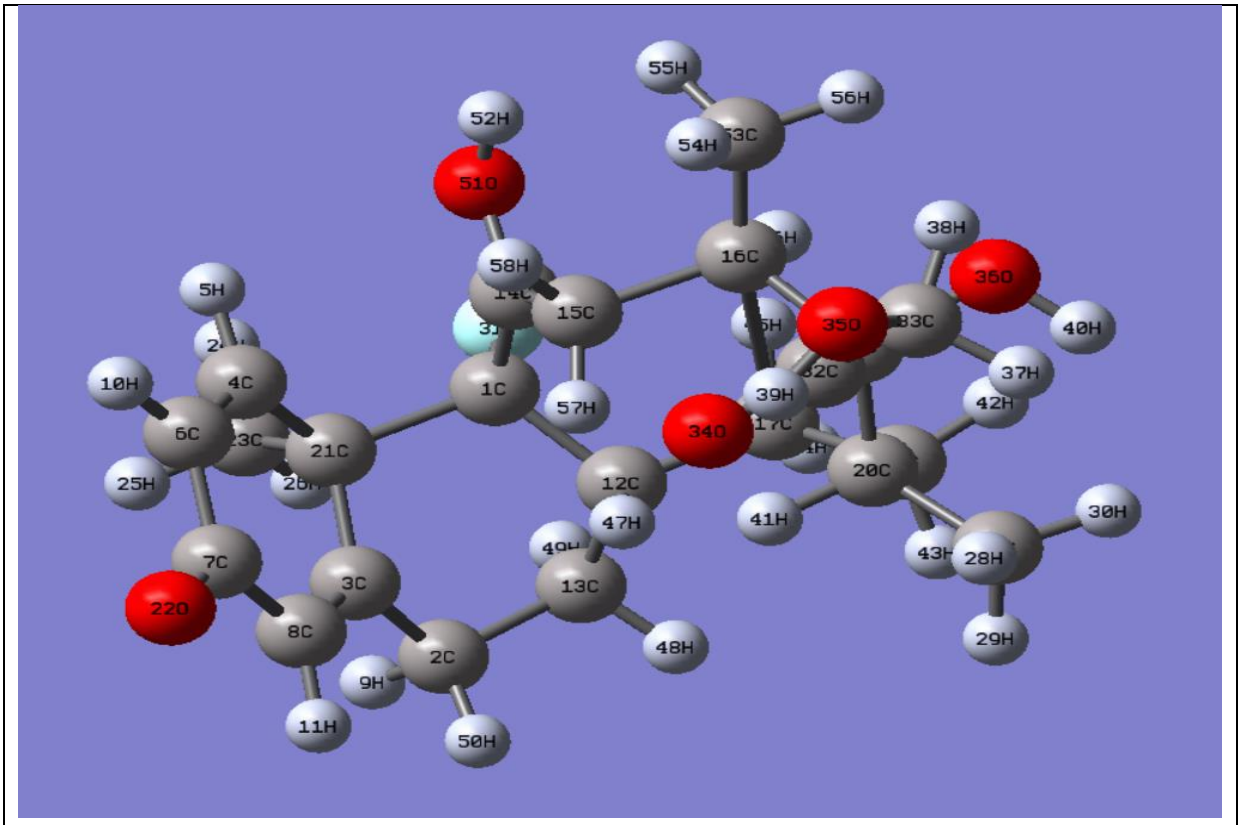

Geometry optimize

Figure (3-3).geometry optimization structure for Betamethasone

Table (3-2). Bond length estimation of Betamethasone, calculated by Semi-empirical (PM3) and DFT(B3LYP) methods at basis set (3-21G and 6-31G)

Chemical bonds	Semi-empirical	DFT(3-21G)	DFT(6-31G)
	Bond length Å	Bond length Å	Bond length Å
R1(C1-C12)	1.4768	1.5796	1.5796
R2(C1-C14)	1.5357	1.5716	1.5716
R3(C1-C21)	1.5468	1.5694	1.5694
R4(C1-F31)	1.3499	1.3716	1.3716
R5(C2-C3)	1.5465	1.5031	1.5031
R6(C2-H9)	1.0703	1.1116	1.1116
R7(C2-C13)	1.5316	1.5436	1.5436
R8(C2-H50)	1.0694	1.1125	1.1125
R9(C3=C8)	1.3262	1.3388	1.3388
R10(C3-C21)	1.5433	1.5406	1.5406
R11(C4-H5)	1.07	1.0863	1.0863
R12(C4=C6)	1.3735	1.334	1.334
R13(C4-C21)	1.5204	1.5193	1.5193
R14(C6-C7)	1.5714	1.5047	1.5047
R15(C6-H10)	1.0698	1.0933	1.0933
R16(C7-C8)	1.5425	1.4854	1.4854
R17(C7=O22)	1.2584	1.2051	1.2051
R18(C8-H11)	1.07	1.0941	1.0941
R19(C12-C13)	1.537	1.5291	1.5291
R20(C12-C17)	1.5064	1.5153	1.5153
R21(C12-H47)	1.07	1.1261	1.1261
R22(C13-H48)	1.0699	1.1105	1.1105
R23(C13-H49)	1.0693	1.1073	1.1073
R24(C14-C15)	1.5836	1.4795	1.4795
R25(C14-O51)	1.4297	1.2986	1.2986
R26(C15-C16)	1.5761	1.5813	1.5813
R27(C15-H57)	1.0692	1.1313	1.1313
R28(C15-H58)	1.0706	1.1175	1.1175
R29(C16-C17)	1.6113	2.7693	2.7693
R30(C16-C18)	1.5908	1.5891	1.5891
R31(C16-H49)	1.0699	1.1259	1.1259
R32(C16-C53)	1.5405	1.5258	1.5258
R33(C17-C19)	1.5258	1.5192	1.5192
R34(C17-H44)	1.07	1.1181	1.1181
R35(C17-H45)	1.0698	1.1311	1.1311
R36(C18-C20)	1.4958	1.5843	1.5843
R37(C18-C32)	1.5406	1.5609	1.5609
R38(C18-O36)	1.4296	1.4273	1.4273
R39(C19-C20)	1.4717	1.5612	1.5612
R40(C19-H42)	1.0699	1.1048	1.1048
R41(C19-H43)	1.0702	1.106	1.106
R42(C20-C27)	1.5412	1.5269	1.5269
R43(C20-H41)	1.0701	1.1264	1.1264

R44(C21-C23)	1.5402	1.5334	1.5334
R45(C23-H24)	1.0698	1.0956	1.0956
R46(C23-H25)	1.0702	1.1035	1.1035
R47(C23-H26)	1.07	1.0999	1.0999
R48(C27-H28)	1.0703	1.1071	1.1071
R49(C27-H29)	1.0697	1.0993	1.0993
R50(C27-H30)	1.0703	1.1011	1.1011
R51(C32-C33)	1.5399	1.526	1.526
R52(C32=O34)	1.2586	1.2103	1.2103
R53(C33-O35)	1.4303	1.4248	1.4248
R54(C33-H37)	1.0699	1.1129	1.1129
R55(C33-H38)	1.0702	1.1059	1.1059
R56(O35-H39)	0.96	0.9902	0.9902
R57(O36-H40)	0.9594	0.9989	0.9989
R58(O51-H52)	0.9601	1.0317	1.0317
R59(C53-H54)	1.0702	1.0969	1.0969
R60(C53-H55)	1.07	1.0934	1.0934
R61(C53-H56)	1.07	1.1113	1.1113

Table (3-3) shows measurements for bond angles of betamethasone compound. The bond angles of the Betamethasone molecule are ranged from 60^{o} into 120^{o}. The bond angle of A59 that has formed by carbon atom 12, carbon atom 17 and carbon atom 19 is equal to 133.5942^{o}. Its first indication about the carbon atom 17 is a very active site towards chemical reaction due to its position in the betamethasone molecule and it may useful for any desired substitution reaction to getting on any new derivatives for betamethasone, same thing may occurs on A24 and A26 [162].

Table(3-3). Bond angle estimation of Betamethasone compound calculated by Semi-empirical(PM3) and DFT(B3LYP) methods at basis set (3-21G and 6-31G)

Bond angles	Semi-empirical(PM3)	DFT(3-21G)	DFT (6-31G)
	Degree	Degree	Degree
A1(C12-C1-C14)	106.9687	117.7737	117.7737
A2(C12-C1-C21)	113.1894	108.5048	108.5048
A3(C12-C1-F31)	107.6194	108.829	108.829
A4(C14-C1-C21)	111.3372	114.1949	114.1949
A5(C14-C1-F31)	109.781	97.341	97.341
A6(C21-C1-F31)	107.8637	109.3823	109.3823
A7(C3-C2-H9)	110.5279	110.0745	110.0745
A8(C3-C2-C13)	111.9651	111.6591	111.6591
A9(C3-C2-H50)	106.9119	110.7698	110.7698
A10(H9-C2-C13)	109.8021	110.6216	110.6216
A11(H9-C2-H50)	109.856	104.0462	104.0462
A12(C13-C2-H50)	107.6851	109.4116	109.4116
A13(C2-C3=C8)	120.0525	122.6114	122.6114
A14(C2-C3-C21)	123.0254	117.118	117.118
A15(C8=C3-C21)	116.7636	120.2584	120.2584
A16(H5-C4=C6)	122.8244	121.1532	121.1532
A17(H5-C4-C21)	122.9795	117.0099	117.0099
A18(C6=C4-C21)	114.1132	121.6851	121.6851
A19(C4=C6-C7)	119.3864	121.1495	121.1495
A20(C4=C6-H10)	120.2757	123.8207	123.8207
A21(C7-C6-H10)	120.3282	115.0263	115.0263
A22(C6-C7-C8)	117.173	113.7705	113.7705
A23(C6-C7=O22)	121.4303	122.0378	122.0378
A24(C8-C7=O22)	121.3567	124.1832	124.1832
A25(C3=C8-C7)	111.8148	122.2718	122.2718
A26(C3=C8-H11)	124.2575	123.1292	123.1292
A27(C7-C8-H11)	123.8219	114.5922	114.5922
A28(C1-C12-C13)	106.5363	108.5522	108.5522
A59(C12-C17-C19)	111.9438	133.5942	133.5942

3-1-3 Potential energy surface

Potential energy surface has been done in two dimension to get on curve for chemical bond dissociation. It is helpful method to estimate the energetic stability of the reactive chemical bonds of betamethasone. The equilibrium energy and the dissociation energy value required to break down a bond (the weakest bond) were determined [163], [164]. Table (3-4) shows a comparative

of energetic values between the reactivity (stability) of chemical bond of betamethasone compound. The bonds C_8-C_{28} and C23-C25 were lower stable bonds than others with 0.77 and 2.99 kcal/mol respectively of the dissociation energy values, while the bonds of O_{24}-H_{51} and C_{23}=O_4 were higher stable with 169.29 and 169.43 kcal/mol respectively of the dissociation energy values than other bonds. Other chemical bonds also have lowest stability, such as O_5-H_{30} and C_{27}-O_2 with 33.35 and 26.09 kcal/mole respectively, they are also reactive bond but with lowest probability.

Figure (3- 5) shows the reactive chemical bonds which have been determined on betamethasone. The chemical bonds of C_8-C_{28}, C_{23}-C_{25}, C_{27}-O_2 and O_5-H_{30} were appeared in red colour line to signify their chemical reactivity than other bonds. The bonds of O_{24}-H_{51} and C_{23}=O_4 have been appeared in yellow colour line to signify their higher chemical stability than other bonds.

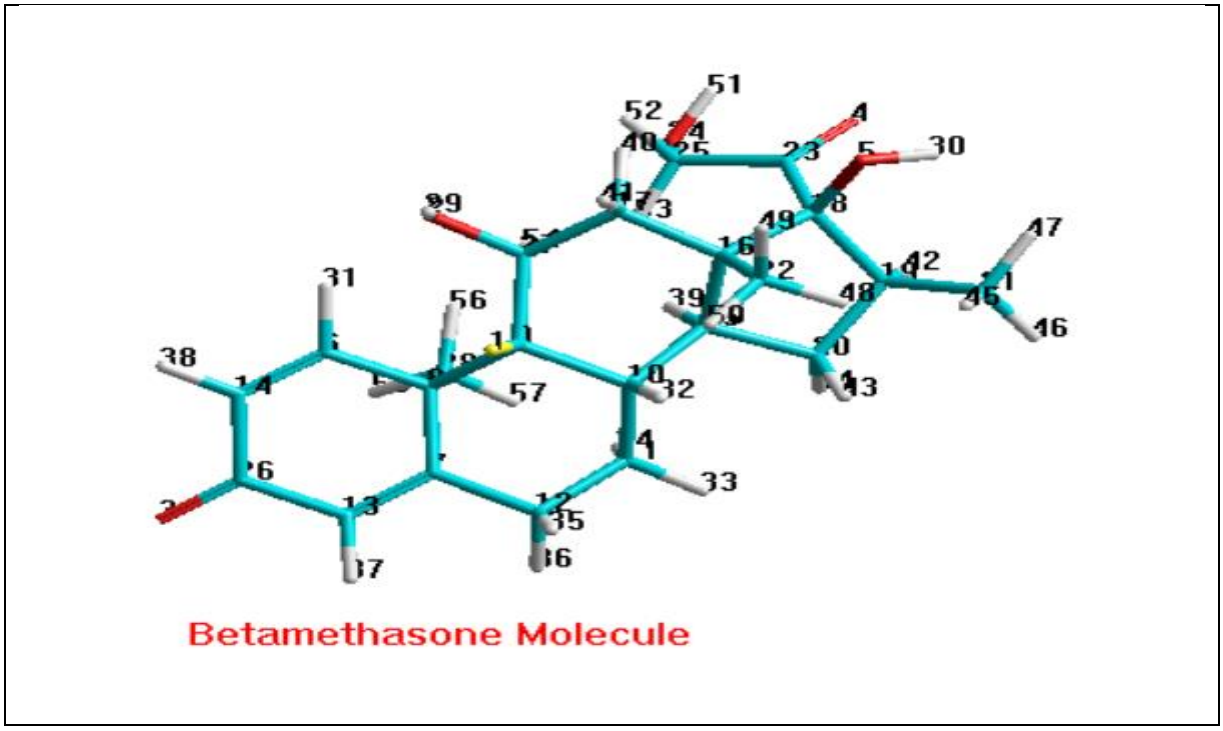

Figure(3-4).Geometry optimization structure for Betamethasone in Hyperchem

Table (3-4).Energetic values of chemical bonds stability of betamethasone

Chemical bonds	Equilibrium length Å	Equilibrium Energy kCal/mol	Dissociation length Å	Dissociation Energy kCal/mol	Energy difference kCal/mol
C26=O3	1.02	-5759.81	2.42	-5618.69	141.12
C14-H38	1.12	-5824.05	2.62	-5664.21	159.84
C13-H37	1.12	-5824.09	2.62	-5664.63	159.45
C8-C28	1.22	-5749.63	2.32	-5748.86	0.77
O5-H30	2.36	-5677.45	2.96	-5644.10	33.35
C9-F1	1.22	-5802.58	2.42	-5702.93	99.65
C27-O2	1.12	-5745.15	2.32	-5719.06	26.09
O2-H29	0.92	-5823.56	2.62	-5654.29	169.27
C17-H40	1.12	-5824.23	2.62	-5684.27	139.96
C17-H41	1.12	-5824.22	2.62	-5677.58	146.64
C18-C23	1.56	-5824.24	2.96	-5720.45	103.79
C18-O5	1.46	-5823.35	2.96	-5674.32	149.03
C23=O4	1.02	-5759.19	2.42	-5589.76	196.43
O24-H51	0.92	-5823.58	2.62	-5654.29	169.29
C23-C25	1.22	-5758.79	2.32	-5755.80	2.99
C23-O24	1.12	-5750.36	2.32	-5711.09	39.27
C25-H52	1.12	-5824.23	2.62	-5687.50	136.73
C25-H53	1.12	-5824.23	2.62	-5693.59	130.64
C19-C21	1.22	-5757.99	2.32	-5741.55	16.44
C19-H42	1.12	-5824.24	2.62	-5678.88	145.36
C21-H47	1.10	-5824.23	2.50	-5681.69	142.54
C21-H46	1.10	-5824.23	2.50	-5677.82	146.41
C21-H45	1.10	-5824.24	2.50	-5685.67	138.57
C20-H43	1.10	-5824.23	2.50	-5684.18	140.05
C20-H44	1.10	-5824.24	2.50	-5682.01	142.23
C10-H32	1.13	-5824.24	2.62	-5686.38	137.86
C11-H33	1.13	-5824.23	2.63	-5675.80	148.33
C11-H34	1.13	-5824.17	2.63	-5682.62	141.55
C12-H35	1.13	-5824.14	2.63	-5678.73	145.41
C12-H36	1.13	-5824.12	2.63	-5676.55	147.57
C6-H31	1.11	-5824.24	2.51	-5688.26	135.98
C28-H55	1.12	-5824.06	2.62	-5676.62	147.44
C28-H56	1.12	-5824.14	2.62	-5684.43	139.71
C28-H57	1.12	-5824.11	2.62	-5686.35	137.76
C27-H54	1.12	-5824.23	2.62	-5693.64	130.59
C16-C22	1.11	-5662.13	2.12	-5773.71	111.58
C22-H48	1.11	-5824.22	2.51	-5693.18	131.04
C22-H49	1.11	-5824.18	2.51	-5678.01	146.17
C22-H50	1.11	-5824.22	2.51	-5684.60	139.62

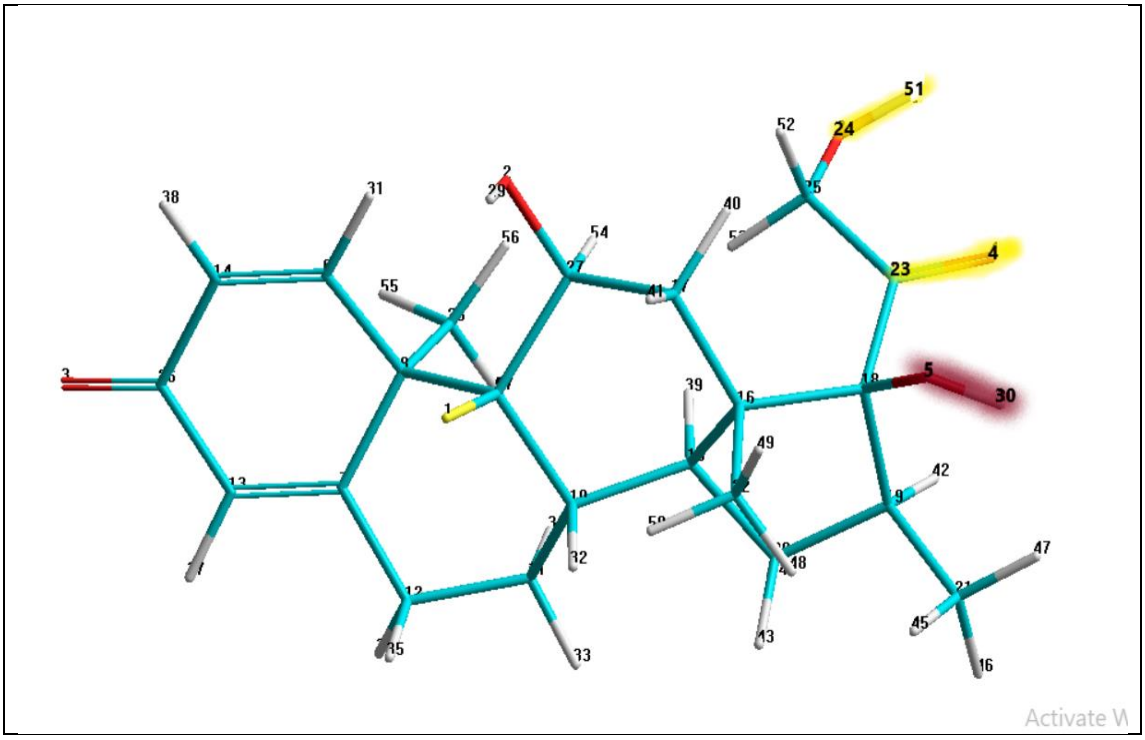

Figure (3-5). Most probable reactive chemical bonds of Betamethasone

Two-dimensions curve of potential energy is estimated for the most chemical bonds of betamethasone. Figure (3-6) illustrates the potential energy stability of bonds onto Betamethasone, the stability energy curve of bond such as C_8-C_{28} is broken down at 2.32 Å(-5748.86 kCal/mol) while the bond O_{24}-H_{51} is broken down at 2.62Å(-5654.29 kCal/mol) these values are closer the experimental values[165].

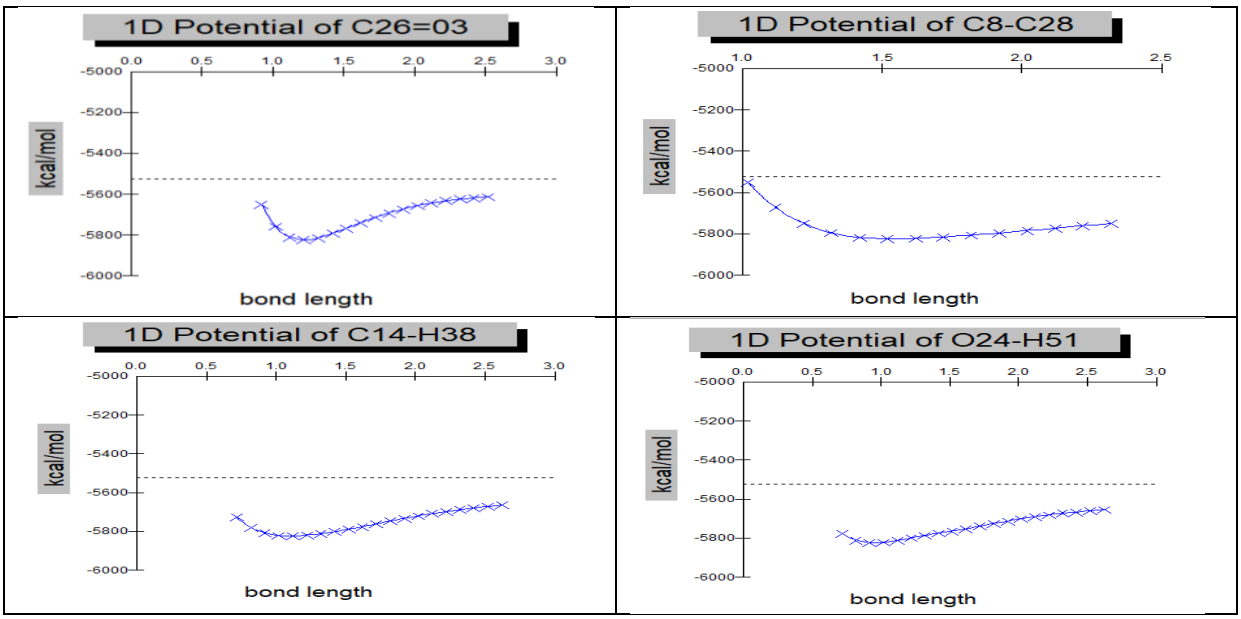

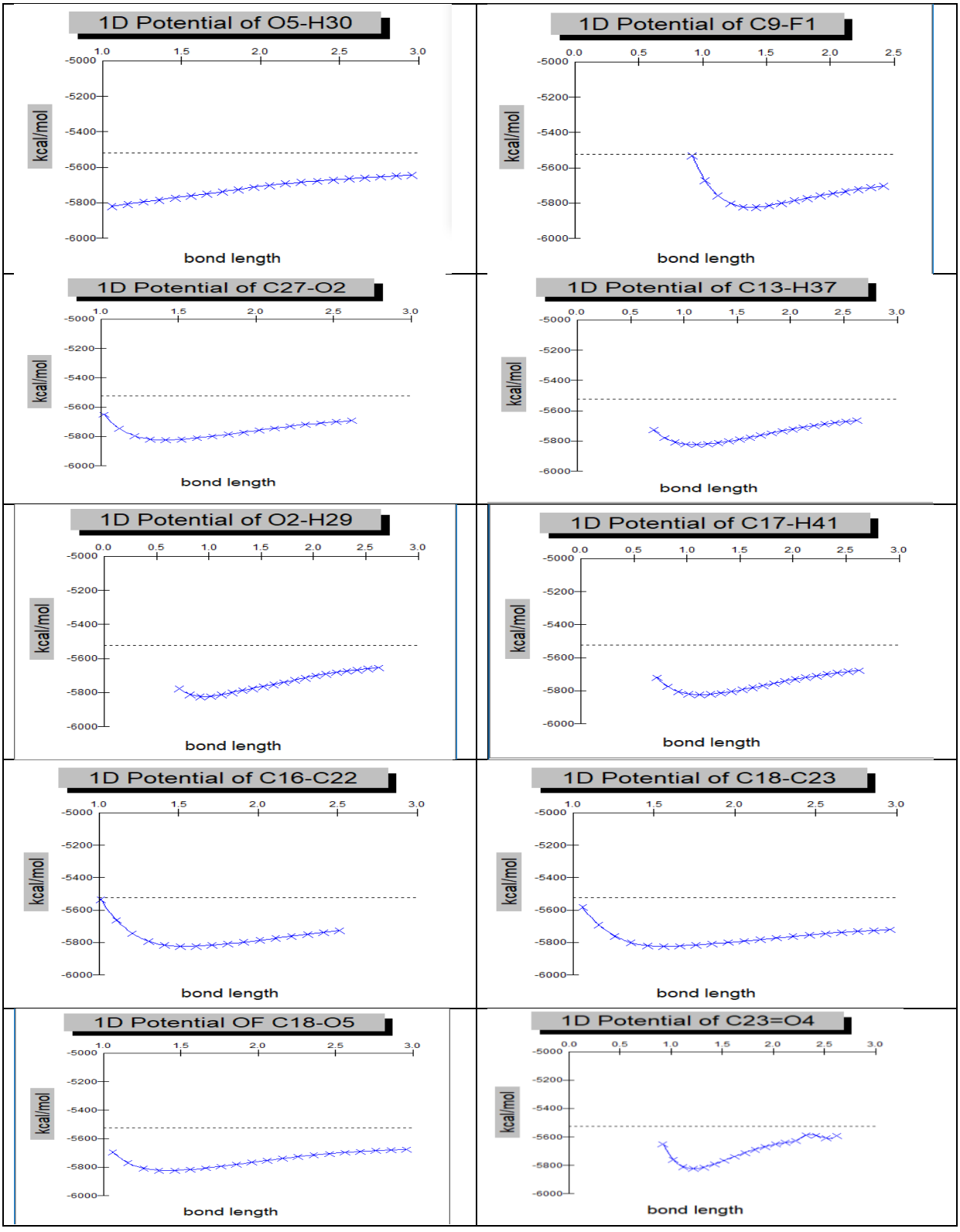
1D Potential of O5-H30
kcal/mol
bond length
1D Potential of C9-F1
kcal/mol
bond length
1D Potential of C27-O2
kcal/mol
bond length
1D Potential of C13-H37
kcal/mol
bond length
1D Potential of O2-H29
kcal/mol
bond length
1D Potential of C17-H41
kcal/mol
bond length
1D Potential of C16-C22
kcal/mol
bond length
1D Potential of C18-C23
kcal/mol
bond length
1D Potential OF C18-O5
kcal/mol
bond length
1D Potential of C23=O4
kcal/mol
bond length

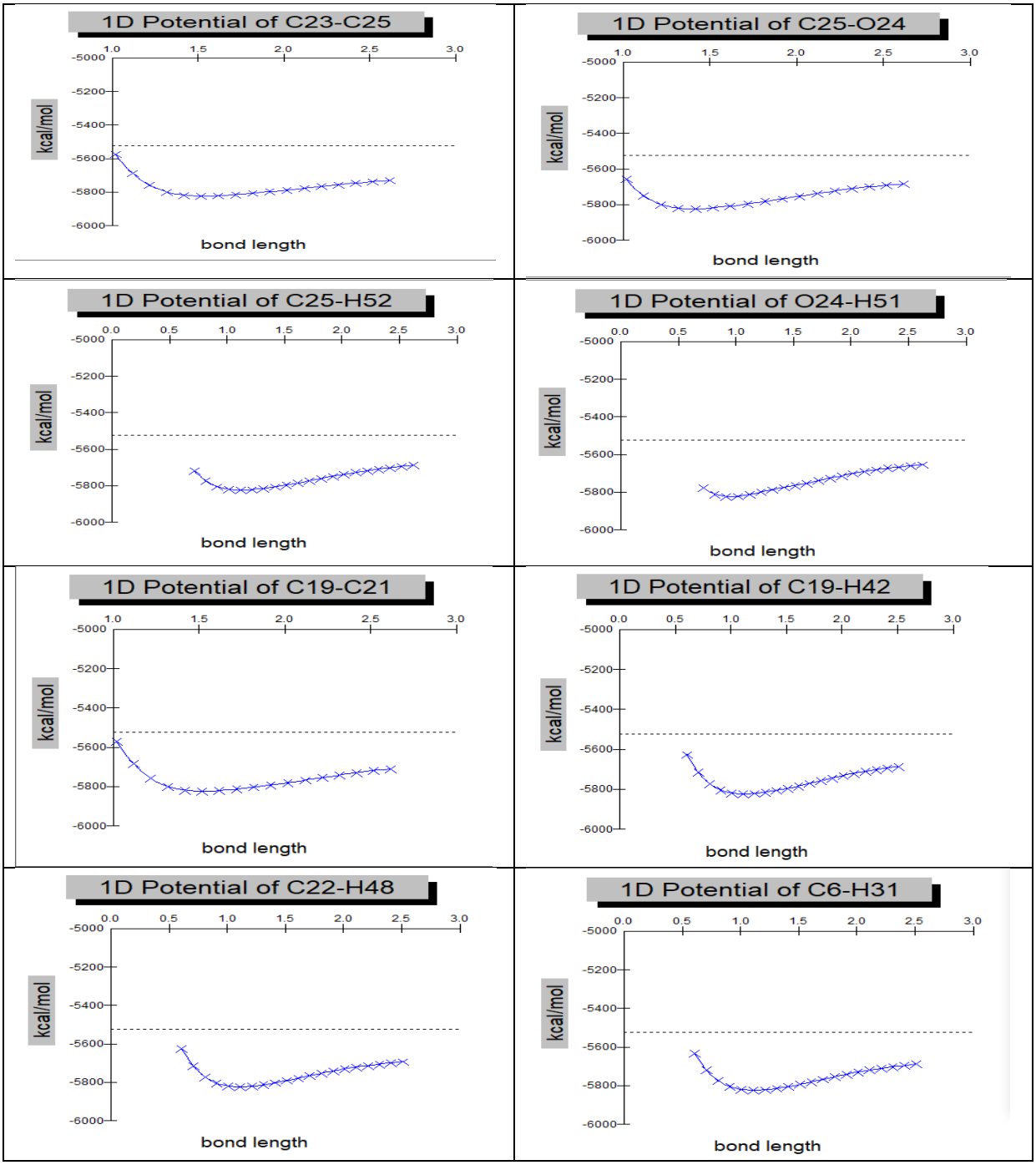

Figure (3-6).Comparative of potential energy stability curve for bond lengths of betamethasone compound calculated at semi-6empirical(PM_3)method

3-2 Molecular Spectrum Identification

Molecular spectrum identification is important tool to improve the actual real chemical structure of betamethasone drug because the manufactured companies may produce the same trade drugs with modified structures, with an additives structure or in different manner. Simulation of molecular spectrum and comparative with the experimental spectrum give a clear view of chemical structure to find a good way of modulation for chemical drugs.

3-2-1 Vibration spectrum

Infrared spectrum of betamethasone has been estimated with range of (4000 - 400 cm^{-1}) as well as for theoretical and experimental to get the comparative investigation in vibrational. Infrared spectrum is frequently used to demonstrate the existence or absence of functional groups with certain vibration frequencies, such as (C-O), (N-H), (O-H), (C-H), and so on [166]. Figure (3-7) shows a comparative between theoretical spectrum and experimental spectrum for betamethasone, which found closer in the vibrational transition.

Table (3-5) shows the comparative of transition frequencies of the betamethasone, since theoretical transitions and experimental transitions are closer from each other. Stretching and bending vibration of bonds (C-C, C=C, C-H, O-H, C-O, C=O) are closely for the two measurements. The main theoretical signal stretching vibration of C-H bond occurs at 3146.83-2964.94cm^{-1} but the experimental value at 3441.12 cm^{-1} due to some effected factors. Theoretical C_{16}-H_{46} bending and C_{20}-H_{41} bending modes observed in the 1351.09cm^{-1}, are a good agreement with the experimental value that's is equal to 1365.65 cm^{-1}[167].The modes are in the range(1507.86-323.01cm^{-1}) due to O-H bending vibration while the experimental value is equal to 1448.59cm^{-1}. The peaks in the range of less than 900 cm^{-1} lead to bending vibrations of C-O and C-C. The modes in the range (3018.44-945.29 cm^{-1}) due to C=C bending while the range (1977.66-1963.58 cm^{-}1) due to C=O stretching and C=O bending at 323.01 cm^{-1} .

The bond C=C is stretching between (1722.04-1670.17 cm^{-1}) and it is bending between (954.73-725.82 cm^{-1}) and the experimental value equal to 964.44cm^{-1} [168], C-O bending in the range (1506.73-1385.41cm^{-1}) while the bond C=O is stretching in the range(1722.04-1667.16 cm^{-1}). The bond O-H is stretching between (3658.03-3539.52 cm^{-1}). Vibration transitions at different levels of calculation give identical parameters for a functional group of drugs comparatively with practical data[169] .

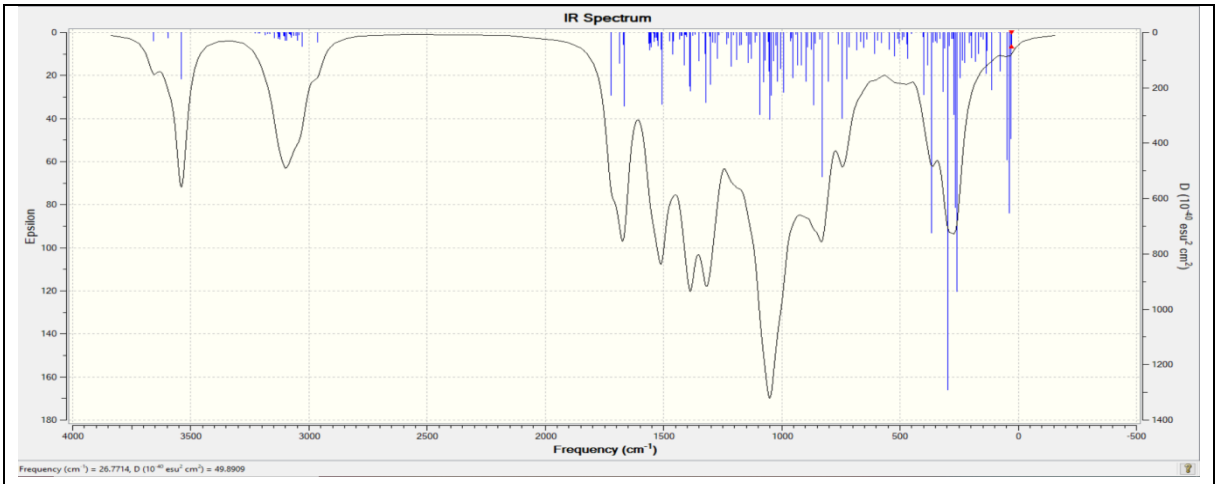

A-Theoretical vibration spectrum

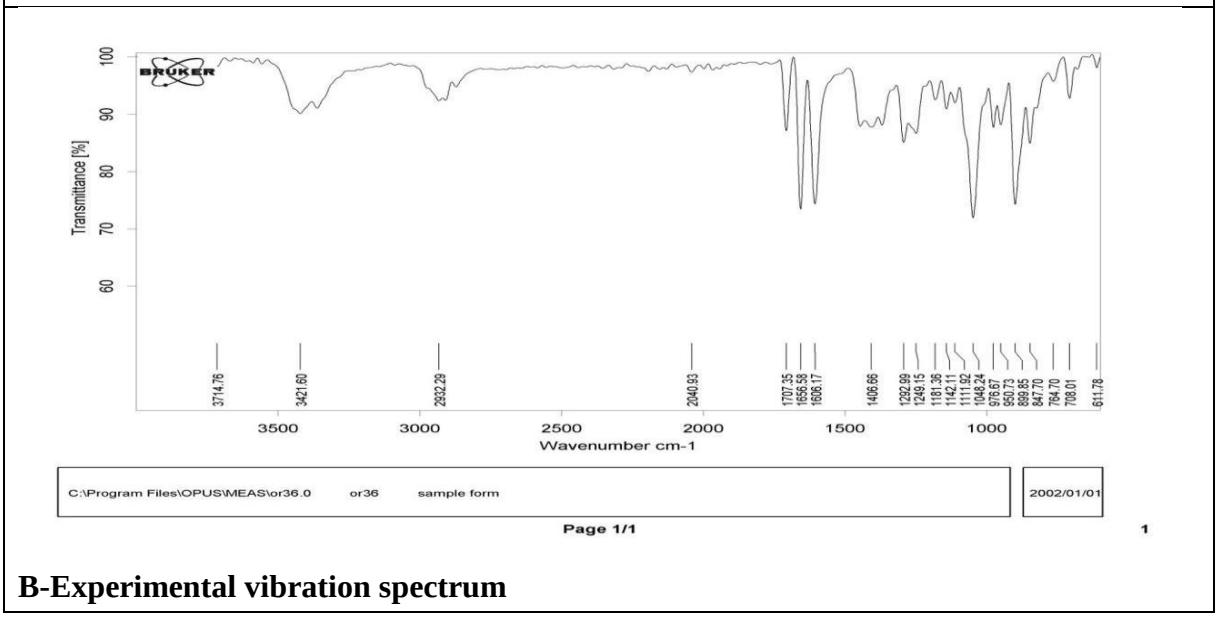

B-Experimental vibration spectrum

Figure (3-7). Comparative of Infrared spectrum of betamethasone

A-Theoretical vibration spectrum. DFT(B_3LYP) at basis set(6-31G) .

B-Experimental vibration spectrum.

Table(3-5).Vibrational frequencies of betamethasone compound calculated at DFT(B3LYP)at basis set(6-31G).

NO. mode	Theoretical		Description	Experimental
	Frequency cm^{-1}	Intensity $Km.mol^{-1}$		Frequency cm^{-1}
54	725.82	30.4826	O51-H52 bend and C4=C6 bend	707.90
64	898.94	39.8242	C2-H9 bend and C8-H11 bend	896.93
65	917.84	27.1181	C53-H55 bend and O36-H40 bend	---
66	932.69	27.6058	C27-H28 bend and C27-H30 bend	947.08
68	954.73	39.1511	C6=C4 bend and C8-H11 bend	964.44
74	1019.48	45.1571	C23-H24 end, C23-H26 bend	---
78	1052.60	82.7539	C33-O35 str. and O35-H39 bend	1049.31
79	1054.87	36.7710	C21-C23 str. Out ring, O51-H52 bend	1049.31
86	1129.45	26.7324	C53-H55 bend and C53-H56 bend	1112.96
88	1142.96	30.9628	C23-H25 bend,C23-H24 bend, O51-H52 bend	1138.04
92	1189.99	29.5963	C6-H10b, C4-H5b	1180.47
94	1213.85	36.9149	C33-H37 bend,C33-H38 bend, O35-H39 bend	1257.63
101	1302.19	60.9075	C15-H57 bend and C15-H58 bend	1294.28
104	1323.74	24.9946	C7-C8 str. in-ring and C7-C6 str. in ring	-------
107	1351.09	34.4935	C16-H46 bend and C20-H41 bend	1365.65
110	1385.41	73.6679	C12-H47 bend,C13H48 bend, C14-O51 bend, and O51-H52 bend	-----
115	1413.18	41.6551	O35-H39 bend,C33-H37 bend, C33-H38 bend	1404.22
120	1461.26	29.1201	C53-H54 bend,C53-H55 bend, C53-H56 bend	1448.59
122	1506.73	98.0277	C14-C15 bend,C15-H57 bend, C14-O51 bend, and O51-H52 bend	-------
135	1667.16	110.8066	C4-H5 bend, C4=C6 str.in ring, C6-C7 bend, C7=O27str. Out ring	1608.09
136	1670.17	18.5432	C3=C8str in ring, C4=C6 str. In ring, C7-O22 str. Out ring , and C7-C8 bend	1660.77
137	1685.92	46.6062	C32=O34 str. andC32-C18 bend	1710.92
138	1722.04	97.9514	C7=O22 str. out ring, C8=C3 str.in ring, C6=4 str. in ring, C4-H10 bend, and C8-H11 bend	-------
139	2964.94	26.0839	C33-H37str. And C33-H38 bend,	2943.47
158	3146.83	15.3214	C27-H28 str., and C27-H29 str.	------
166	3539.52	148.9455	O51-H52 str.	3441.12
168	3658.03	28.7463	O36-H40 str.	-------

3-2-2 Electronic transition

The absorption spectrum of electronic transitions is recorded in the range (200-800 nm) and is separated into two regions: Ultraviolet region (190-400 nm) and visible region (400-800 nm)[170]. Theoretical UV-visible spectrum of betamethasone has been compared with experimental UV-visible spectrum of betamethasone as shown in Figure (3-8). Both the theoretical and experimental electronic spectrum are consisted from two band. The first band occur at wavelength equal to 532 nm refers to the n—π^* transition of the non-bonding electrons of the carbonyl group and other functional group in the compound. The second band occur at 715 nm appears as a tail on the shoulder of 532 nm peak a band. However it´s not pronounced due to the weaker of the absorption band caused by the red shift created by high electron density between the atoms[171], [172].other transitions may occurs but with low intensity such as π-π^* transitions. Electronic absorption spectrum of betamethasone compound illustrate in the table (3-6).There are an agreement between theoretical and experimental data. Figure(3-8) shows the Experimental and Theoretical spectrum of Betamethasone compound.

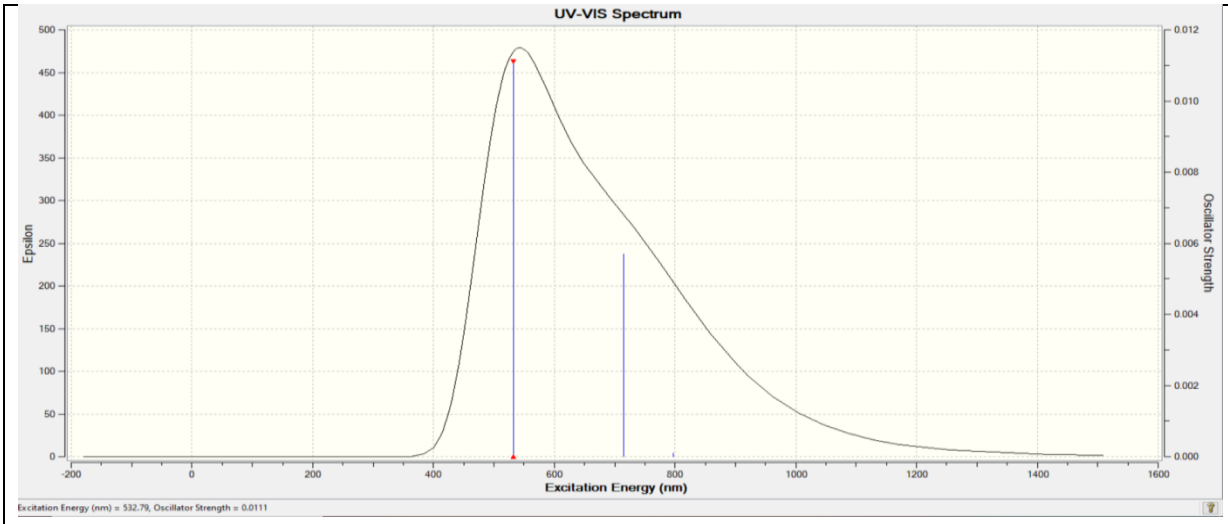

A- Theoretical spectrum

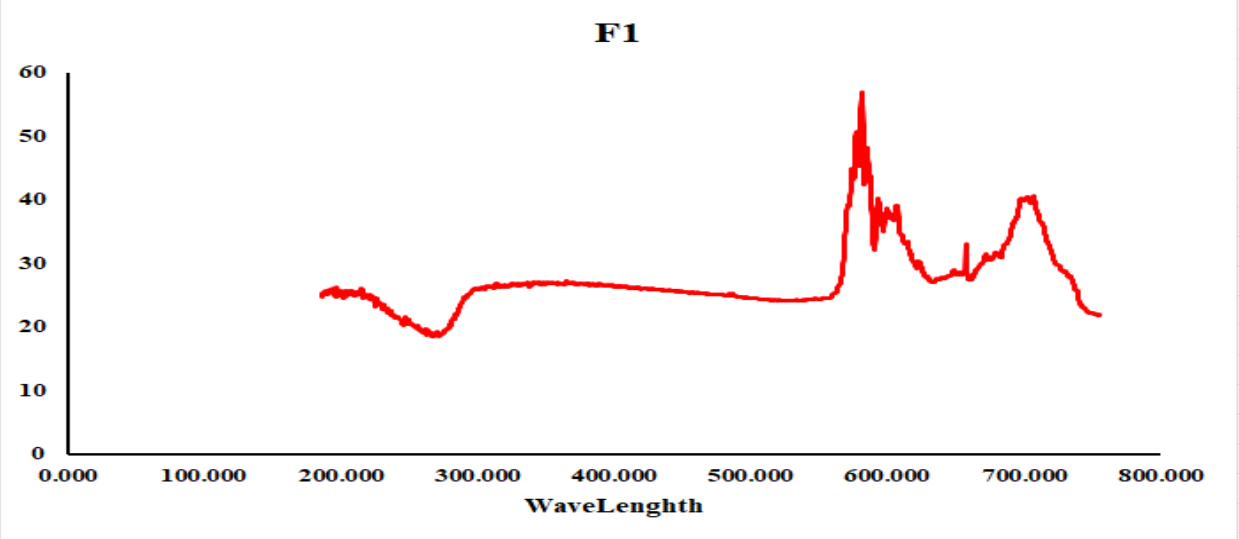

B-Experimental spectrum

Figure (3-8). Absorption spectrum of electronic transitions for betamethasone by DFT(B3LYP)/(6-31G) . A-Theoretical spectrum calculated

B- Experimental spectrum.

Table(3-6). Electronic absorption spectrum of Betamethasone compound calculated by DFT(B3LYP)method at basis set(6-31G) in vacuum

Wave length Experimental nm	Wave length Theoretical nm	Excitation energy eV	Corresponding Transition orbitals	Oscillator Strength(f)	Transition Type
-	796	1.556	(105-106) 0.706	0.0001	n—π*
720	715	1.733	(104-106) 0.703	0.0057	n—π*
580	532	2.327	(101-106) 0.109	0.0111	n—π*

3-2-3 Mass spectroscopy

Mass spectrometry is a destructive way for determining molecular weight and obtaining information about molecular structure which sets it apart from other ways, The material is ionised and not subject to electromagnetic radiation. Fragmentation occurs when ionized molecules are stimulated[173]. The mass spectrum of betamethasone was studied and Figure(3-6) illustrates appearance of the molecular ion equal to 392.3 g/mol which confirms the validity of the molecular structure of this drug. The mass spectrum also showed many fragments due to the dissociation of that drug. It was also noted that the relative abundance of the apparent fragments was acceptable. According to mass spectrum, Scheme (3-1)is represented the suggested fragmentation mechanism for betamethasone depending on the peaks values of radical's moieties. Summation of molecular weight of all species show that the molecular weight of betamethasone is 392.3 g/mol. Losing of fragments occurs gradually and by combination all these species can be now the fundamental structure it is identify with our theoretical mimic structure of betamethasone or not. This process will achieved later by improving the calculations on the pathway of betamethasone synthesis.

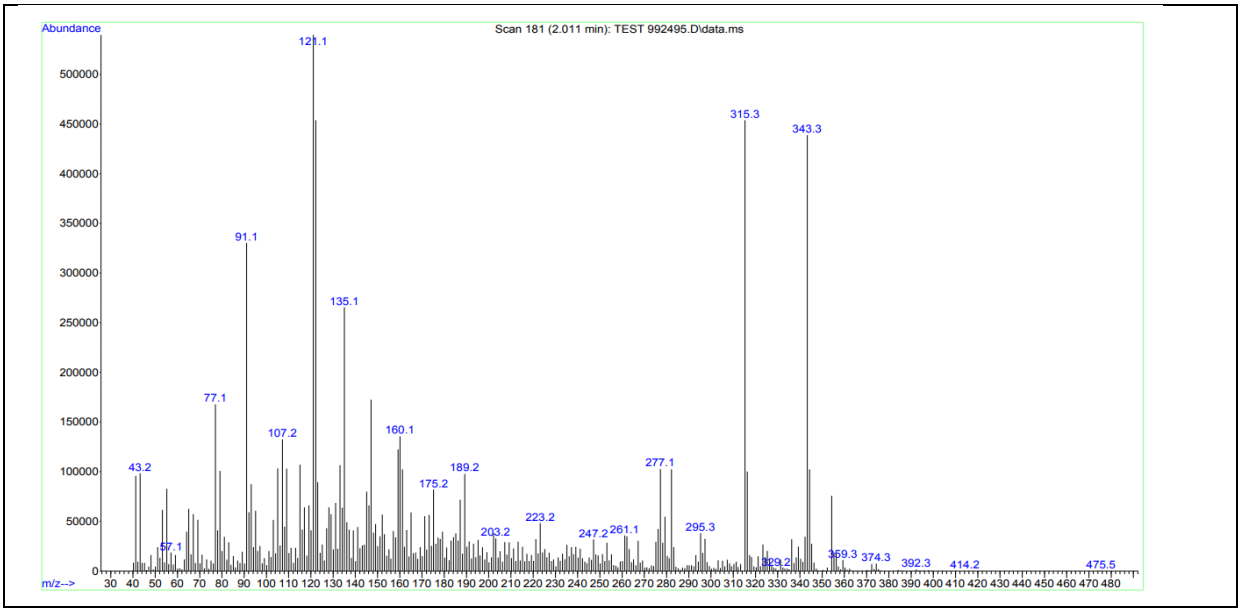

Figure (3-9). Experimental spectrum of Betamethasone compound

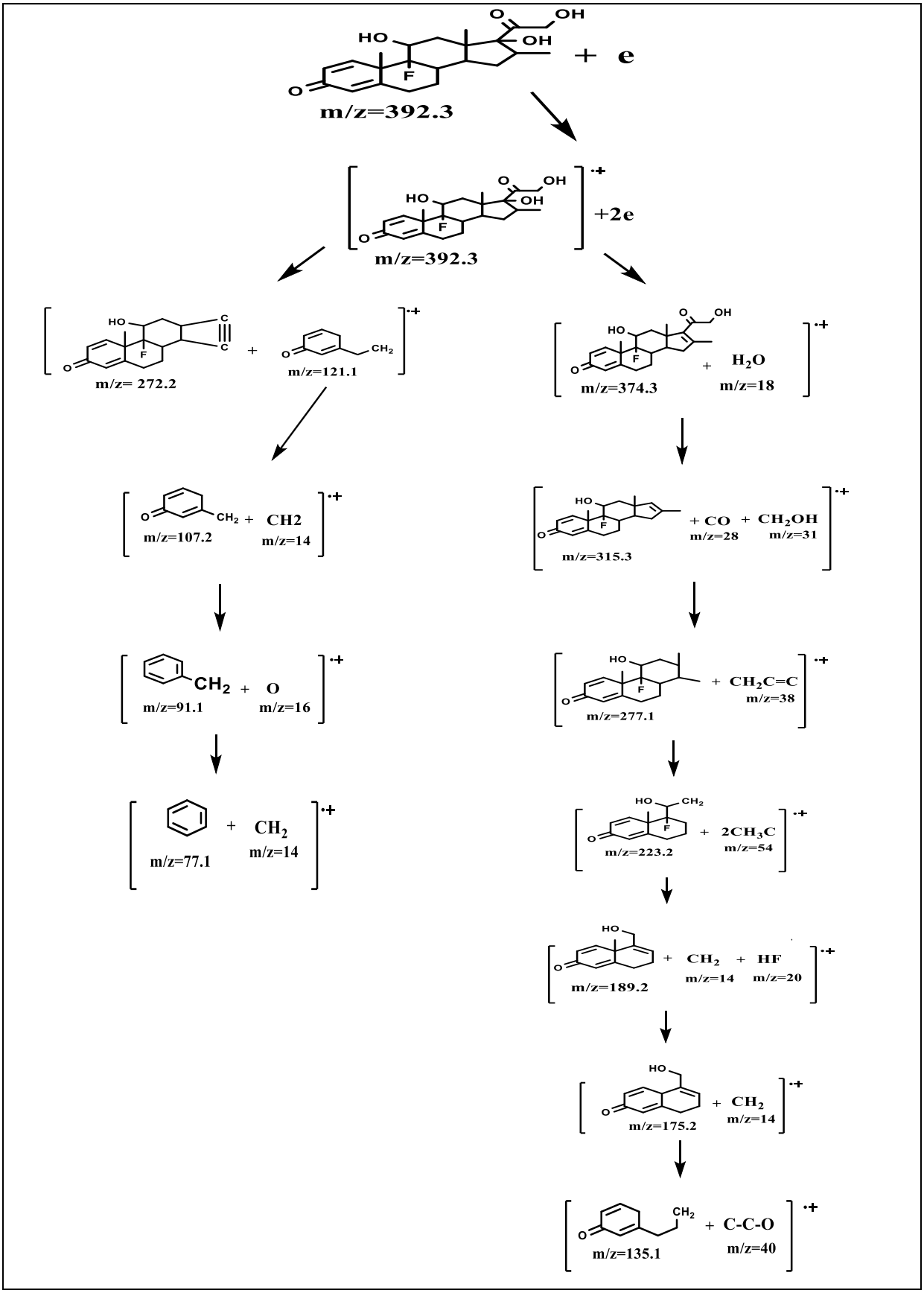

Scheme(3-1). Proposed mechanism of mass fragmentation pathways for Betamethasone molecule

3-3 Thermodynamic Investigation

Thermodynamics function determination is a good tool to understanding the chemical reaction of compound formation. Applying Hess's law of thermal constant summation gives clear idea about the nature and behaviour of chemical reactants through the pathway of compound formation rather than the controlling transition state of the reaction.

3-3-1 Transition states investigation

Four transition states of betamethasone molecule are suggested as represented in Figure (3-10).According to their energetic properties, one of these transition states is most probable for giving the actual path way of betamethasone formation reaction.

Table (3-7) shows energetic properties of proposed transition states of betamethasone formation. From these results ,it can be seen that TS2 is most probable than other transition states due to has the highest of zero-point energy equal to 341.874 kCal/mol and the first imaginary frequency was negative. This meaning TS2 needed to lowest value of activation energy(E_b) for giving the actual path way of Betamethasone formation reaction[174].

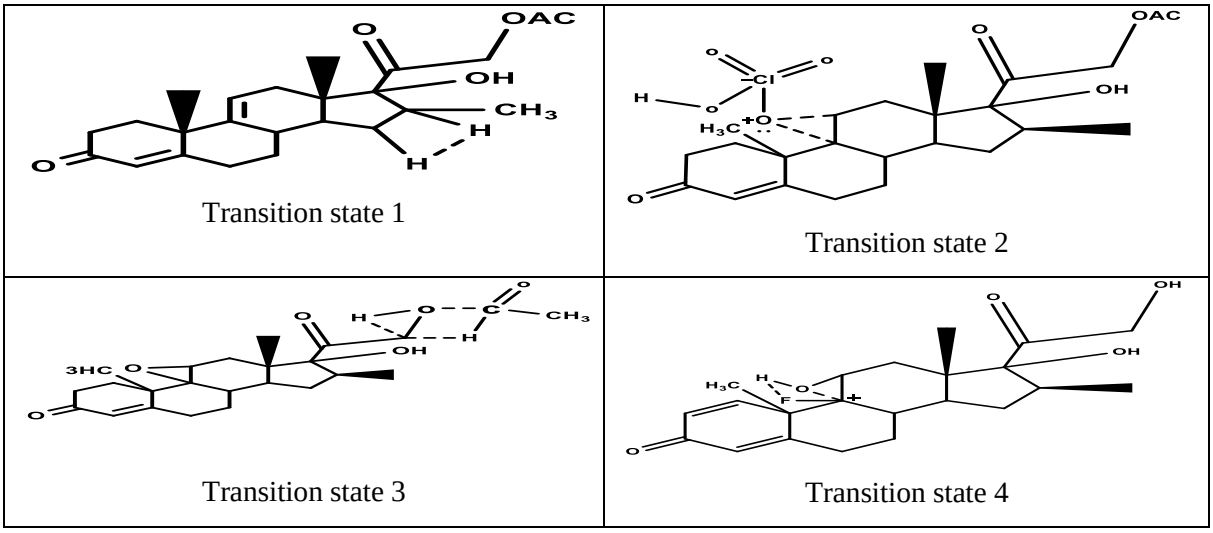

Figure(3-10). Proposed transition states of betamethasone calculated at semi-empirical(PM3) method

Table(3-7).Energetic properties of transition states of Betamethasone

Energetic properties	TS1	TS2	TS3	TS4
Total energy*	-110833.639	-145411.769	-117022.737	-114010.084
Heat of formation*	-195.593	-194.144	347.382	203.765
Zero-point energy*	319.499	341.874	313.687	295.546
Imaginary frequency*	-	-	-	-

*kCal/mol unit.

3-3-2 Chemical Reaction Formation for Betamethasone

Synthesis of glucocorticoids have been carried out by using e 9α-hydroxyandrost-4-ene-3,17-one (9αOH-AD) and 4-ene-3,17-dione (4-AD) readily[175], since use of (9α OH-AD) as a starting material[176]. Figure (3-11). Shows the optimized geometries structures of the reaction component, that's expressed by full IUPAC name and coded names. Energetic parameters and imaginary frequency of betamethasone reaction components are listed in Table(3-8), since the imaginary frequency values estimate the nature of reactant component whether is transition component or stable component .

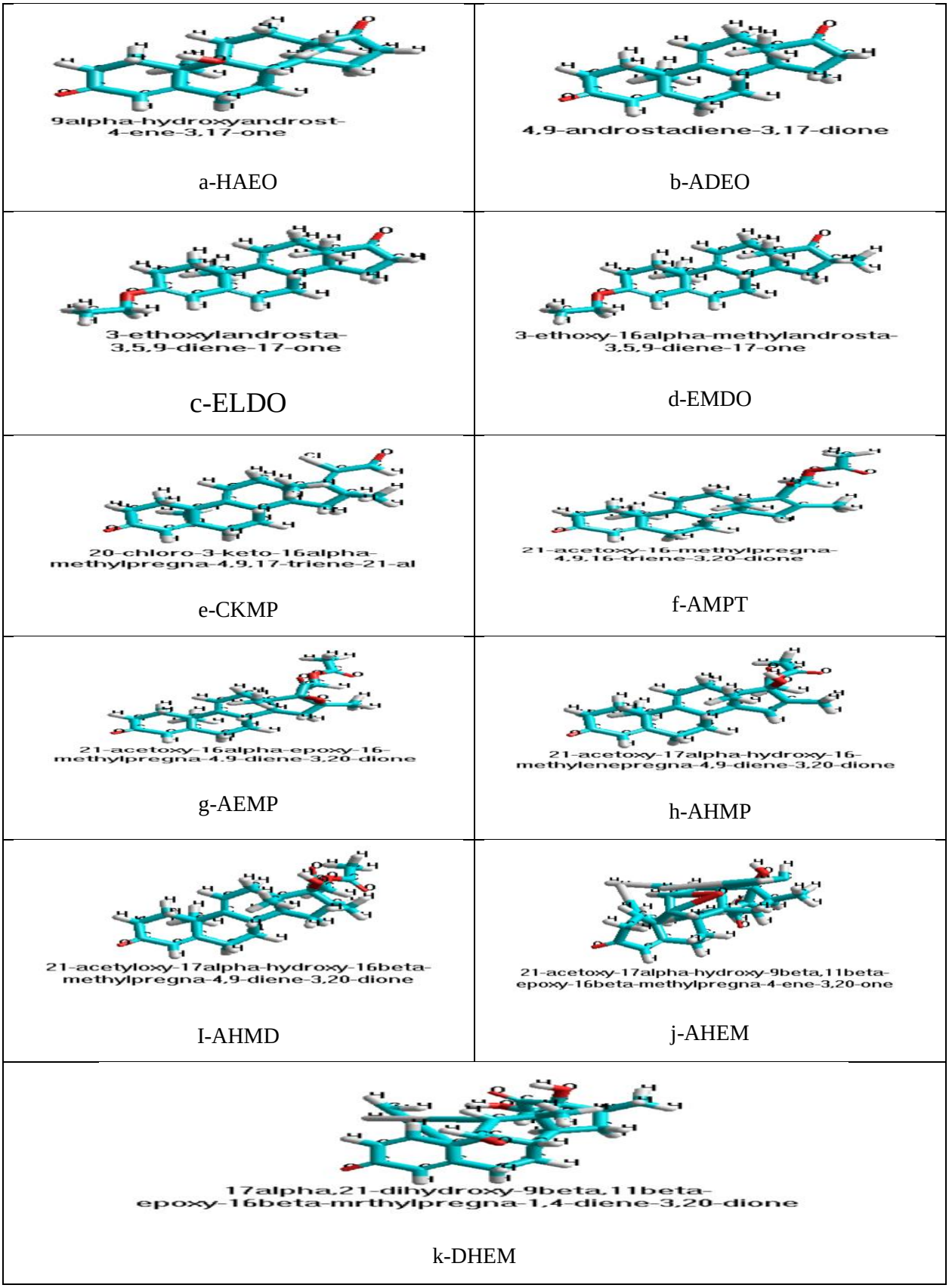

Figure (3-11). Geometry optimized structures of pathway reactions components of betamethasone with their coded names

Table (3-8). Energetic parameters of pathway reaction components of betamethasone formation

Codes of Reaction's components	Total energy kCal/mol	Binding energy kCal/mol	Heat of formation kCal/mol	Zero point energy kcal/mol	HOMO Energy eV	LUMO Energy eV	E_{gap} eV	Imaginary frequency cm^{-1}
HAEO	-81507.098	-4914.737	-134.498	262.087	-10.029	-0.037	9.992	+
ADEO	-74010.942	-4694.050	-77.574	243.433	-9.828	-0.190	9.638	+
ELDO	-80887.704	-5234.755	-68.091	277.580	-8.554	0.250	8.804	+
EMDO	-84336.271	-5515.295	-73.537	294.793	-8.549	0.254	8.803	-
CKMP	-144775.495	-1608.919	-10766.477	270.435	-9.670	-0.475	9.195	-
AMPT	-103347.100	-6050.943	-148.286	308.498	-9.775	-0.165	9.613	+
AEMP	-110091.999	-6123.325	-161.110	310.645	-9.892	-0.205	9.687	-
AHMP	-110111.443	-6142.769	-180.555	311.068	-9.683	-0.093	9.59	-
AHMO	-110843.881	-6272.254	-205.835	325.489	-9.873	-0.207	9.666	-
AHEM	-117418.166	-6173.986	-48.046	316.112	-8.645	-0.787	7.858	-
DHEM	-103847.049	-5611.478	-95.247	286.872	-7.465	-3.263	4.202	+

The pathway of reaction betamethasone formation is consisted from some elemental reaction steps. The first step include dehydration of α11-hyroxy steroid for 9-α-OH-AD(HAEO) to produced ADEO with releasing water molecule at energy barrier of reaction (E_b) equal to 163.67 kCal/mol and ΔH=3.465 kcal/mol. This process can be presented as shown in equation(3-1)

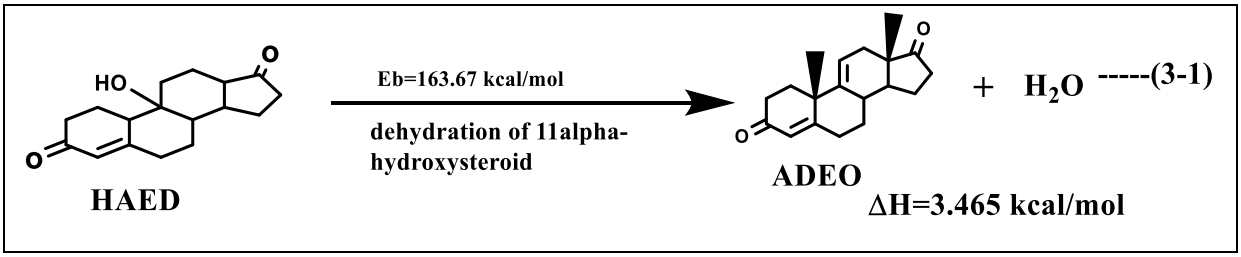

The second step involved ADEO product is interacted with the ethanol molecule which reacted to the terminal 3-keto group accompanied by loss another water molecule and gave ELDO at E_b equal to 328.4 kCal/mol and ΔH=12.991 kCal/mol.

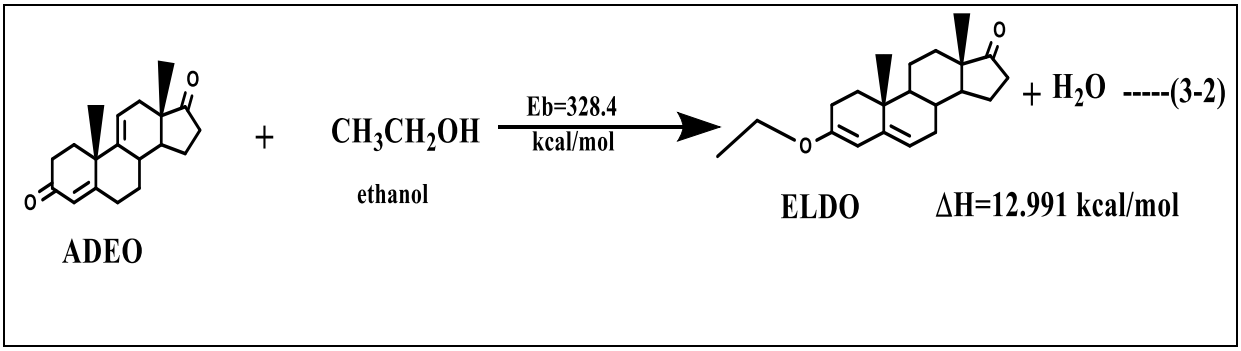

At third step ELDO product is turned in addition to methyl group at the carbon atom (C16).After interaction with bromo methane by loss of hydrogen bromide molecule, to give the EMDO with E_b equal to 13.683 kCal/mol and ΔH=1.885 kCal/mol.

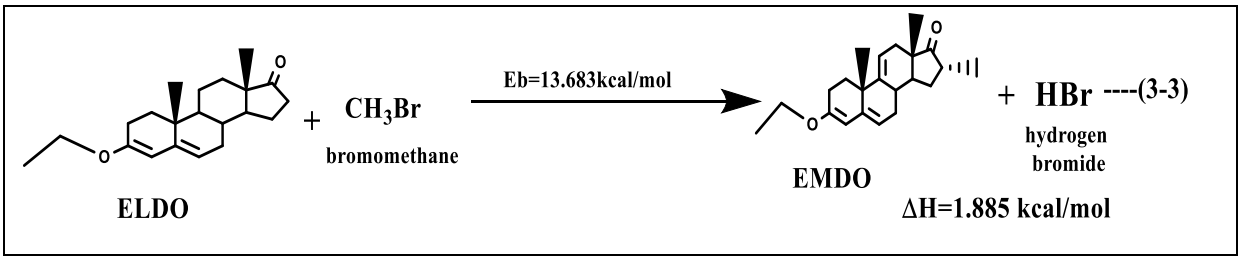

In step Four, EMDO product is interacted with 1-chloro-2-ethoxy ethylene to give CKMP product with ethanol and ethene molecules at E_b equal to 342.199 kCal/mol and ΔH =1.992 kCal/mol.

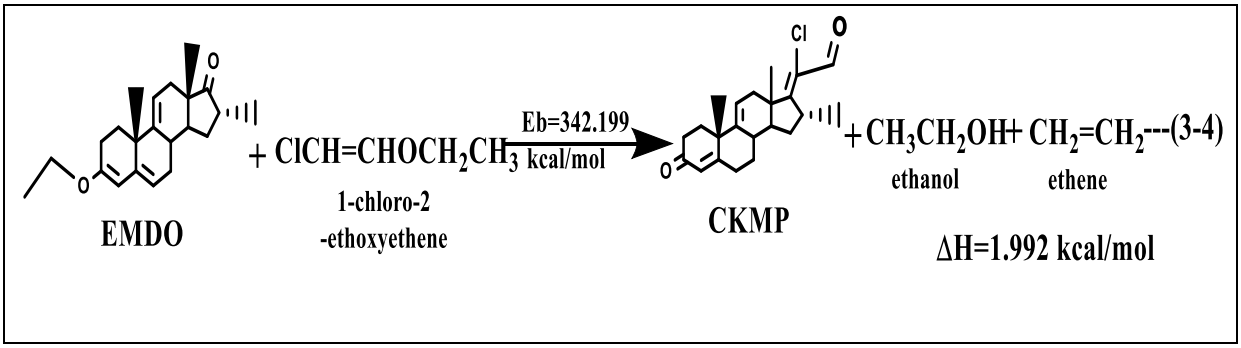

In fifth step, AMPT product is formed after CKMP interaction with sodium acetate accompanied with releasing sodium chloride molecule at E_b equal to -29.09 kCal/mol and ΔH = - 462.484 kCal/mol.

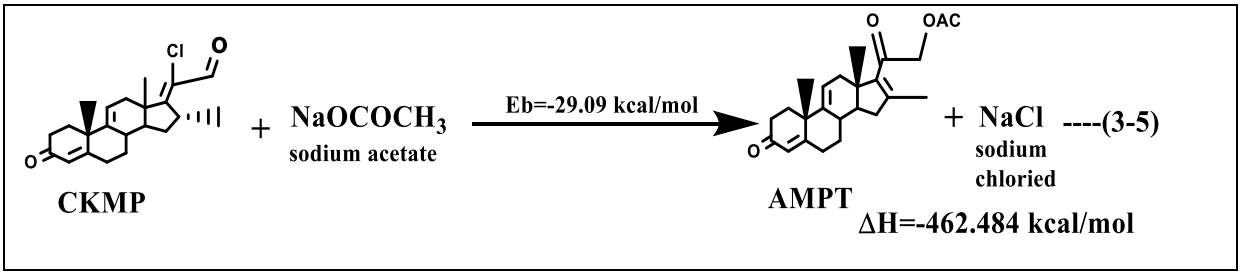

The product AMPT in step fifth is reacted with m-CBPA(meta-chloroperoxy benzoic acid) and after releasing 4-chlorobenzoic acid molecule the AEMP was formed at E_b equal to 240.624 kCal/mol and ΔH=-37.063 kCal/mol(step six).

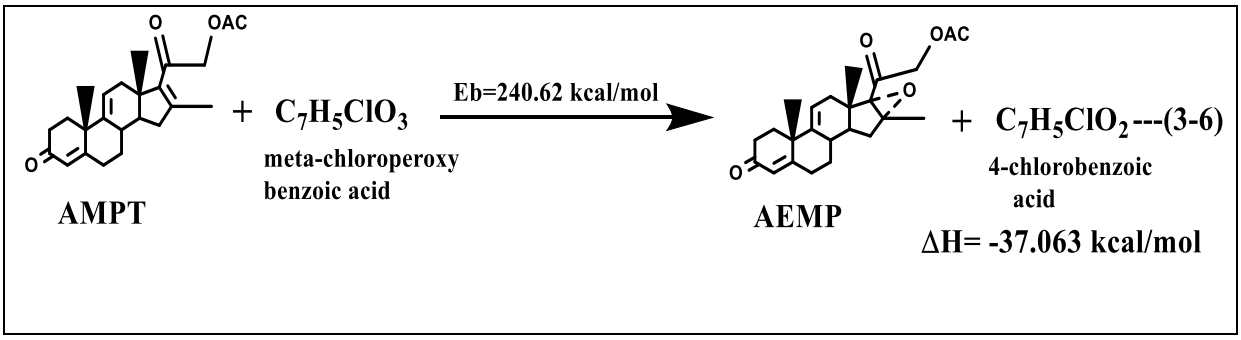

The product of AEMP in step six, which is gave AHMP at the presence of hydrogen bromide as catalytic agent by E_b equal to 39.585 kCal/mol and ΔH=-19.445 kCal/mol(step seven).

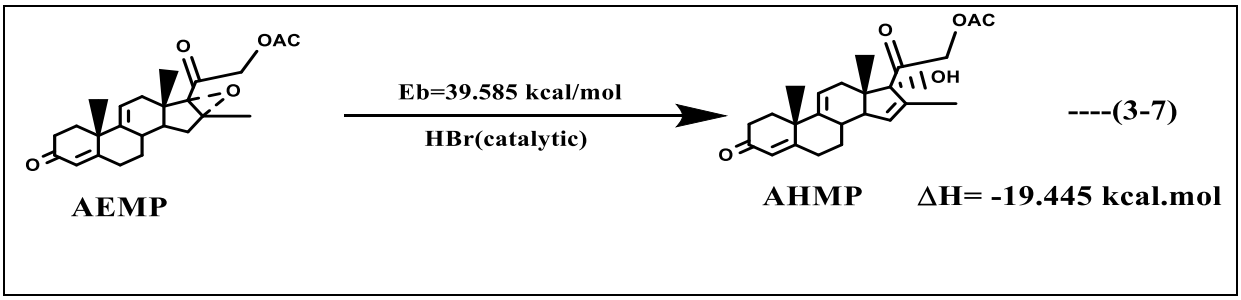

The eighth step include adding hydrogen molecule to AHMP to formation most probable TS1 at E_b equal to 427.085 kCal/mol and ΔH= 39.149 kCal/mol.

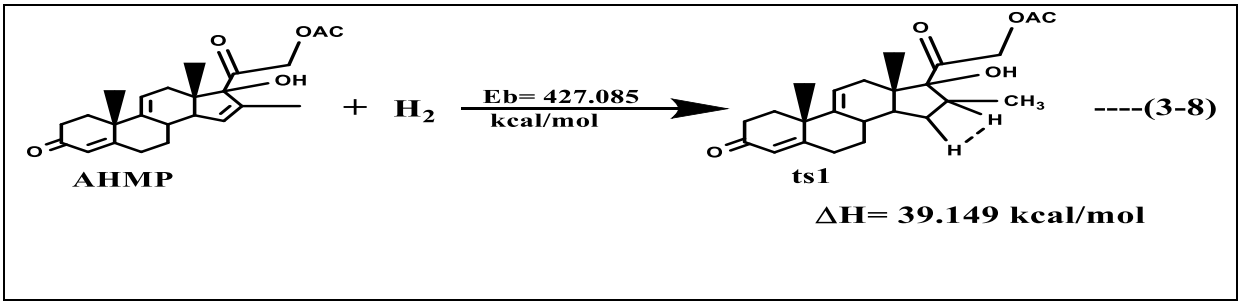

TS1which in turn dissociation to AHMD at E_b equal to 272.633 kCal/mol and ΔH=-399.071 kCal/mol.

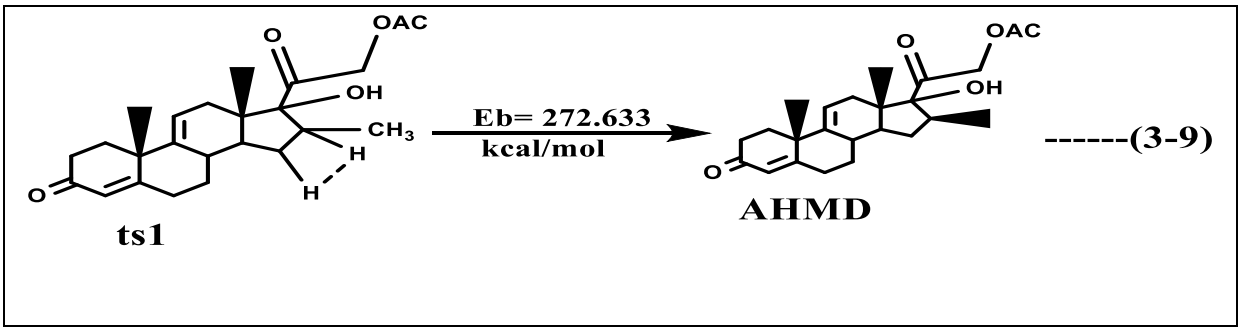

In the ninth step, adding perchloric acid to AHMD to give the most probable TS2 at E_b= 37.931 kCal/mol and ΔH= 52.354 kCal/mol.

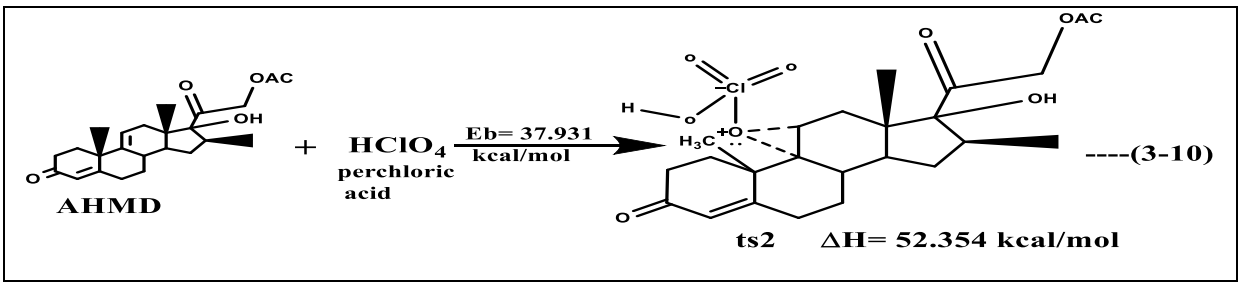

After that TS2 will dissociation to AHEM and chloric acid at E_b = 134.444 kCal/mol and ΔH= 20.274 kCal/mol.

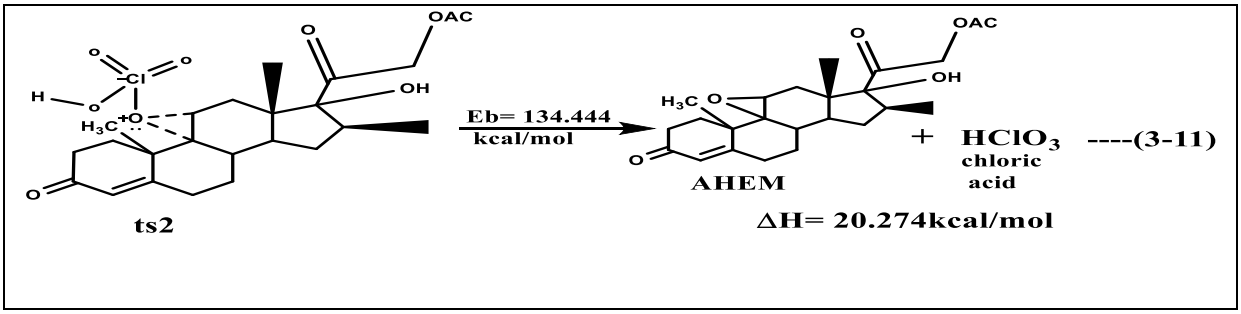

In the tenth step, AHEM give the most probable TS3 at E_b=395.429 kCal/mol and ΔH= 367.847 kCal/mol.

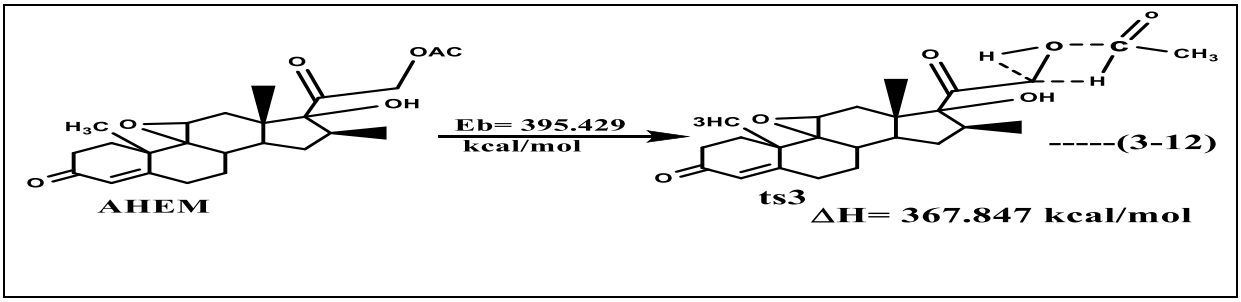

TS3 suffers from rearrangement and 1,2 dehydration to gives DHEM and acetaldehyde molecule at E_b= -518.874 kCal/mol and ΔH= -458.687 kCal/mol.

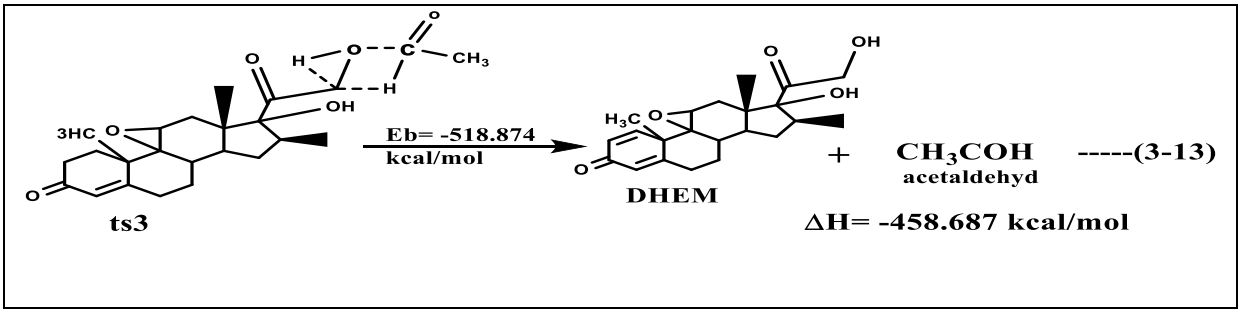

In the eleventh step DHEM is reacted with hydrogen fluoride to give the TS4 at E_b= 361.777 kCal/mol and ΔH= 377.085 kCal/mol.

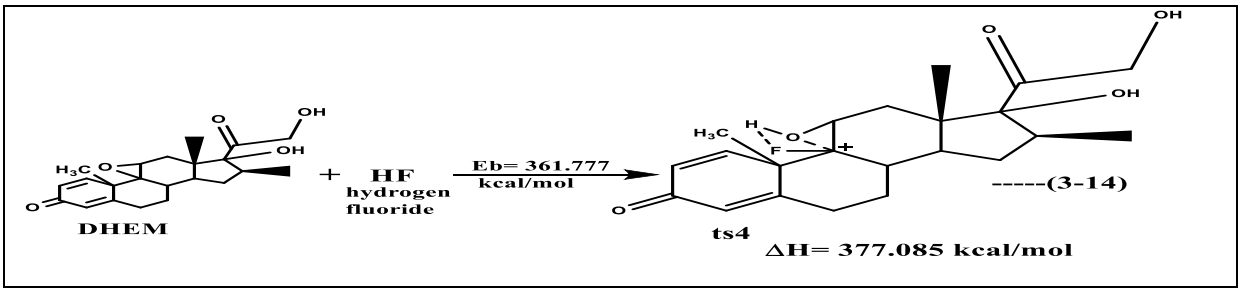

After that TS4 which in turn dissociation to Betamethasone molecule at E_b= -71.349 kCal/mol and ΔH= -451.357 kCal/mol.

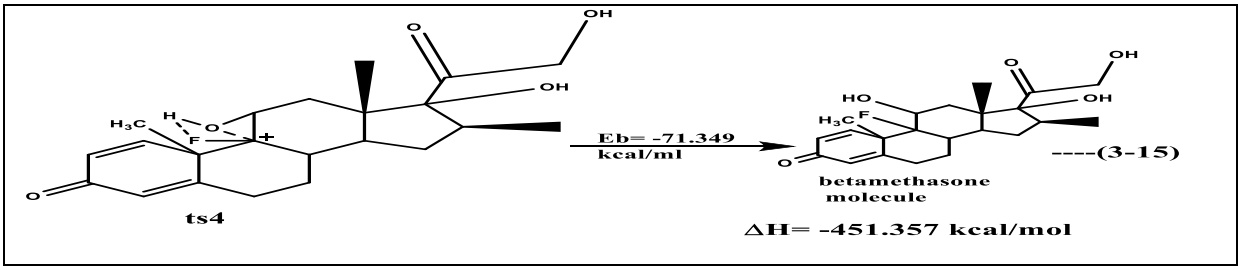

thermodynamics summation of net equation of reaction pathway (3-16) is clarifies that the reaction of betamethasone formation is exothermic reaction at the reaction total enthalpy change equal to - 452.406 kCal/mol.

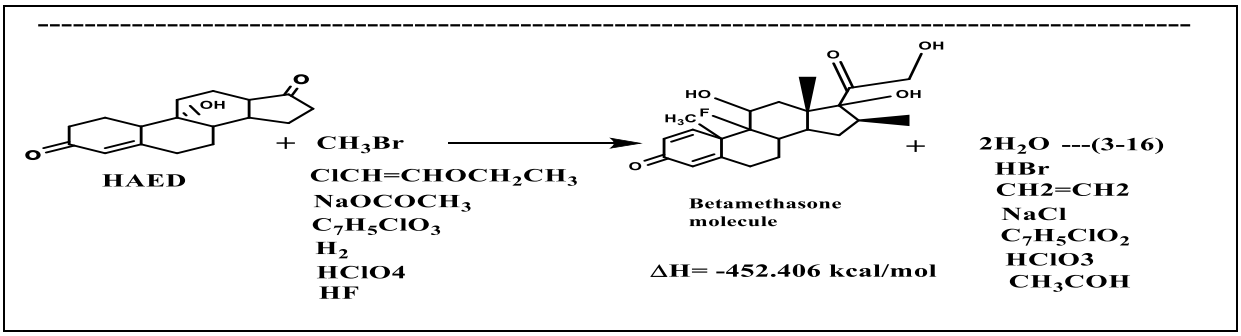

The catalyst are used to realize reaction with minimized energy value and to orient the product toward the desired result[51], [177] .

3-4 Modulation of new suggested derivatives

Modulation of new suggested derivatives for Betamethasone can be done through transition state estimation for rate determining step of reaction mechanism. In this case both of steps, eight and nine in are rate-determining steps in the betamethasone formation; therefore must be studied the transition state formation for any modulation of betamethasone drug. To suggest anew betamethasone's derivatives, must be choice suitable functional groups that has substituted into the molecular structure of betamethasone. Main effect of the introduced functional groups is enclosed in electrostatic potential effect change for reorientation of electronic density around the molecular structure and other stereo isomerism effects . We have choice the amine group ($-NH_2$), ethylamine group ($-CH_3CH_2-NH_2$), Carboxyl group (-COOH) and Carboxyl amide group ($-CONH_2$) due to common uses in the fabrication of drugs modulation [178]. The suggested final structures of derivative have been examined through Reaxys

programme of scientific research definer for preparative chemical material in the world as represented in appendix.

Using various functional groups, which has subsisted into the active site of Betamethasone, this means the newest functional group will attached to carbon atom (C_{17}) through reaction steps eight and nine of chemical reaction formation. Introducing of electron donating or electron withdrawing functional group substitutions on the molecule are very important to determine several critical electronic parameters such as ionization energy, electron affinity, and so on because of these functional groups influence on the activity of molecule [179]–[182]. Donor substituents are increased the energies of highest occupied molecular orbital (HOMO) and lowest unoccupied molecular orbital (LUMO) relative to that of bare molecule, which allows for large modification of the molecular electronic properties. In addition, the electron donating groups increased the effect of electron density onto a molecule through the carbon atom (C17). It is bonded to and decreased the Eg_{ap} value [183]. Electron acceptor functional groups (withdrawing) are decreased the energies of HOMO and LUMO relative to that of bare molecule. Also reduced the electron density onto a molecule through the carbon atom (C17). It is bonded to and increased the E_{gap} which lead to decrease the reactivity of the molecule .

3-4-1 Amino Betamethasone derivative

The first optimized geometry structure of suggested derivative is amino betamethasone (AFHTDPO (Betamethasone.NH_2), Figure(3-12) illustrates the electrostatic behaviour of this derivative. Electrostatic potential is redistributed onto molecular orbitals, because of changes the electronegativity of bounded atoms, which influences HOMO, LUMO, and overall charge density [184]. The nitrogen and oxygen atoms reflect the most electronegative area and these atoms have an excessive negatively charged.

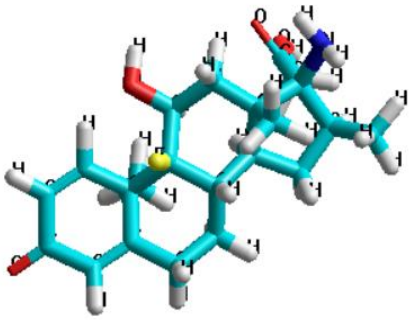

A-Geometry optimization

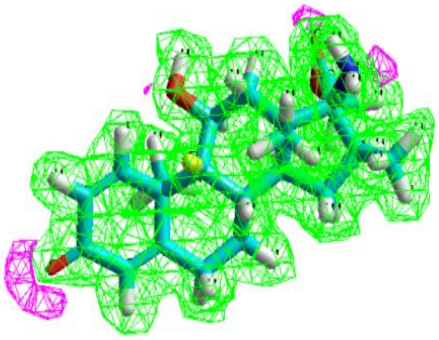

B-Electrostatic potential

Figure (3-12) Energetic properties of AFHTDPO (Betamethasone.NH_2) derivative calculated by semi-empirical (AM1) method

3-4-1-1 Transition states estimation for amino Betamethasone

Four transition states of AFHTDPO(betamethasone.NH_2) are suggested as represented in Figure (3-13).According to their energetic properties ,one of these transition states is most probable for giving the actual path way of AFHTDPO(betamethasone.NH_2) formation reaction [174].

Table (3-9) shows the energetic properties of proposed transition states of AFHTDPO(betamethasone.NH_2) derivative formation. From these results TS2 is most probable than other transition states due to has the highest of zero-point energy equal to 350.951kCal/mol and the first imaginary frequency was negative. this meaning TS2 needed to lowest value of activation energy(E_b) for giving the actual path way of AFHTDPO(betamethasone.NH_2) formation reaction[174].

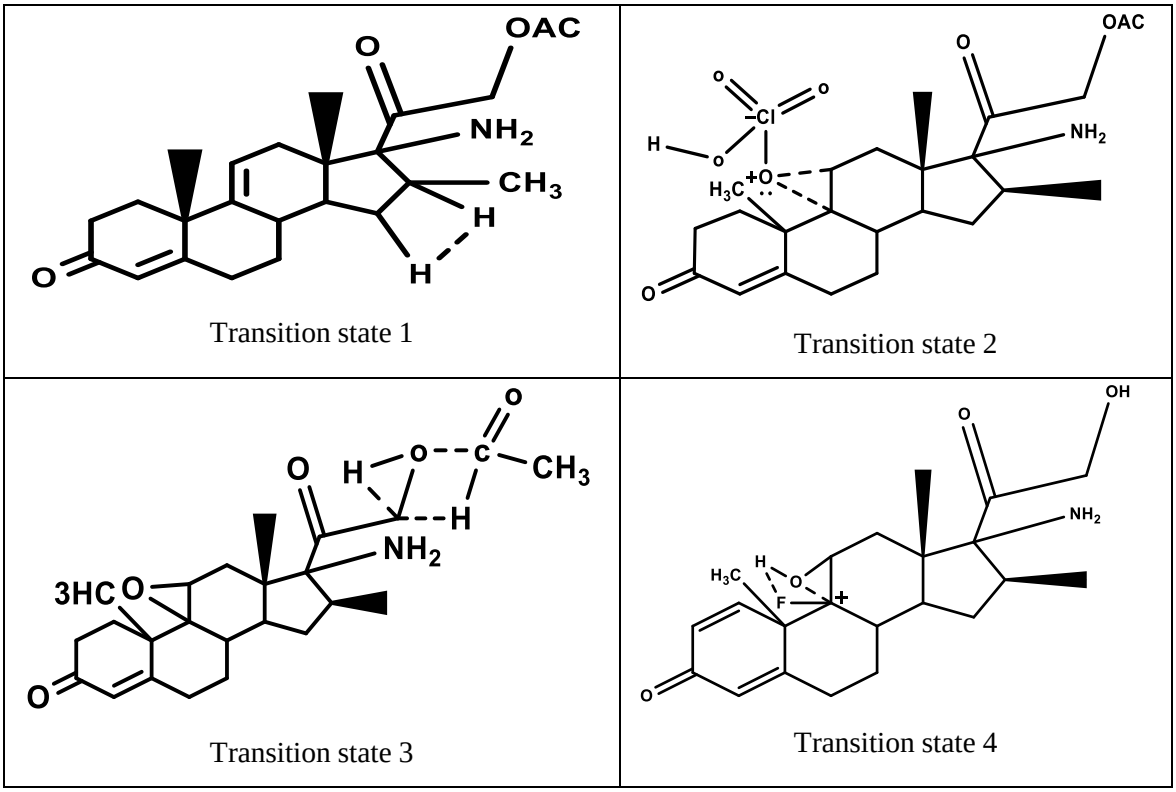

Figure (3-13). Proposed transition states of AFHTDPO(betamethasone.NH_2)

Table(3-9).Energetic properties of transition states of AFHTDPO(betamethasone.NH_2).

Energetic properties	TS 1	TS 2	TS 3	TS 4
Total energy *	-108156.249	-142825.209	-114444.172	-111263.153
Heat of formation *	-148.963	-238.345	295.188	319.936
Zero point energy *	327.008	350.951	333.363	294.040
Imaginary frequency	+	-	-	-

*kCal/mol unit.

3-4-1-2 Amino Betamethasone Formation reaction

Table(3-10).Energetic properties of AFHTDPO(betamethasone.NH_2) derivative components

Derivatives	Total energy*	Heat of formation*	Zero point energy*	Imaginary frequency
AHMP.NH_2	-107433.839	-133.710	318.602	+
AHMD.NH_2	-108165.951	-158.666	333.847	-
AHEM.NH_2	-114916.929	-177.568	335.757	-
DHEM.NH_2	-101177.175	-56.133	299.547	+

*units of kCal/mol

Formation reaction of AFHTDPO(betamethasone.NH_2) derivative , since the first seven steps are the same that of betamethasone formation reaction . The differences in reaction formation steps is began from step eight. Step eighth involved adding ammonium chloride to AHMP to formed the most probable transition state and hydrochloric acid at E_b equal to 0.112 kCal/mol and ΔH=340.006 kCal/mol.

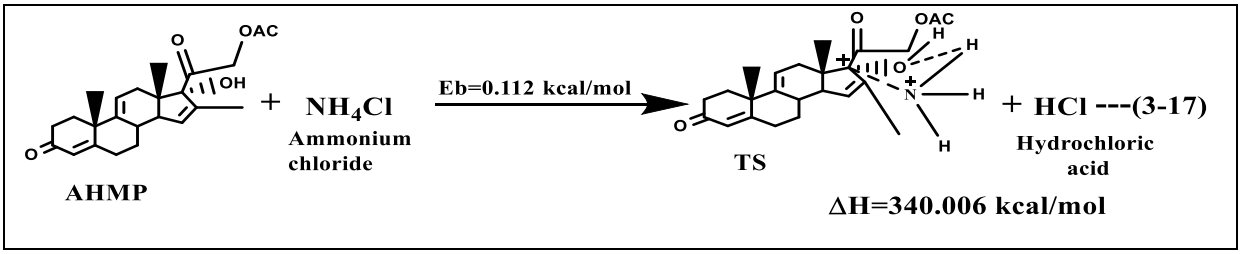

After that the transition state was dissociated to AHMP.NH_2 and water molecule at E_b equal to -436.117 kCal/mol and ΔH=-436.116 kCal/mol.

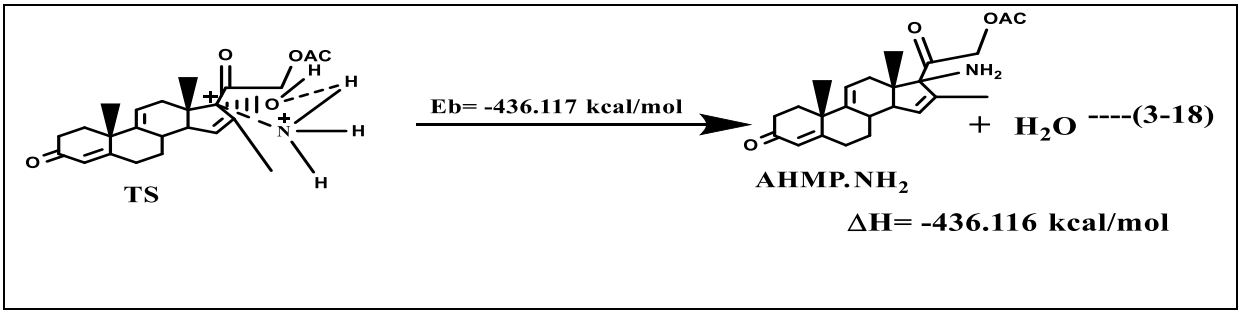

After that AHMP.NH2 interaction with hydrogen molecule to give the most probable TS1 at energy barrier equal to -1.821 kCal/mol and ΔH= -1.84 kCal/mol.

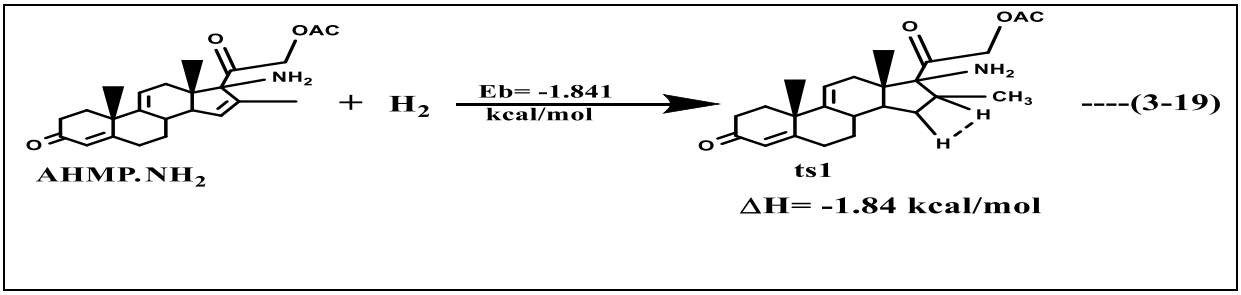

TS1 which in turn dissociation to AHMD.NH_2 at E_b= 235.858 kCal/mol and ΔH= -9.68 kCal/mol.

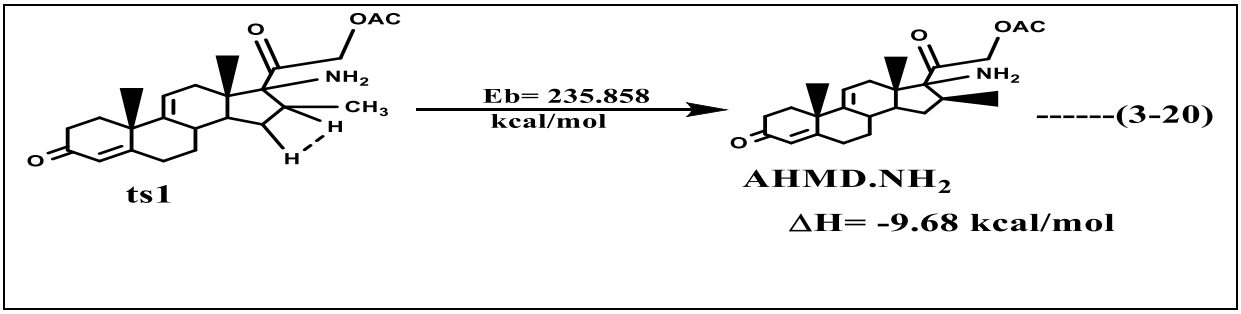

In the ninth step, adding perchloric acid to AHMD.NH_2 to give the most probable TS2 at E_b= -54.439 kCal/mol and ΔH= -74.639 kCal/mol.

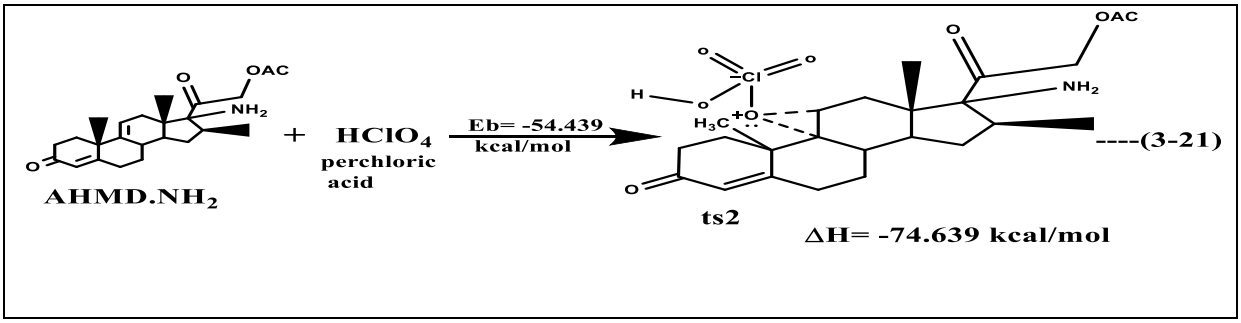

after that TS2 will dissociation to AHEM.NH_2 and chloric acid at E_b = 74.696 kCal/mol and ΔH= -62.424 kCal/mol.

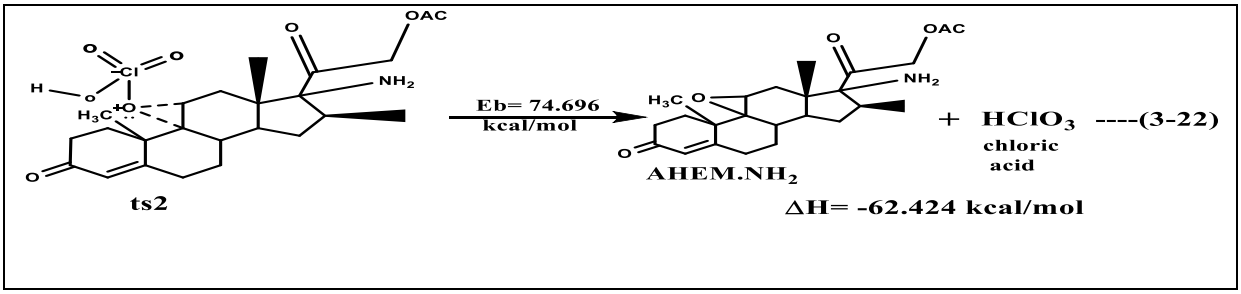

In the tenth step, $AHEM.NH_2$ give the most probable TS3 at E_b=472.756 kCal/mol and ΔH= 380.479 kCal/mol.

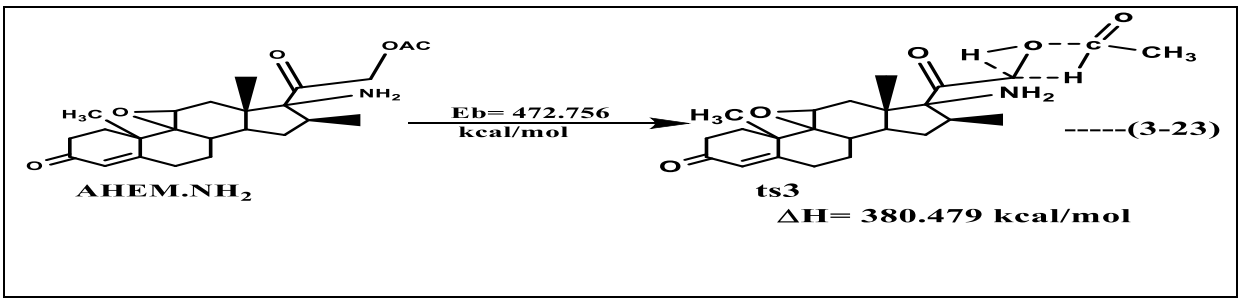

TS3 suffers from rearrangement and 1,2 dehydration to gives $DHEM.NH_2$ and acetaldehyde molecule at E_b= -72699.626 kCal/mol and ΔH= -350.253 kCal/mol.

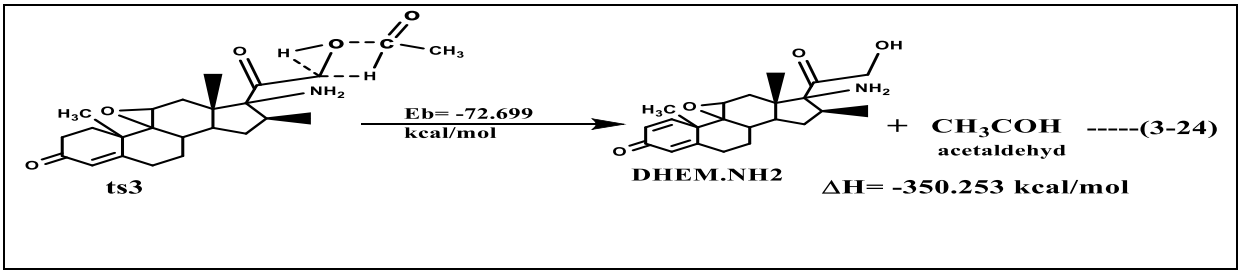

In the eleventh step $DHEM.NH_2$ is reacted with hydrogen fluoride to give the TS4 at E_b= 486.275 kCal/mol and ΔH= -96.6 kCal/mol.

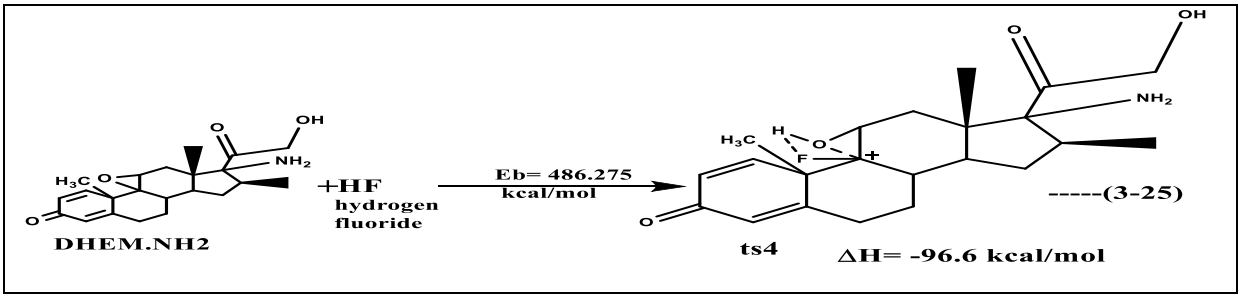

After that TS4 which in turn dissociation to AFHTDPO(betamethasone.$NH_{2)}$ derivative at E_b= -250.608 kCal/mol and ΔH= -445.822 kCal/mol[177].

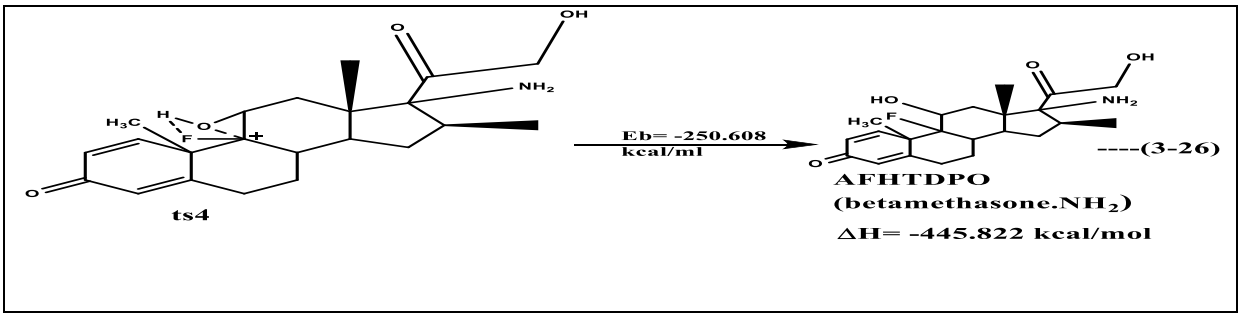

The net equation (3-34) is clarifies the formation of AFHTDPO(betamethasone.NH_2) derivative is exothermic reaction at the reaction enthalpy change equal to -1255.548 kCal/mol.

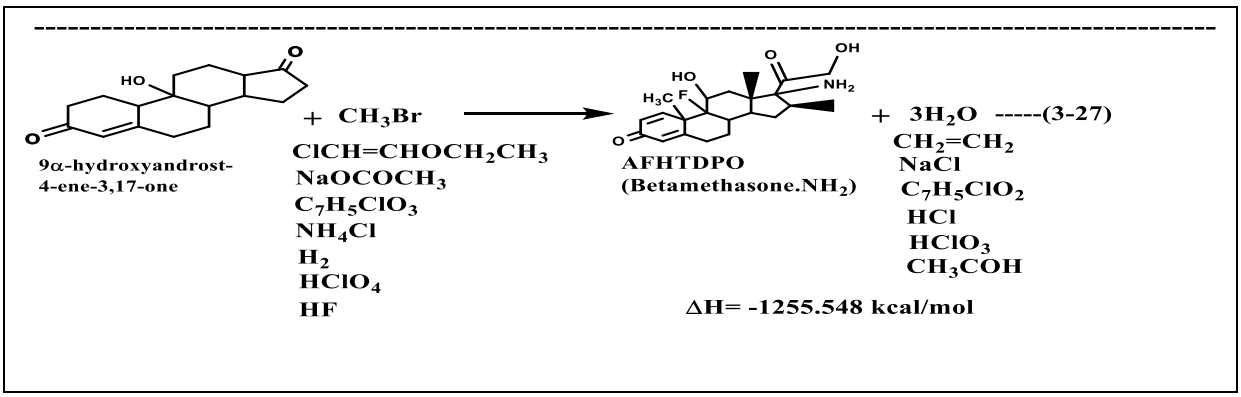

3-4-2 Ethylamine Betamethasone derivative

Ethylamine is a nucleophilic group that is widely used in chemical drugs industry and organic synthesis[185]. Figure (3-14) shows the geometry optimization structure and electrostatic potential of EFHTDPO(Betamethasone.$NHCH_2CH_3$) derivative. Negative electrostatic potential (ESP) areas are seen over oxygen and nitrogen lone pairs, which are coloured red due to the atoms' high electronegativity, while The lowest electron density of the carbon and hydrogen atoms were described by the positive regions in green colour[160].

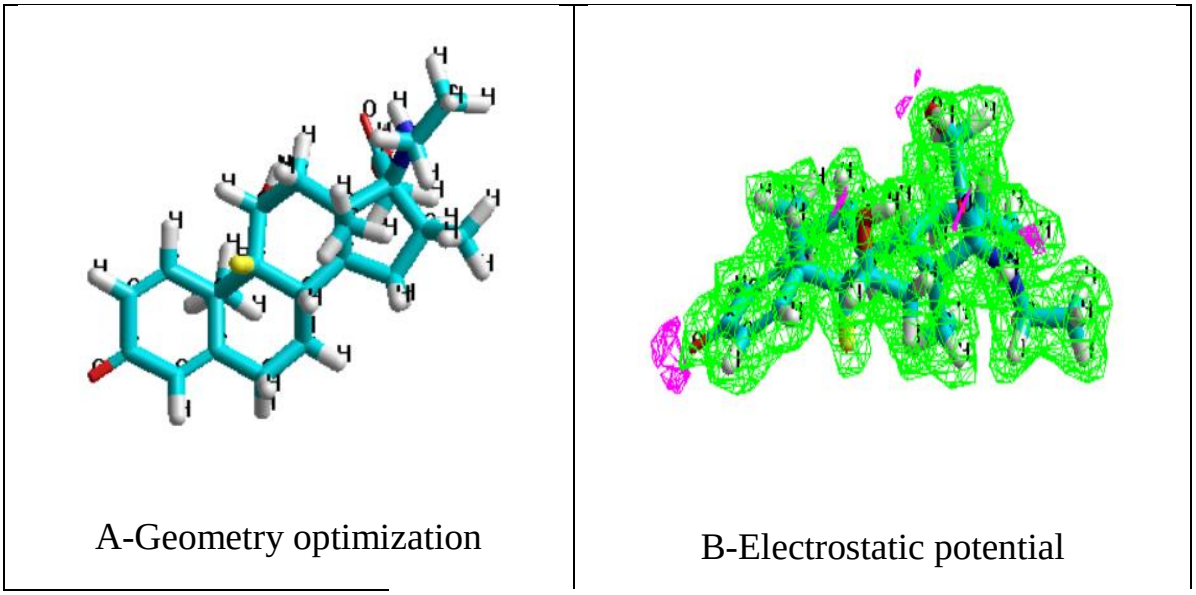

A-Geometry optimization

B-Electrostatic potential

Figure (3-14). Energetic properties of EFHTDPO(Betamethasone.$NHCH_2CH_3$) derivative calculated by semi-empirical(AM1)method in vacuum

3-4-2-1 Transition states estimation for Ethylamine Betamethasone

Four transition states of EFHTDPO (Betamethasone.$NHCH_2CH_3$) derivative are suggested as represented in Figure (3-15). According to their energetic properties one of the transition states is most probable for giving the actual path way of EFHTDPO (Betamethasone.$NHCH_2CH_3$) derivative formation reaction.

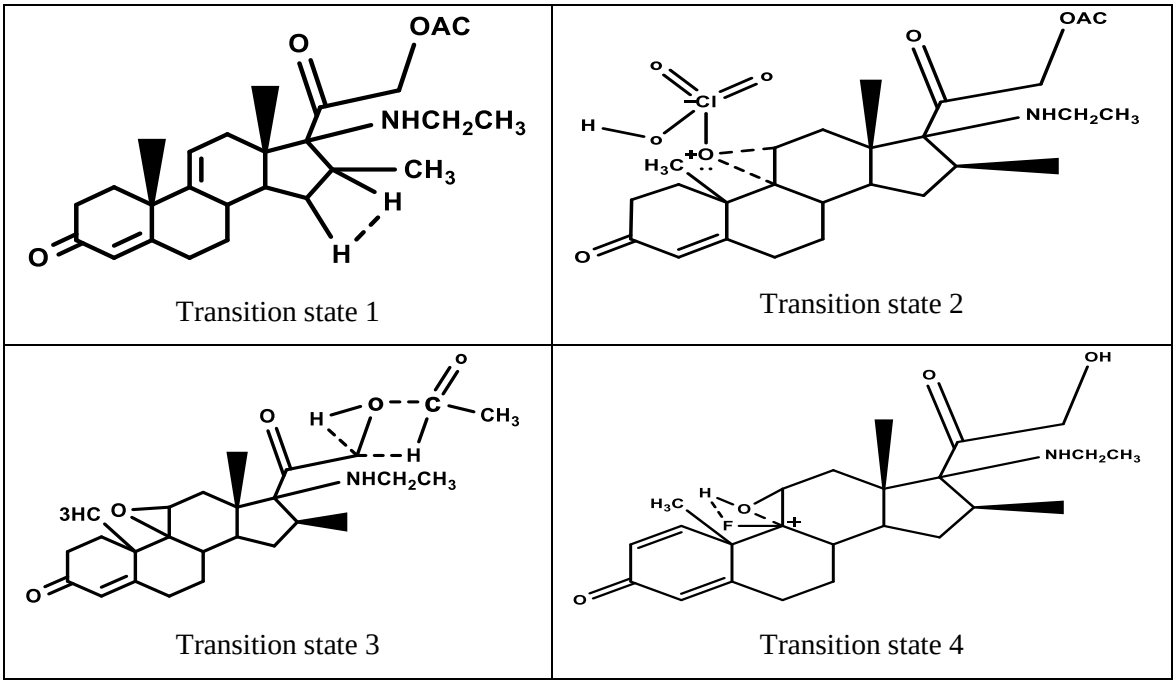

Figure (3-15). Transition states estimation for EFHTDPO (Betamethasone.$NHCH_2CH_3$) derivative

Table (3-11) shows the energetic properties of the suggested transition states of the EFHTTDPO(Betamethasone.$NHCH_2CH_3$) derivative formation. It was found that TS2 is most probable than other transition states for giving the actual path way of EFHTTDPO(Betamethasone.$NHCH_2CH_3$) derivative formation reaction due to the high Zero-point energy value that equal to 384.684 kcal/mol with the negative imaginary frequency[174].

Table (3-11). Energetic properties of the transition states of EFHTTDPO(Betamethasone.$NHCH_2CH_3$)

Energetic properties	TS 1	TS 2	TS 3	TS 4
Total energy*	-115047.297	-149692.228	-121346.332	-118176.960
Heat of formation*	-153.768	-219.119	279.272	292.373
Zero point energy*	361.429	384.684	365.344	335.444
Imaginary frequency	+	-	+	-

*kCal/mol units.

3-4-2-2 Ethylamine Betamethasone formation reaction

Table(3-12) shows the energetic properties of EFHTDPO(Betamethasone.$NHCH_2CH_3$) derivative components.

Table(3-12). Energetic properties of EFHTDPO(Betamethasone.$NHCH_2CH_3$) derivative components

Derivatives	Total energy*	Heat of formation*	Zero point energy*	Imaginary frequency
AHMP.$NHCH_2CH_3$	-114324.558	-138.185	352.975	+
AHMD.$NHCH_2CH_3$	-115057.832	-164.302	368.483	-
AHEM.$NHCH_2CH_3$	-121779.200	-153.595	371.035	-
DHEM.$NHCH_2CH_3$	-108063.088	-55.803	336.098	+

*kCal/mol unit.

The results of multi steps reaction of EFHTDPO(Betamethasone.$NHCH_2CH_3$) derivative. Since the first seven steps are the same that of betamethasone formation reaction. The differences in reaction formation steps is began from step eight. The eighth step include adding 2-chloroethan-1-amine and hydrogen molecule to AHMP to formation most probable TS and hydrochloric acid at E_b equal to 90.676 kCal/mol and ΔH= 393.378 kCal/mol.

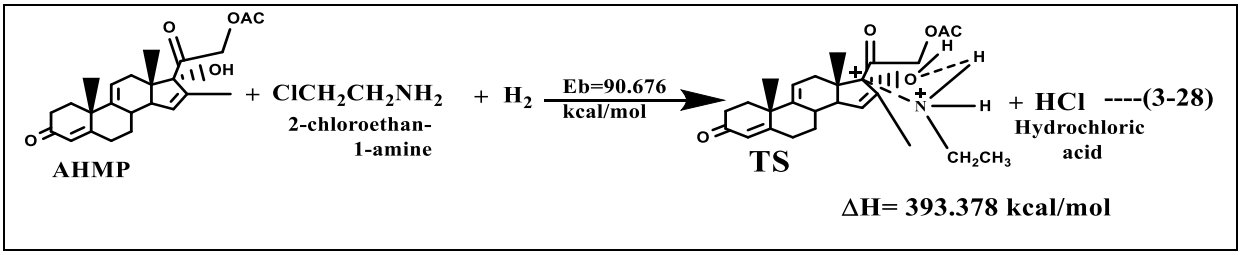

The TS which in turn dissociation to AHMP.NHCH2CH3 and water molecule at E_b equal to -311.988 kCal/mol and ΔH=-396.781 kCal/mol.

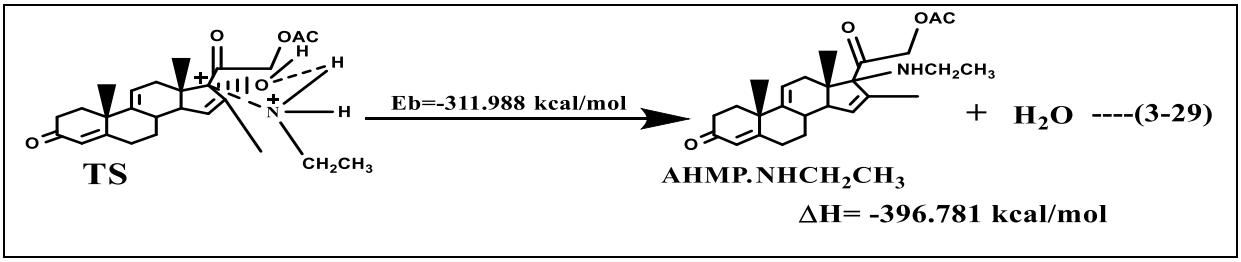

After that AHMP.$NHCH_2CH_3$ interaction with hydrogen molecule to give the most probable TS1 at energy barrier equal to -2.167 kCal/mol and ΔH= -1.64 kCal/mol.

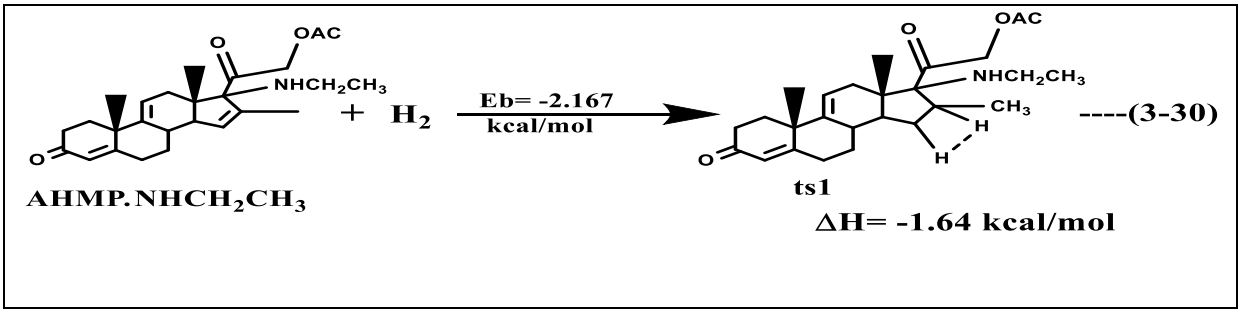

TS1 which in turn dissociation to AHMD.$NHCH_2CH_3$ at E_b= 303.799 kCal/mol and ΔH= -11.062 kCal/mol.

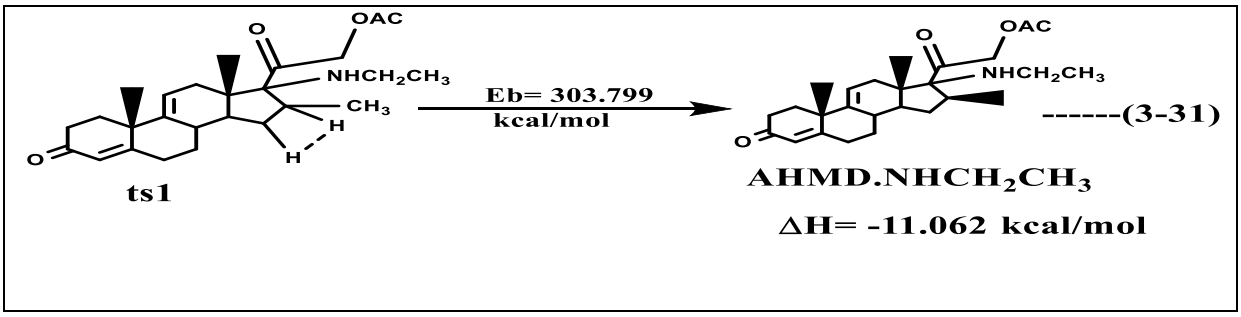

In the ninth step adding perchloric acid to AHMD.$NHCH_2CH_3$ to give the most probable TS2 at E_b= -29.577 kCal/mol and ΔH= -137.842 kCal/mol.

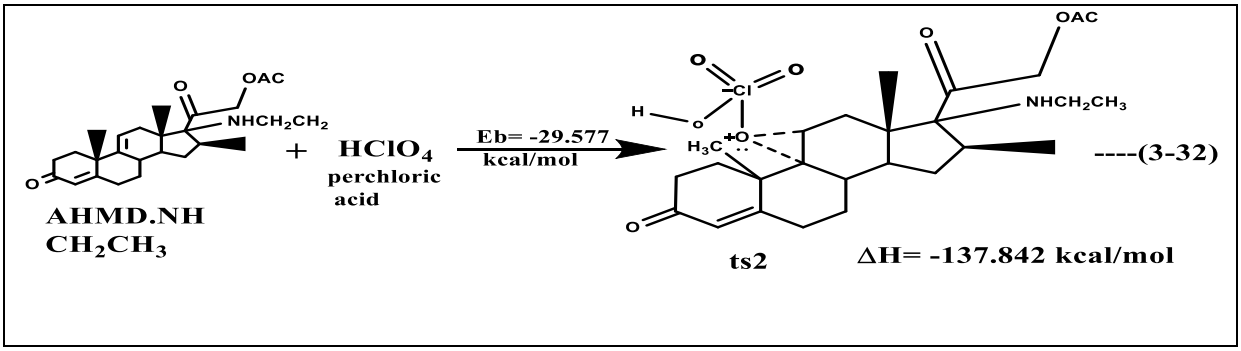

after that TS2 will dissociation to AHEM.$NHCH_2CH_3$ and chloric acid at E_b = 166.719 kCal/mol and ΔH= 66.289 kCal/mol.

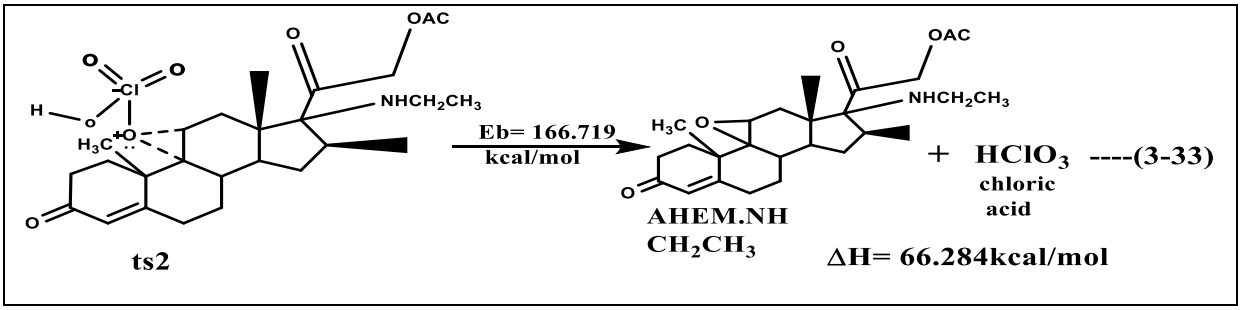

In the tenth step, AHEM.$NHCH_2CH_3$ give the most probable TS3 at E_b=432.868 kCal/mol and ΔH= -71.118 kCal/mol.

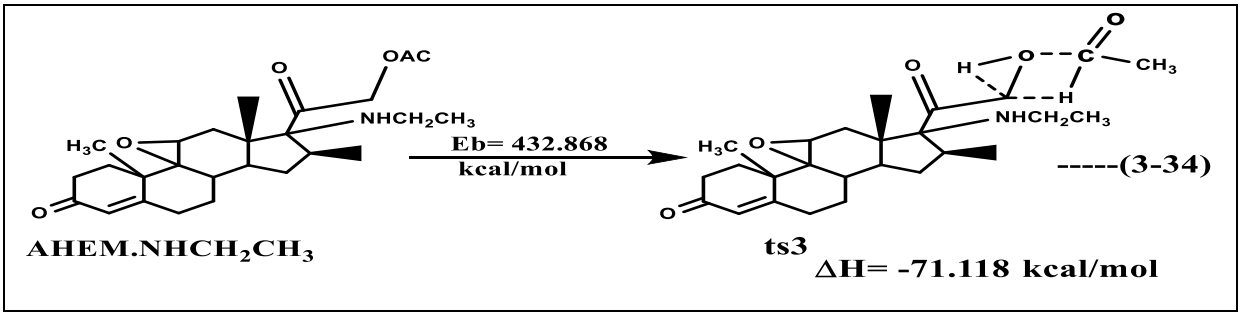

TS3 suffers from rearrangement and 1,2 dehydration to gives DHEM.$NHCH_2CH_3$ and acetaldehyde molecule at E_b= 48.509 kCal/mol and ΔH= -344.155 kCal/mol.

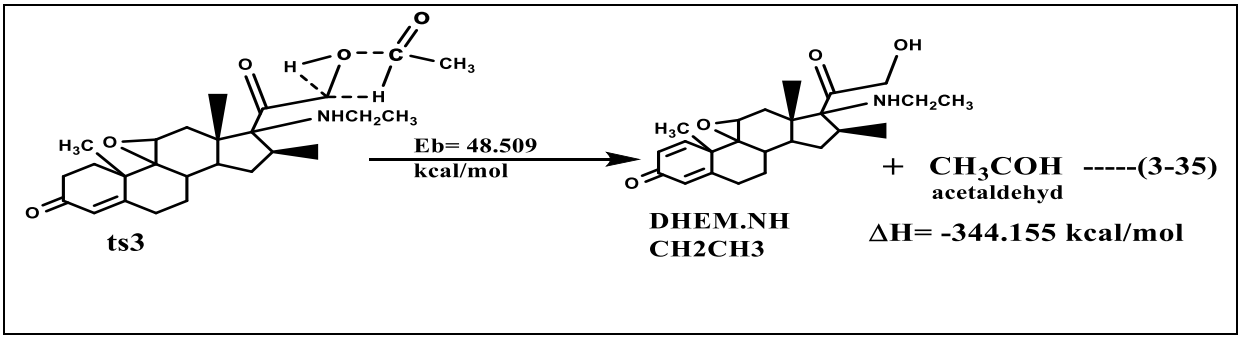

In the eleventh step DHEM.$NHCH_2CH_3$ is reacted with hydrogen fluoride to give the TS4 at E_b= 410.94 kCal/mol and ΔH= 354.572 kCal/mol.

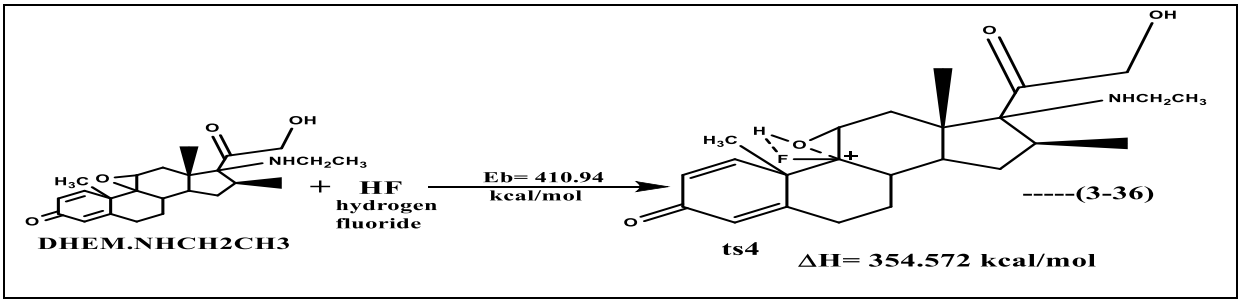

After that, TS4 which in turn dissociation to EFHTDPO(betamethasone.$NHCH_2CH_{3)}$ derivative at E_b= -406.229 kCal/mol and ΔH= -421.554 kCal/mol.

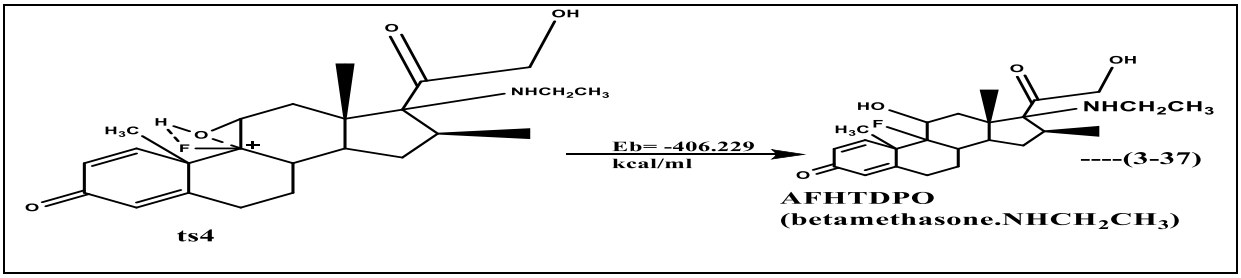

The net equation (3-52) is clarifies the formation of EFHTDPO(Betamethasone.$NHCH_2CH_3$) derivative is exothermic reaction at the reaction enthalpy change equal to -1068.572 kCal/mol.

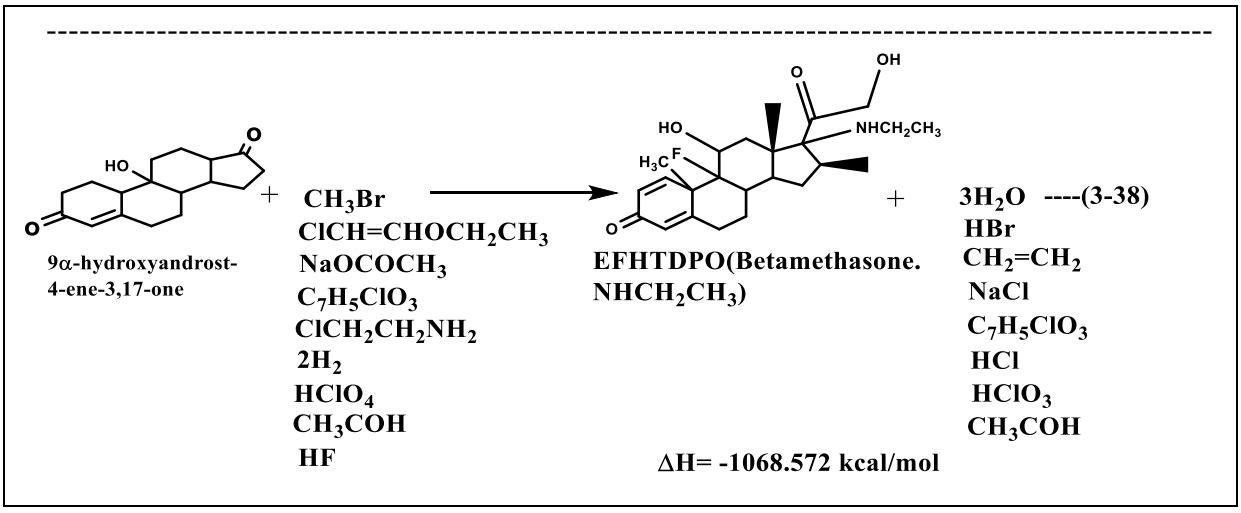

3-4-3 Carboxyl Betamethasone derivative:

Carboxyl group is almost non-existent in the antipsychotic, antidepressant, and hypnotic medication classes, which all work on the central nervous system. CNS-acting medications, as is widely known, must penetrate the blood-brain barrier, which necessitates lipophilicity, which disfavours acid groups [186]. The geometry optimization structure and the electrostatic potential are shows in Figure (3-16). The electrostatic potential mapping is a powerful tool for examining the relation between the molecular structure and physiochemical property. The electrostatic potential of FHCPCC (Betamethasone. COOH) derivative is clearly appears the negative areas around nitrogen and oxygen atoms, which are shown red[187].

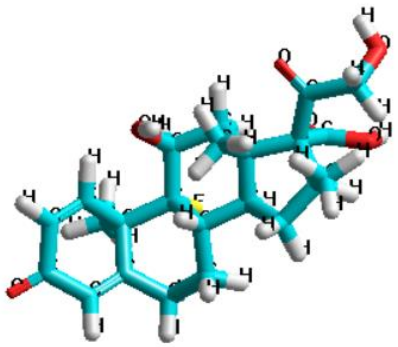

A-Geometry optimization

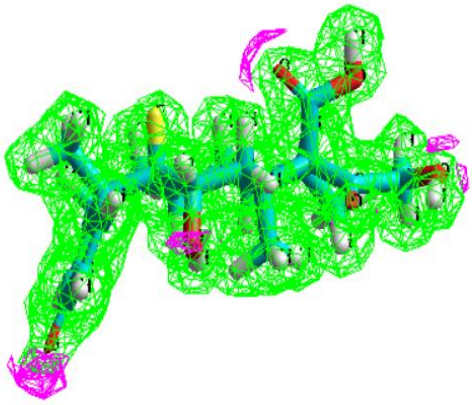

B-Electrostatic potential

Figure (3-16). Energetic properties of FHCPCC(Betamethasone.COOH) derivative calculated by semi-empirical(AM1)method in vacuum.

3-4-3-1 Transition states estimation for Carboxyl Betamethasone:

Four transition states of FHCPCC (Betamethasone. COOH) are suggested as represented in Figure (3-17). According to their energetic properties, one of these transition states is most probable for giving the actual path way of FHCPCC(betamethasone.COOH) derivative formation reaction .

Table (3-13) shows the energetic properties of the suggested transition states of the FHCPCC(Betamethasone.COOH) derivative formation. It was found that TS2 is most probable than other transition states for giving the actual path way of FHCPCC(Betamethasone.COOH) derivative formation reaction due to the high Zero-point energy value that equal to 341.994 kcal/mol with the negative imaginary frequency[174].

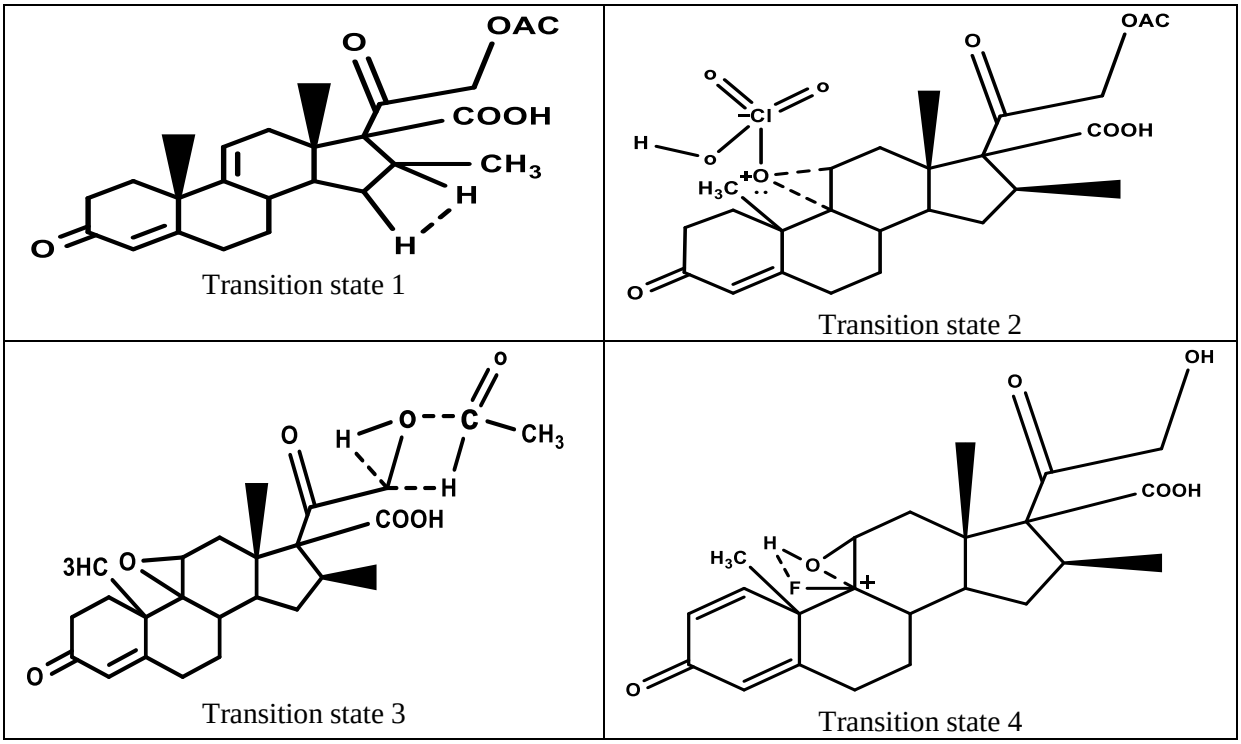

Figure (3-17). Transition states estimation for FHCPCC (Betamethasone. COOH) derivative

Table(3-13). Energetic properties of the transition states of FHCPCC(Betamethasone. COOH) derivative.

Energetic properties	TS1	TS2	TS3	TS4
Total Energy *	-120339.217	-155011.566	-126643.164	-123491.480
Heat of formation *	-233.131	-325.901	194.995	190.408
Zero point energy *	325.695	341.994	327.944	298.164
Imaginary frequency	+	-	-	-

*units of kCal/mol

3-4-3-2 Carboxyl Betamethasone formation Reaction:

The energetic properties of FHCPCC(Betamethasone.COOH) derivative components were shown in Table(3-14).

Table (3-14).Energetic properties of FHCPCC(Betamethasone.COOH) derivative components

Derivatives	Total energy*	Heat of formation*	Zero point energy*	Imaginary frequency
AHMP.COOH	-119616.591	-217.663	317.602	-
AHMD.COOH	-120350.545	-244.460	332.040	-
AHEM.COOH	-127044.441	-206.281	337.109	+
DHEM.COOH	-113412.528	-192.687	298.915	+

*kCal/mol unit.

Results of multi steps formation reaction of FHCPCC(Betamethasone.COOH) derivative , since the first seven steps are the same that of betamethasone formation reaction. The differences in reaction formation steps is began from step eight. In the eighth step the acetic acid adding to AHMP to form most probable TS at E_b equal to 492.74 kcal/mol and ΔH=548.236 kCal/mol.

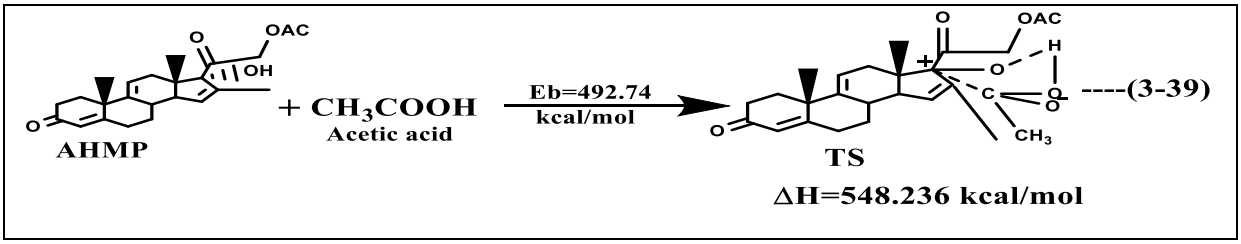

After that TS dissociation to gives AHMP.COOH and methanol molecule at E_b equal to -447.913 kCal/mol and ΔH=-538.183 kCal/mol.

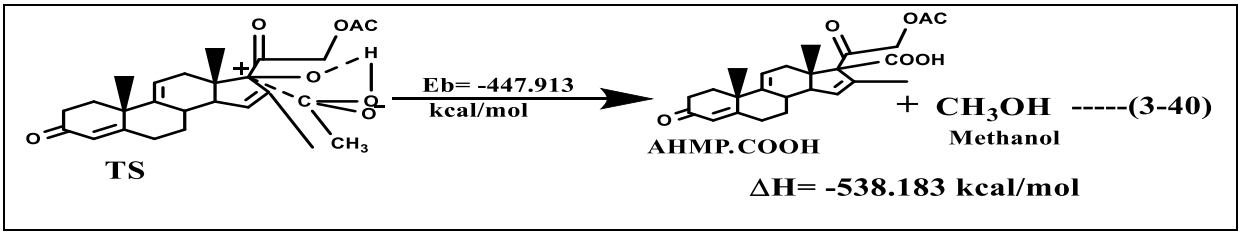

After that AHMP.COOH interaction with hydrogen molecule to give the most probable TS1 at energy barrier equal to -2.067 kCal/mol and ΔH= -1.793 kCal/mol.

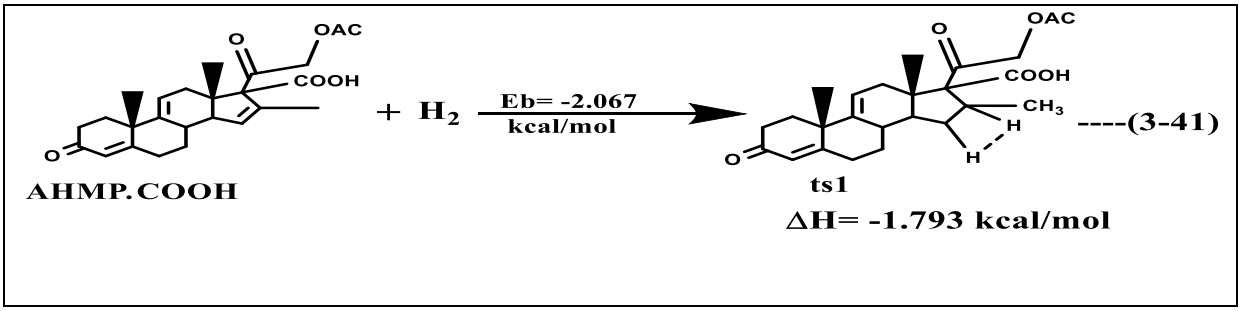

TS1 which in turn dissociated to AHMD.COOH at E_b= -0.029 kCal/mol and ΔH= -11.605 kCal/mol.

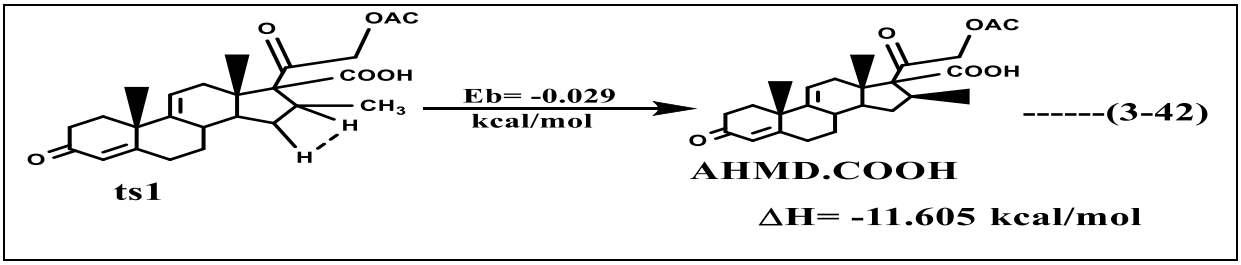

In the ninth step, adding perchloric acid to AHMD.COOH to give the most probable TS2 at E_b= 515.978 kCal/mol and ΔH= -116.62 kCal/mol.

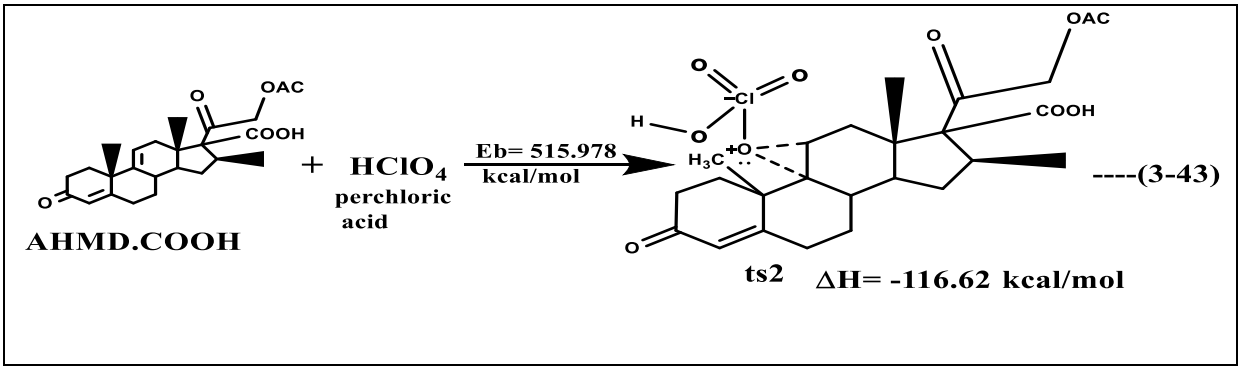

After that TS2 will be dissociated to AHEM.COOH and chloric acid at E_b = 61.413 kCal/mol and ΔH= 72.633 kCal/mol.

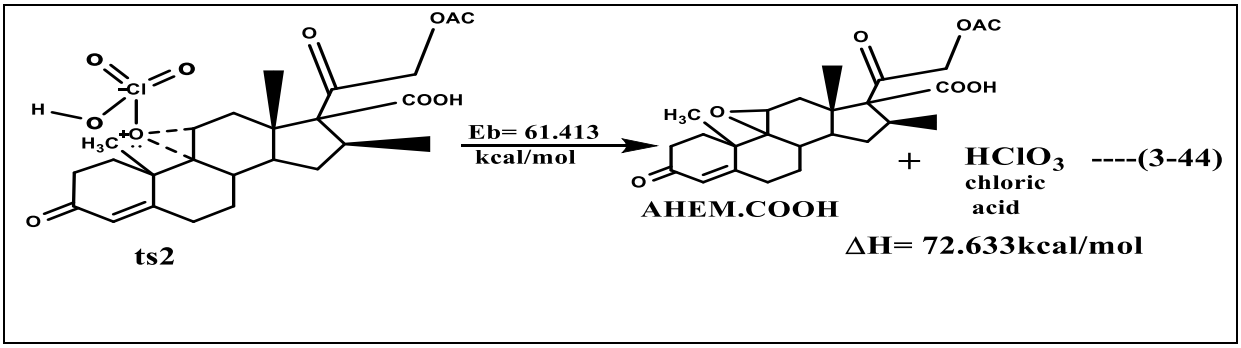

In the tenth step, AHEM.COOH give the most probable TS3 at E_b=426.702 kCal/mol and ΔH= 40.635 kCal/mol.

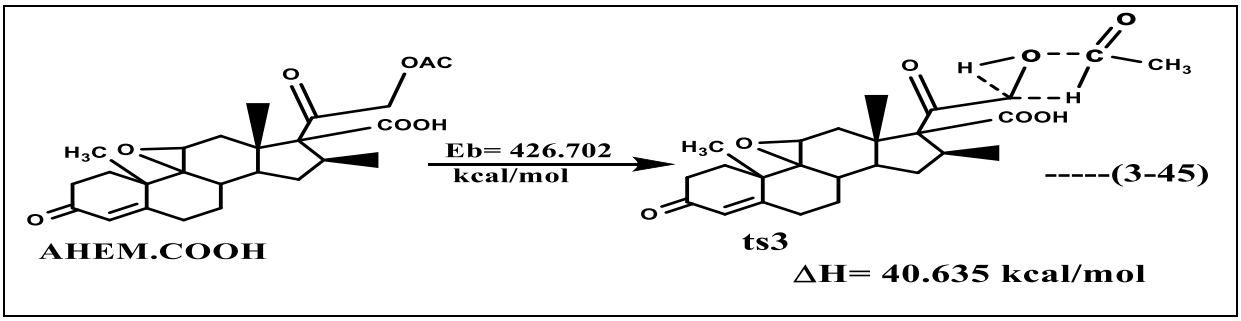

TS3 suffers from rearrangement and 1,2 dehydration to gives DHEM.COOH and acetaldehyde molecule at E_b= -169.145 kCal/mol and ΔH= -401.971 kCal/mol.

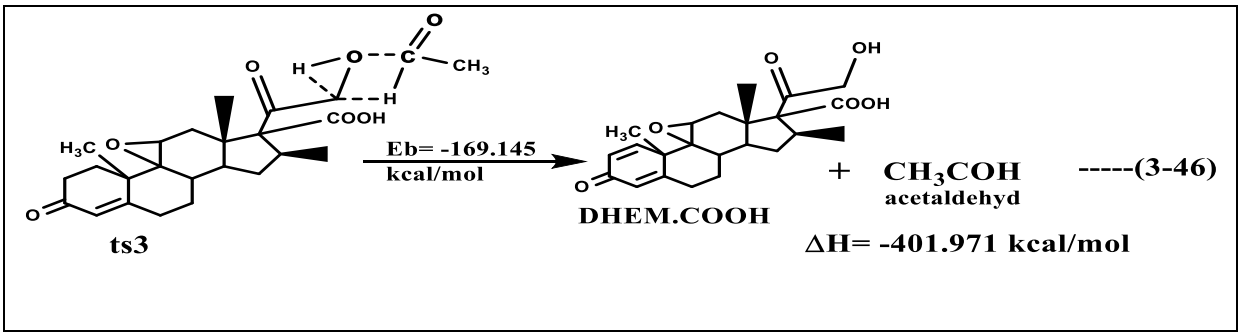

In the eleventh step, DHEM.COOH is reacted with hydrogen fluoride to give the TS4 at E_b= 445.86 kCal/mol and ΔH= 50.461 kCal/mol.

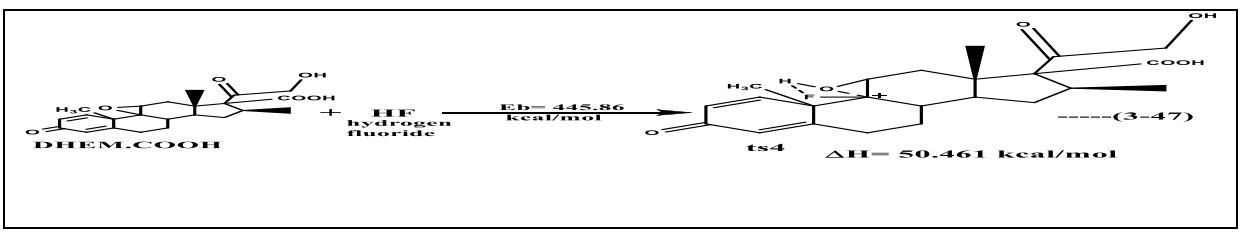

After that TS4 which in turn dissociation to FHCPCC (betamethasone.$NHCH_2CH_{3)}$ derivative at E_b= -463.977 kCal/mol and ΔH= -472.81 kCal/mol.

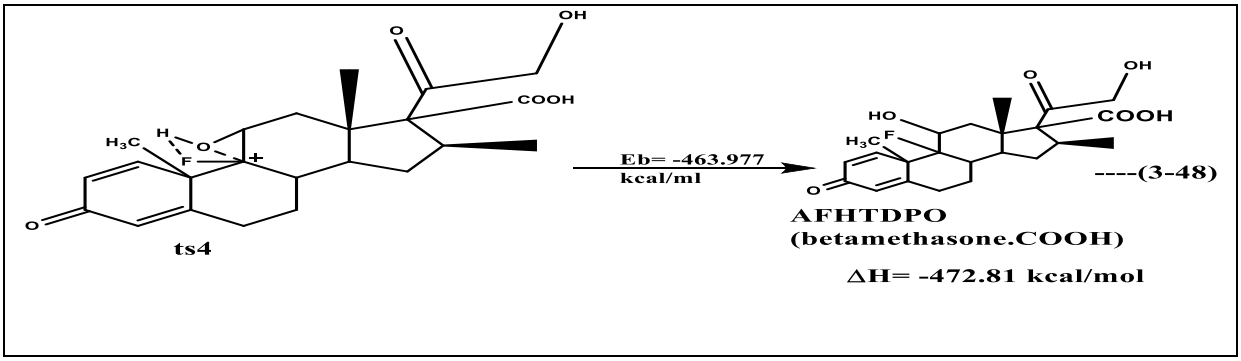

The net equation (3-70) illustrates formation of FHCPCC(Betamethasone.COOH) derivative is exothermic reaction at the reaction enthalpy change equal to -1329.626 kCal/mol.

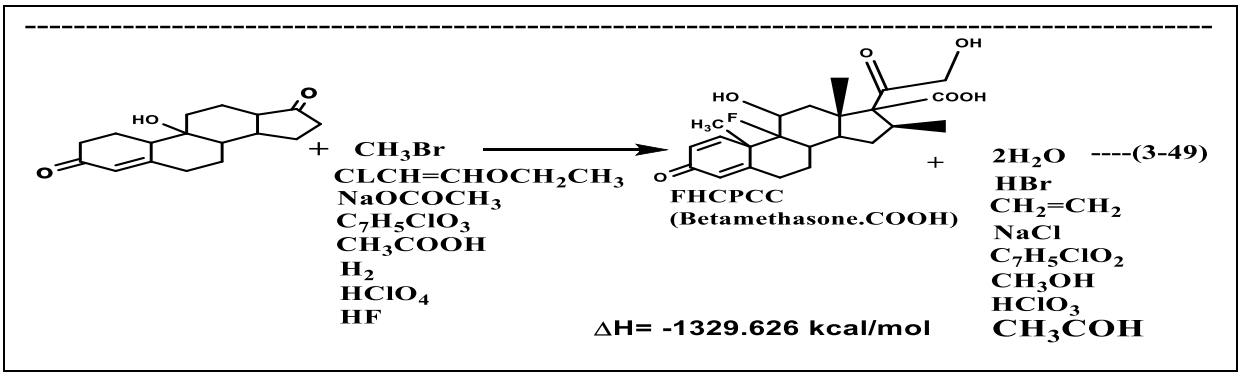

3-4-4 Carboxamide Betamethasone derivative:

Carboxamide group, among the common organic functional groups investigated appears frequently in the CMC database as well as in the numerous medication classes studied because that In a hydrogen bond, it has both hydrogen-accepting and hydrogen-donating abilities, neutral group, hydrophilic and chemically stable[186].Figure (3-18) is illustrated the geometry optimization structure and electrostatic potential of FHACPC(Betamethasone.$CONH_2$) derivative. The negative and positive

potentials zones in the Electro static potential maps correspond to the electron-rich and electron-deficient areas, respectively[188].

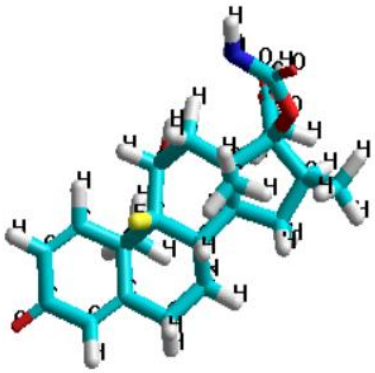

A-Geometry optimization

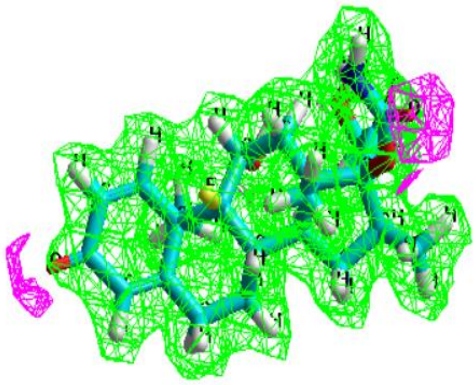

B-electrostatic potential

Figure(3-18) Energetic properties of FHACPC(Betamethasone.$CONH_2$) derivative

3-4-4-1 Transition states estimation for Carboxamide betamethasone

Geometrical optimization structure of different four transition states have been suggested are represented in Figure(3-19). According to their energetic properties (Total energy, heat of formation, zero-point energy and imaginary frequency), one of the transition state is most probable for giving the actual path way of FHACPC(Betamethasone.$CONH_2$)derivative formation reaction[189]. Energetic values are recorded in Table(3-15) of suggested transition states. It was found TS2 is most probable for giving actual path way of the FHACPC(Betamethasone.$CONH_2$) derivative than other transition states due to has high zero-point energy value which equal to 359.323 kCal/mol and the negative imaginary frequency[190]. Zero-point energy of TS yields a lower activation energy value than other transition states. Hilltop structure is a structure with more than one negative frequency [191].

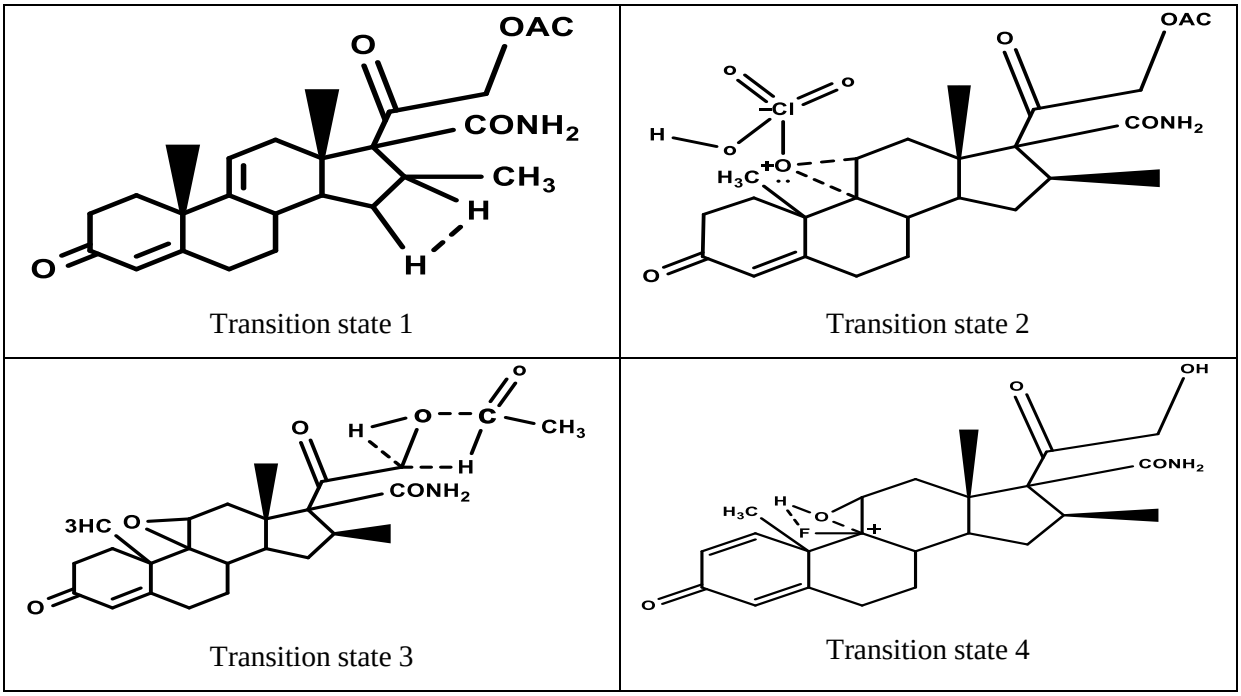

Figure (3-19). Transition states estimation for Carboxamide betamethasone derivative

Table(3-15). Energetic properties of the transition states of FHACPC(Betamethasone .$CONH_2$) derivative

Energetic properties	TS 1	TS 2	TS 3	TS 4
Total energy *	-124431.768	-159122.991	-130777.341	-127620.548
Heat of formation*	-228.368	-336.011	162.133	162.655
Zero point energy*	335.835	359.323	345.119	312.256
Imaginary frequency	-	-	-	-

*kCal/mol unit.

3-4-4-2 Carboxamide Betamethasone Formation Reaction

Table(3-16) shows the energetic properties of FHACPC(Betamethasone.$CONH_2$) derivative components.

Table(3-16).Energetic properties of FHACPC(Betamethasone.$CONH_2$) derivative components

Derivatives	Total energy*	Heat of formation*	Zero point energy*	Imaginary frequency
AHMP.CONH2	-123707.658	-207.414	327.266	-
AHMD.CONH2	-124440.409	-233.009	343.009	-
AHEM.CONH2	-131190.546	-251.071	346.651	-
DHEM.CONH2	-117506.220	-185.064	309.559	+

*kCal/mol unit.

Results of multi steps formation reaction of FHACPC(Betamethasone.$CONH_2$) derivative. Since the first seven steps are the same that of betamethasone formation reaction. The differences in reaction formation steps is began from step eight. In the eighth step the AHMP was reacted with carbamic acid to gives the most probable TS at E_b equal to 501.64 kcal/mol and ΔH=426.259 kCal/mol.

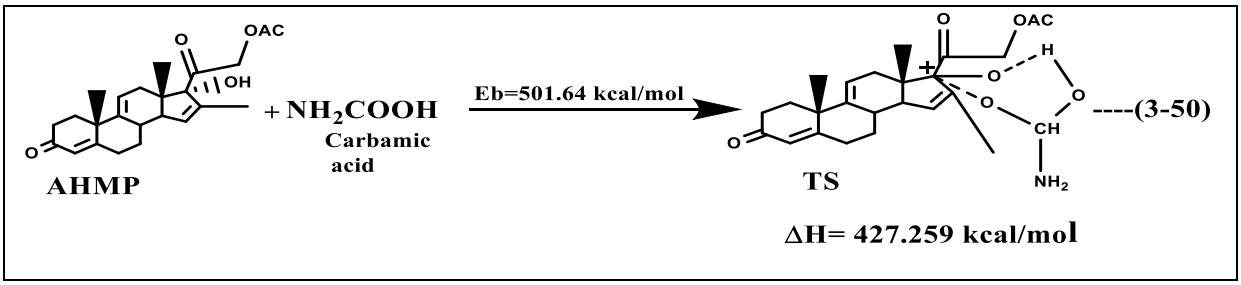

After that, TS dissociated to AHMP.$CONH_2$ and water molecule at E_b equal to -338.337 kCal/mol while ΔH= -412.361 kCal/mol.

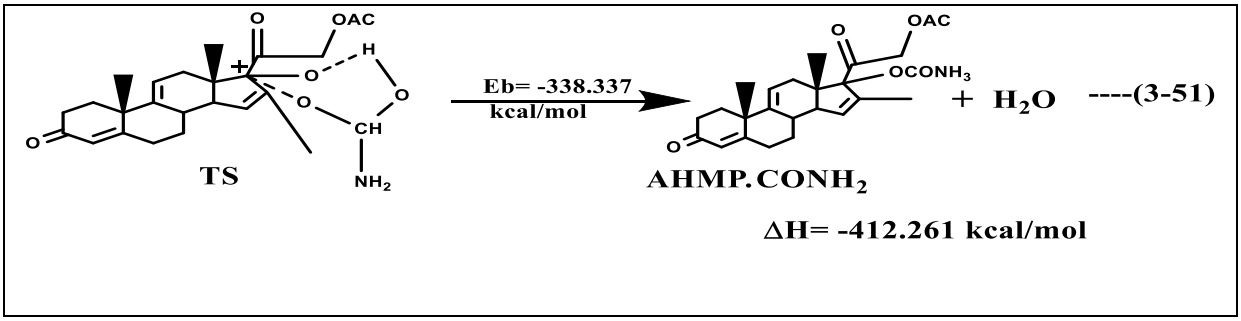

After that, $AHMP.CONH_2$ interaction with hydrogen molecule to give the most probable TS1 at energy barrier equal to -1.69 kCal/mol and ΔH= -98.29 kCal/mol.

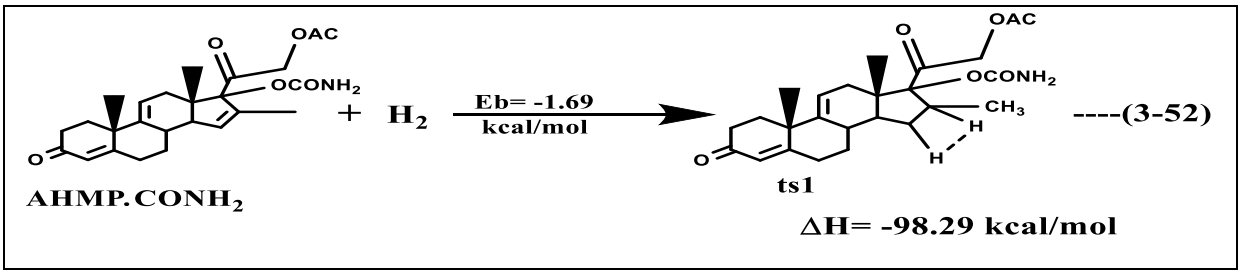

TS1 which in turn dissociation to $AHMD.CONH_2$ at E_b= -1.84 kCal/mol and ΔH= -10.492 kCal/mol.

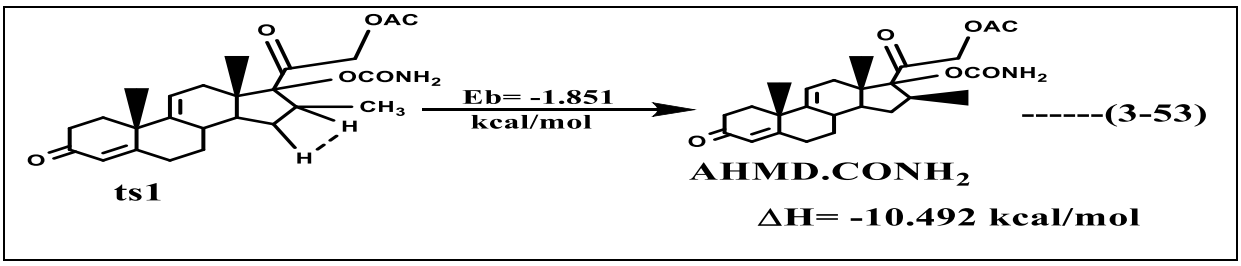

In the ninth step, adding perchloric acid to $AHMD.CONH_2$ to give the most probable TS2 at E_b= -76.763 kCal/mol and ΔH= -81.216 kCal/mol.

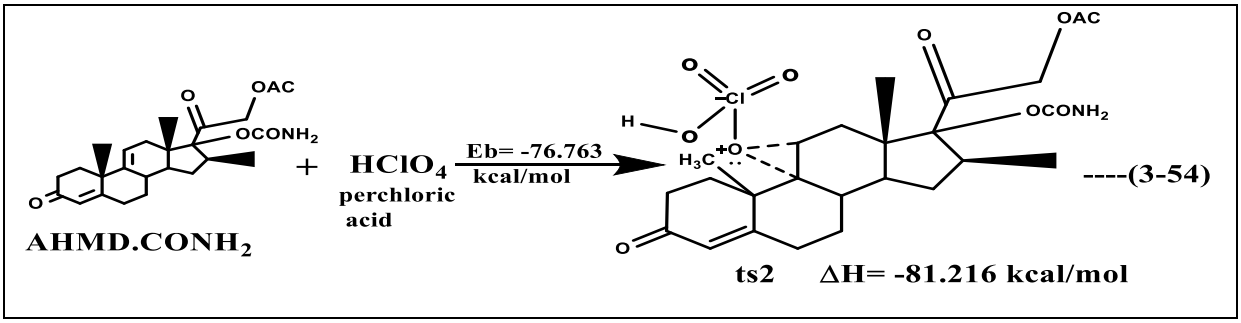

after that, TS2 will dissociation to AHEM.COOH and chloric acid at E_b = 107.151 kCal/mol and ΔH= -18.506 kCal/mol.

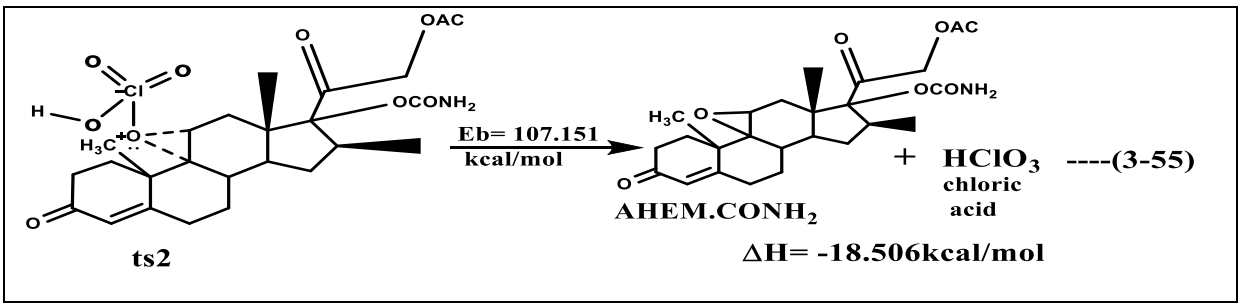

In the tenth step, $AHEM.CONH_2$ give the most probable TS3 at E_b=412.704 kCal/mol and ΔH= -46.722 kCal/mol.

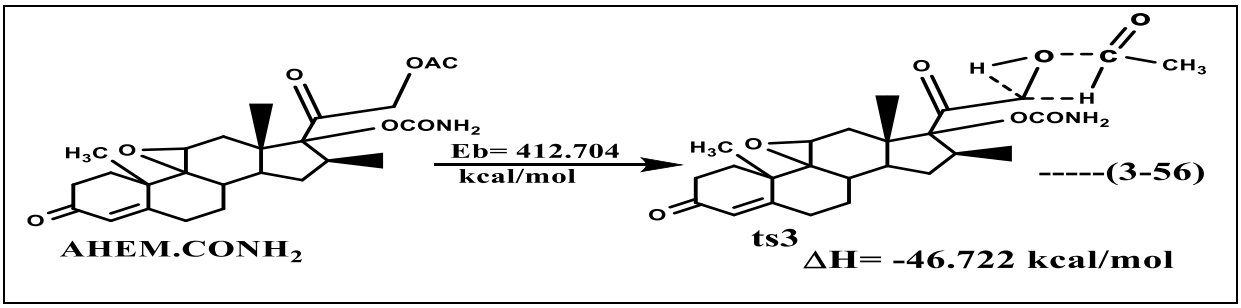

TS3 suffers from rearrangement and 1,2 dehydration to gives $DHEM.CONH_2$ and acetaldehyde molecule at E_b= -96.826 kCal/mol and ΔH= -525.995 kCal/mol.

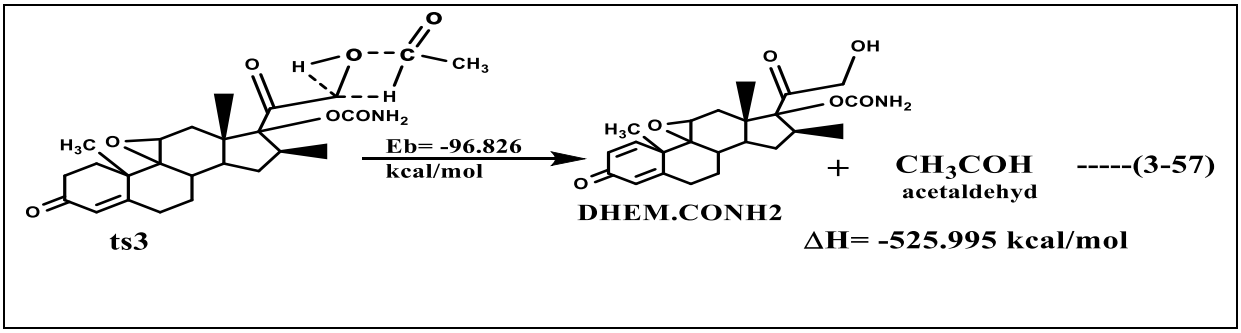

In the eleventh step, DHEM.$CONH_2$ is reacted with hydrogen fluoride to give the TS4 at E_b= 396.226 kCal/mol and ΔH= 98.07 kCal/mol.

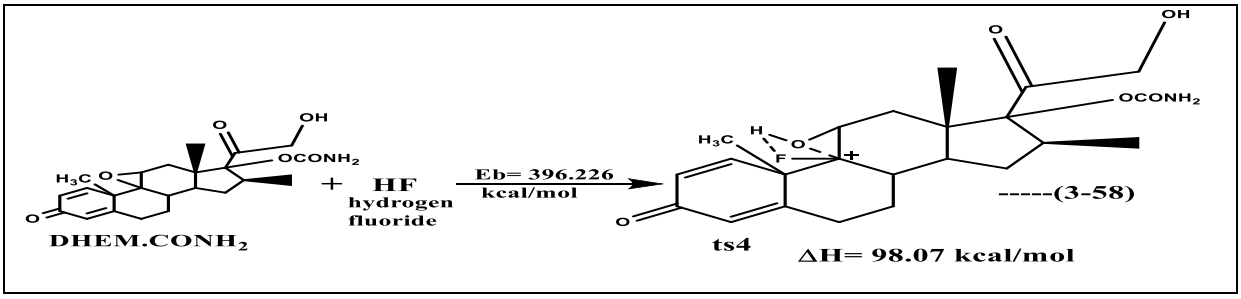

After that TS4 which in turn dissociation to Betamethasone.$CONH_2$ derivative at E_b= -338.788 kCal/mol and ΔH= -408.437 kCal/mol.

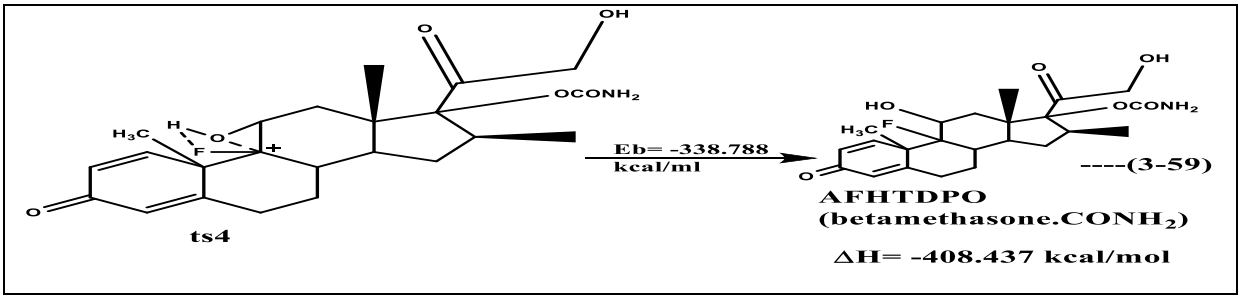

the net equation (3-88) illustrates formation of FHACPC(Betamethasone.$CONH_2$) derivative is exothermic reaction at the reaction enthalpy change equal to -1576.349 kCal/mol.

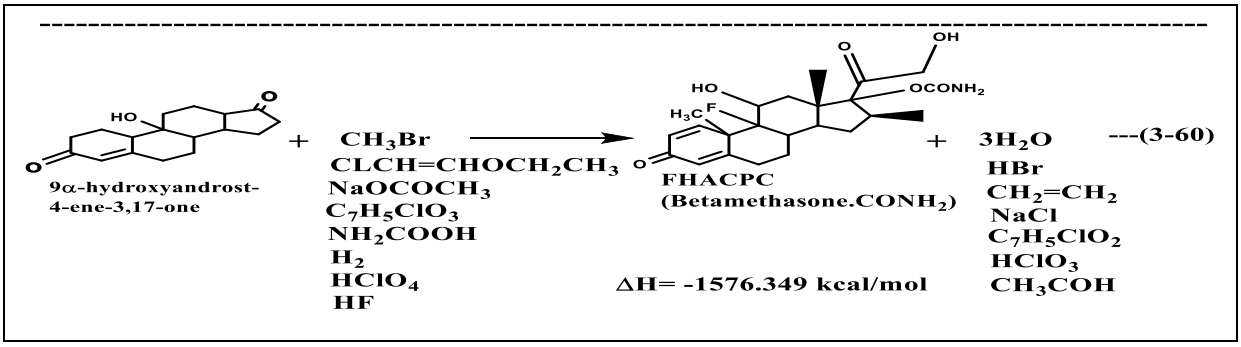

3-5 Comparative of major transition states:

To compare between original moiety of Betamethasone and new suggested derivatives. Transition state formation for reactions eight and nine will be estimation to find the optimized transited state of derivatives. Figure (3-20) shows geometry optimized view of transition states formation through rate determinate step for original molecule of betamethasone and their new derivatives. To compare the energetic properties of these transition states, Table (3-17) show numerical values for the energetic properties of each the original betamethasone and their suggested derivatives. We found the total energy value of geometry optimized transition state for betamethasone is equal to -110444.927 kCal/mol. This value of energy liberated through relaxation process is lowest than for the newest transition states of suggested derivatives. At the same time, the fourth suggested derivative (FHACPC(Beta.$CONH_{2)}$) has the largest value of energy liberated(-130713.608 kCal/mol) through relaxation process than original betamethasone and other suggested derivatives. The Binding energy value of transition state for betamethasone, which has the lowest value (-5833.301 kCal/mol) than other transition states of suggested derivatives, while the second suggested derivatives(EFHTDPO(Beta.$NHCH_2CH_3$)) liberated -6980.832 kCal/mol than original betamethasone and other derivatives. Heat of formation values are described another factor, since the transition state of Betamethasone needed to absorb 233.117 kCal/mol of formation, while the other transition states of first

and second suggested derivatives (AFHTDPO (Beta.NH_2) and EFHTDPO(Beta.$NHCH_2CH_3$)) are liberated -111.421 and -118.032 kCal/mol respectively. The important factor of comparison between the transition state formation for the Betamethasone and their suggested derivatives is zero point energy. Transition state of betamethasone has lowest reactivity to give product by 314.278 kCal/mol. Transition states for both the second and third derivatives (EFHTDPO(Beta.$NHCH_2CH_3$) and FHCPCC(Beta. COOH)) are the most reactive transition states than other derivatives with 358.376 and 348.659 kCal/mol respectively to release the desired product of reaction.

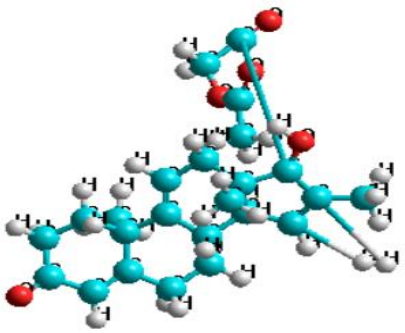

Transition state of
Betamethasone Molecule

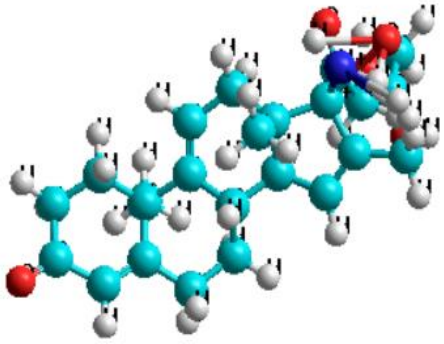

Transition state of Betamethasone.NH2

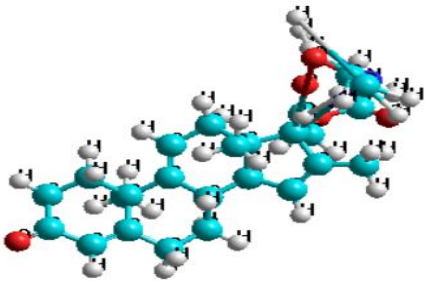

Transition state of
Betamethasone.NHCH2CH3

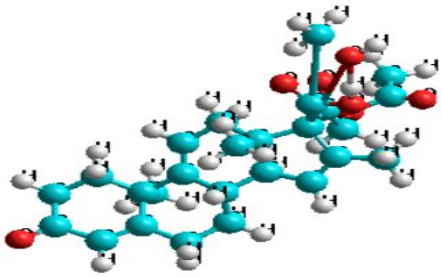

Transition state of
Betamethasone.COOH

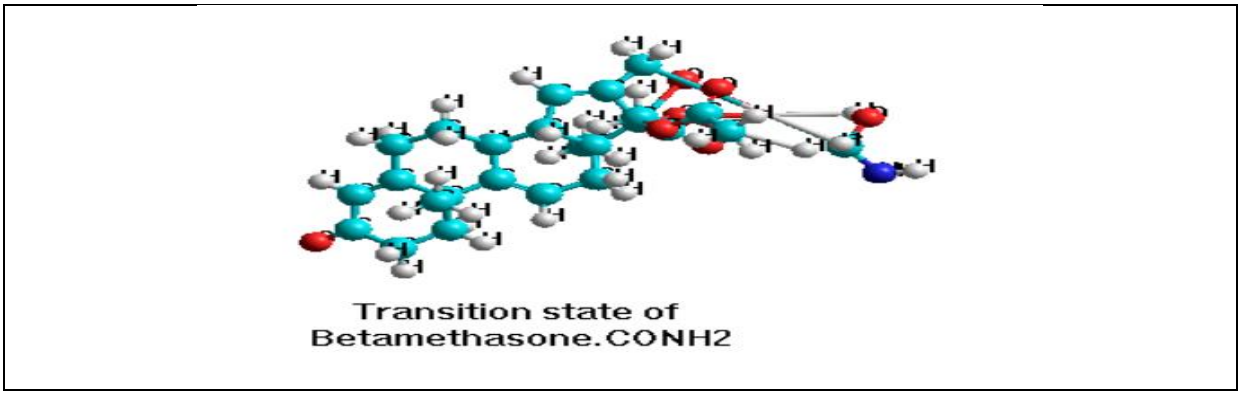

Figure (3-20).Geometry optimization structure of transition states of Betamethasone and their derivatives

Table (3-17). Comparative for energetic properties of transition states of Betamethasone and their derivatives

Transition states	Total energy kCal/mol	Binding energy kCal/mol	Heat of formation kCal/mol	Zero-point energy kCal/mol	Dipole moment Debye	Imaginary frequency
Betamethasone	-110444.927	-5833.301	233.117	314.278	42.935	-
AFHTDPO (Beta.NH_2)	-122502.061	-6424.034	-111.421	330.376	1.722	-
EFHTDPO (Beta.$NHCH_2CH_3$)	-129394.916	-6980.832	-118.032	358.376	4.586	-
FHCPCC (Beta. COOH)	-130071.197	-6421.435	210.085	348.659	40.928	-
FHACPC (Beta.$CONH_2$)	-130713.608	-6295.662	225.866	341.543	29.672	-

3-6 Comparative of Global index Chemical Reactivity

Second comparative was conducted in terms of chemical reactivity that's an excellent indicator to characterize of local reactivity in molecules[113], [192].

Comparative according to Global index values of Betamethasone compound and four new derivatives are shown in Table (3-19). Both of the EFHTDPO(beta.$NHCH_2CH_3$) and AFHTDPO(beta.NH_2) derivatives have lower stability, higher activity and softness molecules more than other derivatives due to have the lower values of E_{gap} which equal to 9.069 ev and 9.47 eV respectively[193], [194]. The dipole moment in a compound is relies on the distribution of positive and negative charges. The dipole moment is raised when

the electronic density of atoms increases, and all atoms contribute one or two pair electrons, thus increasing electron density [195], Therefore the EFHTDPO(beta.$NHCH_2CH_3$) and AFHTDPO(beta.NH_2) derivatives have higher values of the dipole moment that equal to 6.975 eV and 5.547 respectively, because they contain of $CH_3CH_2NH_2$ and NH_2 functional groups which in turn increase the electron density of the molecules because these functional groups are donating electrons.

According to the results in Table (3-18) the EFHTDPO(beta.$NHCH_2CH_3$) and AFHTDPO(beta.NH_2) derivatives have been lower stability, higher activity more than other derivatives due to have low values of ionization potential that equal to 9.489 eV and 9.815 eV respectively.

The chemical hardness of a molecule is represented by the HOMO-LUMO gap. Increases in hardness result in the system's movement towards a more stable configure ration. High values of softness would lead to increased chemical reactivity[196] . The EFHTDPO(beta.$NHCH_2CH_3$) and AFHTDPO(beta.NH_2) derivatives have been higher reactivity than other derivatives due to low values of hardness which equal to 4.535 eV and 4.735 eV while have high values of softness that equal to 0.110 ev and 0.105 eV respectively .the low values of electrophilicity is a good nucleophile while higher values signals a good electrophile[197].

The obtained results showed lower dissociation energy equal to 33.35 kcal/mol than other bonds. Substituted functional groups are globally recognized groups in drug manufacturing that have a significant impact on drug characteristics, such as $–NH_2$,-$CH_3CH_2NH_2$,-COOH and -$CONH_2$ [178]. After substituted four different functional group at active site on the Betamethasone compound, estimated the structure energetic properties for all derivatives and compare between them.

Table(3-18).Global index values of Betamethasone compound and four new derivatives

Global index	betamethasone	AFHTDPO (beta.NH_2)	EFHTDPO (beta.$NHCH_2CH_3$)	FHCPCC (beta.COOH)	FHACPC (beta.$CONH_2$)
Total energy (Kcal/mol)	-114446.232	-111766.974	-118654.883	-123949.713	-128041.883
Dipole moment$_{(Debye)}$	4.513	6.975	5.547	6.032	4.503
Energy of HOMO$_{(ev)}$	-10.126	-9.815	-9.489	-10.148	-10.187
Energy of LUMO$_{(ev)}$	-0.468	-0.345	-0.420	-0.404	-0.515
Egap $_{(ev)}$	9.658	9.47	9.069	9.744	9.672
$\mu_{(ev)}$	-5.297	-5.08	-4.955	-5.276	-5.351
IP$_{(ev)}$	10.126	9.815	9.489	10.148	10.187
EA$_{(ev)}$	0.468	0.345	0.420	0.404	0.515
$X_{(ev)}$	5.297	5.08	4.955	5.276	5.351
$\eta_{(ev)}$	4.829	4.735	4.535	4.872	4.836
$S_{(ev)}$	0.104	0.105	0.110	0.102	0.102
$\omega_{(ev)}$	2.905	2.725	2.707	2.857	2.960
ΔN	1.096	1.072	1.092	1.083	1.106

3-7 **Energetic comparative:**

Table (3-20) shows a comparison for energetic properties of betamethasone and their proposed derivatives. It was found, that the two derivatives EFHTDPO(Beta.$NHCH_2CH_3$) and AFHTDPO(Beta.NH_2) are more effective than betamethasone drug due to they have lower values of E_{gap} and higher values of zero-point energy. EFHTDPO(Beta.$NHCH_2CH_3$) derivative is highest effectiveness due to has lower value of E_{gap} equal to 9.069 eV while AFHTDPO(Beta.NH_2) derivative has E_{gap} equal to 9.47 eV.

Table(3-19):Structural energetic properties of Betamethasone and their derivatives

Derivatives	Total Energy kcal/mol	Heat of formation kCal/mol	Zero-point Energy kCal/mol	Energy of HOMO eV	Energy of LUMO eV	Egap eV
Betamethasone	-114446.232	-232.383	302.619	-10.126	-0.468	9.658
AFHTDPO(Beta.NH_2)	-111766.974	-183.885	309.986	-9.815	-0.345	9.47
EFHTDPO(Beta.NHCH_2CH_3)	-118654.883	-185.549	346.347	-9.489	-0.420	9.069
FHCPCC(Beta.COOH)	-123949.713	-267.824	308.777	-10.148	-0.404	9.744
FHACPC(Beta.CONH_2)	-128041.883	-258.679	318.663	-10.187	-0.515	9.672

3-8 CONCLOUSIONS

From the obtained results in the current study it can be concluded the following points.

1. Geometry optimization structure of Betamethasone showed total energy and energy gap equal to -1331.653 a.u and 0.079 eV, respectively.
2. Chemical reactivity of Betamethasone is controlled through the O_5-H_{30} bond, which is appeared most probable to break down with bond dissociation energy equal to 33.35 kCal/mol.
3. Theoretical spectra gave good identification to some clear peaks of Betamethasone molecule as well as showing identical parameters for functional groups of drug comparatively with practical data.
4. Mass spectra of Betamethasone illustrate appearance of a molecular ion equal to (392.3 m/z^+) which confirms the validity of the molecular structure of Betamethasone drug.
5. Betamethasone synthesis from (9-α OH-AD) as the starting material which is reacted in sequentially steps to yield ΔH= - 452.406 kCal/mol.
6. Four new models are suggested as anti Covied-19 drugs by substituted functional groups on the original structure of Betamethasone.
7. Two new suggested models of anti Covied-19 drugs were more chemical effectively [AFHTDPO(Betamethasone.NH_2) and EFHTDPO(Betamethasone.$NHCH_2CH_3$)] than the Betamethasone molecule while FHCPCC(Betamethasone. COOH) and FHACPC(Betamethasone.$CONH_2$) are less chemical effective.

3-9 Recommendations

1. Investigation chemical reactivity of O_5-H_{30} bond in all derivatives .
2. Estimation chemical reactivity of derivatives toward the chemical reactions with DNA-bases.
3. Preparation new derivatives to conduct on their chemical properties and after that compare with their theoretical data.
4. Investigation antibacterial activities for the preparative derivatives of Betamethasone must be examine.

References

[1] A. Stylee, “SARS-CoV-2, a member of the subfamily Coronavirinae Virus classification e.”

[2] E. V Koonin, T. G. Senkevich, and V. V Dolja, “The ancient Virus World and evolution of cells,” *Biol. Direct*, vol. 1, no. 1, pp. 1–27, 2006.

[3] E. V Koonin and P. Starokadomskyy, “Are viruses alive? The replicator paradigm sheds decisive light on an old but misguided question,” *Stud. Hist. Philos. Sci. part C Stud. Hist. Philos. Biol. Biomed. Sci.*, vol. 59, pp. 125–134, 2016.

[4] E. Rybicki, “The classification of organisms at the edge of life or problems with virus systematics,” *S. Afr. J. Sci.*, vol. 86, no. 4, p. 182, 1990.

[5] E. C. Holmes, “Viral evolution in the genomic age,” *PLoS Biol.*, vol. 5, no. 10, p. e278, 2007.

[6] D. Khaykelson and U. Raviv, “Studying viruses using solution X-ray scattering,” *Biophys. Rev.*, vol. 12, no. 1, pp. 41–48, 2020.

[7] J. C. Vázquez and D. Redolar-Ripoll, “COVID-19 outbreak impact in Spain: A role for tobacco smoking?,” *Tob. Induc. Dis.*, vol. 18, 2020.

[8] H. Nishiura, Hiroshi Jung, Sung-mok Linton, Natalie M Kinoshita, Ryo Yang, Yichi Hayashi, Katsuma Kobayashi, Tetsuro Yuan, Baoyin Akhmetzhanov and Andrei R ., “The extent of transmission of novel coronavirus in Wuhan, China, 2020,” *Journal of clinical medicine*, vol. 9, no. 2. Multidisciplinary Digital Publishing Institute, p. 330, 2020.

[9] A. Hafeez, S. Ahmad, S. A. Siddqui, M. Ahmad, and S. Mishra, “A review of COVID-19 (Coronavirus Disease-2019) diagnosis, treatments and prevention,” *EJMO*, vol. 4, no. 2, pp. 116–125, 2020.

[10] D. Neil, Desley Moran, Linda Horsfield, Catherine Curtis, Elizabeth Swann, Olivia Barclay, Wendy Hanley, Brian Hollinshead, Michael Roufosse and Candice., “Ultrastructure of cell trafficking pathways and coronavirus: how to recognise the wolf amongst the sheep,” *J. Pathol.*, vol. 252, no. 4, pp. 346–357, 2020.

[11] Z.-L. Chen, Ze-Liang Zhang, Wen-Jun Lu, Yi Guo, Cheng Guo, Zhong-Min Liao, Cong-Hui Zhang, Xi Zhang, Yi Han, Xiao-Hu Li and Qian-Lin ., “From severe acute respiratory syndrome-associated coronavirus to 2019 novel coronavirus outbreak: similarities in the early epidemics and prediction of future trends,” *Chin. Med. J. (Engl).*, vol. 133, no. 9, p. 1112, 2020.

[12] Y. Bai, Yan Yao, Lingsheng Wei, Ta Tian, Fei Jin, Dong-YanChen, Lijuan Wang and Meiyun ., “Presumed asymptomatic carrier transmission of COVID-19,” *Jama*, vol. 323, no. 14, pp. 1406–1407, 2020.

[13] W. H. Organization, “Infection prevention and control during health care when novel coronavirus (nCoV) infection is suspected: interim guidance, 25 January 2020,” World Health Organization, 2020.

[14] Q. Ma, Qinhai Li, Runfeng Pan, Weiqi Huang, Wenbo Liu, Bin Xie, Yuqi Wang, ZhoulangLi, Chufang Jiang, Haiming Huang and Jicheng ., “Phillyrin (KD-1) exerts anti-viral and anti-inflammatory activities against novel coronavirus (SARS-CoV-2) and human coronavirus 229E (HCoV-229E) by suppressing the nuclear factor kappa B (NF-κB) signaling pathway,” *Phytomedicine*, vol. 78, p. 153296, 2020.

[15] A. R. Fehr and S. Perlman, “Coronaviruses: an overview of their replication and pathogenesis,” *Coronaviruses*, pp. 1–23, 2015.

[16] E. De Wit, N. Van Doremalen, D. Falzarano, and V. J. Munster, “SARS and MERS: recent insights into emerging coronaviruses,” *Nat. Rev. Microbiol.*, vol. 14, no. 8, pp. 523–534, 2016.

[17] P. Zhou, Peng Yang, Xing-Lou Wang, Xian-Guang Hu, Ben Zhang, Lei Zhang, Wei Si, Hao-Rui Zhu, Yan Li, Bei Huang and Chao-Lin ., “A pneumonia outbreak associated with a new coronavirus of probable bat origin,” *Nature*, vol. 579, no. 7798, pp. 270–273, 2020.

[18] F. B. Mayr, Florian B Yende, Sachin Linde-Zwirble, Walter T Peck-Palmer, Octavia M Barnato, Amber E Weissfeld, Lisa A Angus and Derek C ., “Infection rate and acute organ dysfunction risk as explanations for racial differences in severe sepsis,” *Jama*, vol. 303, no. 24, pp. 2495–2503, 2010.

[19] E. E. Team, “Note from the editors: World Health Organization declares novel coronavirus (2019-nCoV) sixth public health emergency of international concern,” *Eurosurveillance*, vol. 25, no. 5, p. 200131e, 2020.

[20] J. Acosta-Quiroz and S. Iglesias-Osores, “Salud mental en trabajadores expuestos a COVID-19,” *Rev. Neuropsiquiatr.*, vol. 83, no. 3, pp. 212–213, 2020.

[21] W. Y. M. Ren-LL and Z. Q. Wu, “Identification of a novel coronavirus causing severe pneumonia in human,” *Chin Med J*, vol. 133, no. 9, pp. 1015–1024, 2020.

[22] X. Yang, Xiaobo Yu, Yuan Xu, Jiqian Shu, Huaqing Liu, Hong Wu, Yongran Zhang, Lu Yu, Zhui Fang, Minghao Yu and Ting ., "Clinical course and outcomes of critically ill patients with SARS-CoV-2 pneumonia in Wuhan, China: a single-centered, retrospective, observational study," *Lancet Respir. Med.*, vol. 8, no. 5, pp. 475–481, 2020.

[23] R. V. Kashid, A. A. Shidhore, M. M. Kazi, and S. Patil, "Awareness of COVID-19 amongst undergraduate dental students in India–A questionnaire based cross-sectional study," 2020.

[24] C. Huang, Chaolin Wang, Yeming Li, Xingwang Ren, LiliZhao, JianpingnHu, Yi Zhang, LiFan, Guohui Xu, Jiuyang Gu and Xiaoying ., "Clinical features of patients infected with 2019 novel coronavirus in Wuhan, China," *Lancet*, vol. 395, no. 10223, pp. 497–506, 2020.

[25] J. Koh, S. U. Shah, P. E. Y. Chua, H. Gui, and J. Pang, "Epidemiological and clinical characteristics of cases during the early phase of COVID-19 pandemic: a systematic review and meta-analysis," *Front. Med.*, vol. 7, p. 295, 2020.

[26] S. Law, A. W. Leung, and C. Xu, "Severe acute respiratory syndrome (SARS) and coronavirus disease-2019 (COVID-19): From causes to preventions in Hong Kong," *Int. J. Infect. Dis.*, vol. 94, pp. 156–163, 2020.

[27] A. Zumla, J. F. W. Chan, E. I. Azhar, D. S. C. Hui, and K.-Y. Yuen, "Coronaviruses—drug discovery and therapeutic options," *Nat. Rev. Drug Discov.*, vol. 15, no. 5, pp. 327–347, 2016.

[28] M. L. Holshue, C. DeBolt, and S. Lindquist, "Clinical characteristics of coronavirus disease 2019 in China," *N Eng J Med*, vol. 382, pp. 1–13, 2020.

[29] A. Bhimraj, Adarsh Morgan, Rebecca L Shumaker, Amy Hirsch Lavergne, Valery Baden, Lindseyn Cheng, Vincent Chi-Chung Edwards, Kathryn M Gandhi, Rajesh Muller, William J O'Horo and John C ., "Infectious Diseases Society of America guidelines on the treatment and management of patients with COVID-19," *Clin. Infect. Dis.*, 2020.

[30] J. M. Sanders, M. L. Monogue, T. Z. Jodlowski, and J. B. Cutrell, "Pharmacologic treatments for coronavirus disease 2019 (COVID-19): a review," *Jama*, vol. 323, no. 18, pp. 1824–1836, 2020.

[31] J. Gao and S. Hu, "Update on use of chloroquine/hydroxychloroquine to treat coronavirus disease 2019 (COVID-19)," *Biosci. Trends*, 2020.

[32] N. J. Mercuro, Nicholas J Yen, Christina F Shim, David J Maher, Timothy R McCoy, Christopher M Zimetbaum, Peter J Gold and Howard S ., "Risk of QT interval prolongation associated with use of hydroxychloroquine with or without concomitant azithromycin among hospitalized patients testing positive for coronavirus disease 2019 (COVID-19)," *JAMA Cardiol.*, vol. 5, no. 9, pp. 1036–1041, 2020.

[33] L. Zhang and Y. Liu, "Potential interventions for novel coronavirus in China: A systematic review," *J. Med. Virol.*, vol. 92, no. 5, pp. 479–490, 2020.

[34] W. B. PGrant, W B Lahore, H McDonnell, S L Baggerly, C A French, C B Aliano and J L Bhattoa, H ., "Evidence that vitamin D supplementation could reduce risk of influenza and COVID-19 infections and deaths. Nutrients. 2020; 12 (4): 988," *Extern. Resour. Crossref*, 2020.

[35] P. Bergman, Å. U. Lindh, L. Björkhem-Bergman, and J. D. Lindh, "Vitamin D and respiratory tract infections: a systematic review and meta-analysis of randomized controlled trials," *PLoS One*, vol. 8, no. 6, p. e65835, 2013.

[36] A. Özdemir, H. Kazdal, L. Kazancıoğlu, T. Koyuncu, A. Hızal, and T. Ersöz, "Adjuvan Tedavilerin COVID-19 Pozitif Yoğun Bakım Hastaların Morbidite ve Mortalitelerine Etkisi," *Turk J Intensive Care*, vol. 18, pp. 31–38, 2020.

[37] M. Elhidsi, F. Fachrucha, and R. Y. Irawan, "N-Acetylcysteine for COVID-19: A Potential Adjuvant Therapy," *J. Heal. Sci.*, vol. 11, no. 1, pp. 1–6, 2021.

[38] V. Haage, Verena de Oliveira-Filho, Edmilson Ferreira Moreira-Soto, Andres Kühne, Arne Fischer, Carlo Sacks, Jilian A Corman, Victor Max Müller, Marcel A Drosten, Christian Drexler and Jan Felix ., "Impaired performance of SARS-CoV-2 antigen-detecting rapid tests at elevated and low temperatures," *J. Clin. Virol.*, 2021.

[39] J.M. Pérez, Jesús M Molina, Lucía Ureña-Gutiérrez, Benjamín Espinosa, José López-Montoya, Antonio J Boos, Mathieu Granados, José E Cano-Manuel, Francisco J Azorit and Concepción., "Individual stress responses to Sarcoptes scabiei infestation in Iberian ibex, Capra pyrenaica," *Gen. Comp. Endocrinol.*, vol. 281, pp. 1–6, 2019.

[40] J. Vandewalle, A. Luypaert, K. De Bosscher, and C. Libert, "Therapeutic mechanisms of glucocorticoids," *Trends Endocrinol. Metab.*, vol. 29, no. 1, pp. 42–54, 2018.

[41] L. Mazzini, Letizia Gelati, Maurizio Profico, Daniela Celeste Sgaravizzi, Giada Pensi, Massimo Projetti Muzi, Gianmarco Ricciolini, Claudia Nodari, Laura Rota Carletti, Sandro Giorgi and Cesare ., "Human neural stem cell transplantation in ALS: initial results from a phase I trial," *J. Transl. Med.*, vol. 13, no. 1, pp. 1–16, 2015.

[42] L. Rahimi, A. Rajpal, and F. Ismail-Beigi, "Glucocorticoid-induced fatty liver disease," *Diabetes, Metab. Syndr. Obes. targets Ther.*, vol. 13, p. 1133, 2020.

[43] D. Cruz-Topete and J. A. Cidlowski, "One hormone, two actions: anti-and pro-inflammatory effects of glucocorticoids," *Neuroimmunomodulation*, vol. 22, no. 1–2, pp. 20–32, 2015.

[44] C. MacLeod, P. W. F. Hadoke, and M. Nixon, "Glucocorticoids: Fuelling the Fire of Atherosclerosis or Therapeutic Extinguishers?," *Int. J. Mol. Sci.*, vol. 22, no. 14, p. 7622, 2021.

[45] F. A. Britto, Florian A Cortade, Fabienne Belloum, Yassine Blaquière, Marine Gallot, Yann S Docquier, Aurélie Pagano, Allan F Jublanc, Elodie Bendridi, Nadia Koechlin-Ramonatxo, Christelle ., "Glucocorticoid-dependent REDD1 expression reduces muscle metabolism to enable adaptation under energetic stress," *BMC Biol.*, vol. 16, no. 1, pp. 1–17, 2018.

[46] M. L. Kmieć, A. Pajor, and G. Broniarczyk-Dyła, "Evaluation of biophysical skin parameters and assessment of hair growth in patients with acne treated with isotretinoin.," *Postep. dermatologii i Alergol.*, vol. 30, no. 6, pp. 343–349, Dec. 2013, doi: 10.5114/pdia.2013.39432.

[47] P. Pharmacopoeia, "Polish Pharmaceutical Society," *Warsaw, Pol.*, 2011.

[48] M. V Donova, "Transformation of steroids by actinobacteria: a review," *Appl. Biochem. Microbiol.*, vol. 43, no. 1, pp. 1–14, 2007.

[49] T. S. Savinova, T S Dovbnya, D V Khomutov, S M Kazantsev, A V Huy, L D Lukashev and N V Donova, M V ., "Conversion of Soybean Phytosterol into Androsta-4, 9 (11)-diene-3, 17-dione," *Appl. Biochem. Microbiol.*, vol. 56, no. 4, pp. 459–466, 2020.

[50] T. G. Lobastova, S. M. Khomutov, A. A. Shutov, and M. V Donova, "Microbiological synthesis of stereoisomeric 7 (α/β)-hydroxytestololactones and 7 (α/β)-hydroxytestolactones," *Appl. Microbiol. Biotechnol.*, vol. 103, no. 12, pp. 4967–4976, 2019.

[51] J. Tang, X. Liu, C. Zeng, H. Meng, M. Tian, and C. Guo, "A novel route for the preparation of betamethasone from 9α-hydroxyandrost-4-ene-3, 17-dione (9αOH-AD) by chemical synthesis and fermentation," *J. Chem. Res.*, vol. 41, no. 5, pp. 266–270, 2017.

[52] L. Uva, Luís Miguel, Diana Pinheiro, Catarina Antunes, Joana Cruz, Diogo Ferreira, Joao Filipe, Paulo., "Mechanisms of action of topical corticosteroids in psoriasis," *Int. J. Endocrinol.*, vol. 2012, 2012.

[53] F. F. Abrantes, Fabiano Ferreira Moraes, Marianna Pinheiro Moraes de Albuquerque Filho, José Marcos Vieira de Alencar, Jéssica Monique Dias Lopes, Alexandre Bussinger Pinto, Wladimir Bocca Vieira de Rezende Souza, Paulo Victor Sgobbi de Oliveira, Enedina Maria Lobato de Oliveira, Acary de Souza Bulle de Pedroso and José Luiz ., "Immunosuppressors and immunomodulators in Neurology-Part I: a guide for management of patients underimmunotherapy," *Arq. Neuropsiquiatr.*, vol. 79, pp. 1012–1025, 2021.

[54] L. Ni, Y. Pan, C. Tang, W. Xiong, X. Wu, and C. Zou, "Antenatal exposure to betamethasone induces placental 11β-hydroxysteroid dehydrogenase type 2 expression and the adult metabolic disorders in mice," *PLoS One*, vol. 13, no. 9, p. e0203802, 2018.

[55] G. Sliwoski, S. Kothiwale, J. Meiler, and E. W. Lowe, “Computational methods in drug discovery,” *Pharmacol. Rev.*, vol. 66, no. 1, pp. 334–395, 2014.

[56] M. De Vivo, M. Masetti, G. Bottegoni, and A. Cavalli, “Role of molecular dynamics and related methods in drug discovery,” *J. Med. Chem.*, vol. 59, no. 9, pp. 4035–4061, 2016.

[57] A. F. Eweas, I. A. Maghrabi, and A. I. Namarneh, “Advances in molecular modeling and docking as a tool for modern drug discovery,” *Der Pharma Chem.*, vol. 6, no. 6, pp. 211–228, 2014.

[58] L. A. Vu, P. T. C. Quyen, and N. T. Huong, “In silico drug design: Prospective for drug lead discovery,” *Int. J. Eng. Sci. Invent.*, vol. 4, no. 10, pp. 2319–6734, 2015.

[59] L. Di and E. Kerns, *Drug-like properties: concepts, structure design and methods from ADME to toxicity optimization*. Academic press, 2015.

[60] A. W. Dombrowski, A. L. Aguirre, A. Shrestha, K. A. Sarris, and Y. Wang, “The Chosen Few: Parallel Library Reaction Methodologies for Drug Discovery,” *J. Org. Chem.*, 2021.

[61] F. Mao, Fei Ni, Wei Xu, Xiang Wang, Hui Wang, Jing Ji, Min Li and Jian ., “Chemical structure-related drug-like criteria of global approved drugs,” *Molecules*, vol. 21, no. 1, p. 75, 2016.

[62] S. Purser, P. R. Moore, S. Swallow, and V. Gouverneur, “Fluorine in medicinal chemistry,” *Chem. Soc. Rev.*, vol. 37, no. 2, pp. 320–330, 2008.

[63] H. Mei, J. Han, S. Fustero, R. Román, R. Ruzziconi, and V. A. Soloshonok, “Recent progress in the application of fluorinated chiral sulfinimine reagents,” *J. Fluor. Chem.*, vol. 216, pp. 57–70, 2018.

[64] P. Shah and A. D. Westwell, “The role of fluorine in medicinal chemistry,” *J. Enzyme Inhib. Med. Chem.*, vol. 22, no. 5, pp. 527–540, 2007.

[65] K. L. Kirk, “Fluorine in medicinal chemistry: Recent therapeutic applications of fluorinated small molecules,” *J. Fluor. Chem.*, vol. 127, no. 8, pp. 1013–1029, 2006.

[66] C. J. Cramer, *Essentials of computational chemistry: theories and models*. John Wiley & Sons, 2013.

[67] P. Ramasami, “A Learning Experience: Conformational Studies of Ethane and 1, 2-Disubstituted ethanes using Molecular Mechanics,” *Guid. Contrib. to Aust. J. Educ. Chem.*, p. 16, 2005.

[68] S. Sowlati Hashjin, “Computational investigations of some molecular properties, their perturbation by external electric fields, and their use in quantitative structure-to-activity relationships,” 2013.

[69] R. J. Weber, *Computational modeling of small molecules*. University of North Texas, 2015.

[70] J. B. Foresman, “Computational Chemistry: A Practical Guide for Applying Techniques to Real World Problems By David Young (Cytoclonal Pharmaceutics Inc.). Wiley-Interscience: New York. 2001. xxvi+ 382 pp. $69.95. ISBN: 0-471-33368-9.” ACS Publications, 2001.

[71] E. G. Lewars, “Introduction to Quantum Mechanics in Computational Chemistry,” in *Computational Chemistry*, Springer, 2016, pp. 101–191.

[72] P. W. Atkins and R. S. Friedman, *Molecular quantum mechanics*. Oxford University press, 2011.

[73] C. B. R. Santos, Cleydson B R Lobato, Cleison C Braga, Francinaldo S Morais, Sílvia S S Santos, Cesar F Fernandes, Caio P Brasil, Davi S B Hage-Melim, Loran IS Macêdo, Williams J C Carvalho and José C T ., "Application of Hartree-Fock method for modeling of bioactive molecules using SAR and QSPR," *Comput. Mol. Biosci.*, vol. 2014, 2014.

[74] M. W. Schmidt, Michael W Baldridge, Kim K Boatz, Jerry A Elbert, Steven T Gordon, Mark S Jensen, Jan H Koseki, Shiro Matsunaga, Nikita Nguyen, Kiet A Su and Shujun ., "General atomic and molecular electronic structure system," *J. Comput. Chem.*, vol. 14, no. 11, pp. 1347–1363, 1993.

[75] B. N. Plakhutin, E. V Gorelik, and N. N. Breslavskaya, "Koopmans' theorem in the ROHF method: Canonical form for the Hartree-Fock Hamiltonian," *J. Chem. Phys.*, vol. 125, no. 20, p. 204110, 2006.

[76] E. R. Davidson and B. N. Plakhutin, "Koopmans's theorem in the restricted open-shell Hartree–Fock method. II. The second canonical set for orbitals and orbital energies," *J. Chem. Phys.*, vol. 132, no. 18, p. 184110, 2010.

[77] B. N. Plakhutin and E. R. Davidson, "Canonical form of the Hartree-Fock orbitals in open-shell systems," *J. Chem. Phys.*, vol. 140, no. 1, p. 14102, 2014.

[78] K. R. Glaesemann and M. W. Schmidt, "On the ordering of orbital energies in high-spin ROHF," *J. Phys. Chem. A*, vol. 114, no. 33, pp. 8772–8777, 2010.

[79] M. T. Hussein and T. Kasim, "Ab–initio method with Density Functional Theory using to Study of the electronic structure and mechanical properties of BN Nanocrystals," 2016.

[80] M.-C. Kim, E. Sim, and K. Burke, “Ions in solution: Density corrected density functional theory (DC-DFT),” *J. Chem. Phys.*, vol. 140, no. 18, p. 18A528, 2014.

[81] D. J. Singh, “Density functional theory and applications to transition metal oxides,” *Correl. electrons from Model. to Mater.*, vol. 2, pp. 1–2, 2012.

[82] V. K. Shukla, “Vibrational analysis and electronic structure Calculations of small organic molecules using first Principles,” 2015.

[83] J. Kwon, “Applications of semi-empirical quantum mechanical calculations to simple molecular systems.” 2012.

[84] P. O. Dral, Pavlo O Wu, Xin Spörkel, Lasse Koslowski, Axel Weber, Wolfgang Steiger, Rainer Scholten, Mirjam Thiel and Walter ., “Semiempirical quantum-chemical orthogonalization-corrected methods: theory, implementation, and parameters,” *J. Chem. Theory Comput.*, vol. 12, no. 3, pp. 1082–1096, 2016.

[85] R. C. Bingham, M. J. S. Dewar, and D. H. Lo, “Ground states of molecules. XXV. MINDO/3. Improved version of the MINDO semiempirical SCF-MO method,” *J. Am. Chem. Soc.*, vol. 97, no. 6, pp. 1285–1293, 1975.

[86] J. A. Pople, M. Head-Gordon, and K. Raghavachari, “Quadratic configuration interaction. A general technique for determining electron correlation energies,” *J. Chem. Phys.*, vol. 87, no. 10, pp. 5968–5975, 1987.

[87] B. A. AL-Razak, R. R. A. AL-Ani, N. J. ALObaidi, and T. T. Al-Nahari, “Synthesis, Ab initio and PM3 studies of the 2-(5-Hydrazine-4H-1, 2, 4-Triazol-3-yl) Phenol and Some of Their Transition Metal Complexes,” *Al-Mustansiriyah J. Sci.*, vol. 21, no. 7, 2010.

[88] R. Szostak, J. Aubé, and M. Szostak, “Determination of Structures and Energetics of Small-and Medium-Sized One-Carbon-Bridged Twisted Amides using ab Initio Molecular Orbital Methods: Implications for Amidic Resonance along the C–N Rotational Pathway,” *J. Org. Chem.*, vol. 80, no. 16, pp. 7905–7927, 2015.

[89] A. K. Sachan, “Applications of ab initio quantum chemistry to small organic molecules,” 2015.

[90] M. Lepeltier, F. Morlet-Savary, B. Graff, J. Lalevée, D. Gigmes, and F. Dumur, “Efficient blue green organic light-emitting devices based on a monofluorinated heteroleptic iridium (III) complex,” *Synth. Met.*, vol. 199, pp. 139–146, 2015.

[91] J. C. Slater, “Atomic shielding constants,” *Phys. Rev.*, vol. 36, no. 1, p. 57, 1930.

[92] S. F. Boys, “Electronic wave functions-I. A general method of calculation for the stationary states of any molecular system,” *Proc. R. Soc. London. Ser. A. Math. Phys. Sci.*, vol. 200, no. 1063, pp. 542–554, 1950.

[93] H. Simka, B. G. Willis, I. Lengyel, and K. F. Jensen, “Computational chemistry predictions of reaction processes in organometallic vapor phase epitaxy,” *Prog. Cryst. growth Charact. Mater.*, vol. 35, no. 2–4, pp. 117–149, 1997.

[94] M. S. Gordon, J. S. Binkley, J. A. Pople, W. J. Pietro, and W. J. Hehre, “Self-consistent molecular-orbital methods. 22. Small split-valence basis sets for second-row elements,” *J. Am. Chem. Soc.*, vol. 104, no. 10, pp. 2797–2803, 1982.

[95] R. Ditchfield, W. J. Hehre, and J. A. Pople, “Self-consistent molecular-orbital methods. IX. An extended Gaussian-type basis for molecular-orbital studies of organic molecules,” *J. Chem. Phys.*, vol. 54, no. 2, pp. 724–728, 1971.

[96] A. V Mitin and K. M. Merz Jr, “Erratum: An improved 6-31G* basis set for atoms Ga through Kr,” *Int. J. Quantum Chem.*, vol. 109, no. 5, p. 1158, 2009.

[97] W. J. Hehre and W. A. Lathan, “Self-Consistent Molecular Orbital Methods. XIV. An Extended Gaussian-Type Basis for Molecular Orbital Studies of Organic Molecules. Inclusion of Second Row Elements,” *J. Chem. Phys.*, vol. 56, no. 11, pp. 5255–5257, 1972.

[98] M. P. McGrath, “On the 6-311G basis set of bromine,” *J. Chem. Phys.*, vol. 130, no. 17, p. 176101, 2009.

[99] M. C. J. Lee, “Correlations between MO Eigenvectors and the Thermochemistry of Simple Organic Molecules, Related to Empirical Bond Additivity Schemes.” The University of Waikato, 2008.

[100] F. Jensen, “Polarization consistent basis sets. III. The importance of diffuse functions,” *J. Chem. Phys.*, vol. 117, no. 20, pp. 9234–9240, 2002.

[101] B. L. Kormos, J. F. Liebman, and C. J. Cramer, “298 K enthalpies of formation of monofluorinated alkanes: theoretical predictions for methyl, ethyl, isopropyl and tert-butyl fluoride,” *J. Phys. Org. Chem.*, vol. 17, no. 8, pp. 656–664, 2004.

[102] V. Bakken and T. Helgaker, “The efficient optimization of molecular geometries using redundant internal coordinates,” *J. Chem. Phys.*, vol. 117, no. 20, pp. 9160–9174, 2002.

[103] D. E. Woon and T. H. Dunning Jr, “Gaussian basis sets for use in correlated molecular calculations. III. The atoms aluminum through argon,” *J. Chem. Phys.*, vol. 98, no. 2, pp. 1358–1371, 1993.

[104] E. G. Lewars, “The concept of the potential energy surface,” in *Computational Chemistry*, Springer, 2016, pp. 9–49.

[105] H. B. Schlegel, “Exploring potential energy surfaces for chemical reactions: an overview of some practical methods,” *J. Comput. Chem.*, vol. 24, no. 12, pp. 1514–1527, 2003.

[106] H. B. Schlegel, “Ab initio molecular dynamics with Born-Oppenheimer and extended Lagrangian methods using atom centered basis functions,” *Bull. Korean Chem. Soc.*, vol. 24, no. 6, pp. 837–842, 2003.

[107] J. Long, “Use of potential energy surfaces (PES) in spectroscopy and reaction dynamics,” 2010.

[108] W. Quapp, M. Hirsch, and D. Heidrich, “An approach to reaction path branching using valley–ridge inflection points of potential-energy surfaces,” *Theor. Chem. Acc.*, vol. 112, no. 1, pp. 40–51, 2004.

[109] K. L. Williamson and K. M. Masters, *Macroscale and microscale organic experiments*. Cengage Learning, 2016.

[110] C. Peng, P. Y. Ayala, H. B. Schlegel, and M. J. Frisch, “Using redundant internal coordinates to optimize equilibrium geometries and transition states,” *J. Comput. Chem.*, vol. 17, no. 1, pp. 49–56, 1996.

[111] H. B. Schlegel, “Geometry optimization,” *Wiley Interdiscip. Rev. Comput. Mol. Sci.*, vol. 1, no. 5, pp. 790–809, 2011.

[112] S. K. Burger and P. W. Ayers, “Methods for finding transition states on reduced potential energy surfaces,” *J. Chem. Phys.*, vol. 132, no. 23, p. 234110, 2010.

[113] J. Melin, F. Aparicio, V. Subramanian, M. Galván, and P. K. Chattaraj, “Is the Fukui Function a Right Descriptor of Hard− Hard Interactions?,” *J. Phys. Chem. A*, vol. 108, no. 13, pp. 2487–2491, 2004.

[114] J. Zevallos and A. Toro-Labbé, “A theoretical analysis of the Kohn-Sham and Hartree-Fock orbitals and their use in the determination of electronic properties,” *J. Chil. Chem. Soc.*, vol. 48, no. 4, pp. 39–47, 2003.

[115] J. P. Perdew, R. G. Parr, M. Levy, and J. L. Balduz Jr, “Density-functional theory for fractional particle number: derivative discontinuities of the energy,” *Phys. Rev. Lett.*, vol. 49, no. 23, p. 1691, 1982.

[116] S. Pal, R. Roy, and A. K. Chandra, “Change of hardness and chemical potential in chemical binding: a quantitative model,” *J. Phys. Chem.*, vol. 98, no. 9, pp. 2314–2317, 1994.

[117] P. O. Ameh and N. O. Eddy, “Theoretical and experimental studies on the corrosion inhibition potentials of 3-nitrobenzoic acid for mild steel in 0.1 M H2SO4,” *Cogent Chem.*, vol. 2, no. 1, p. 1253904, 2016.

[118] D. Sajan, K. U. Lakshmi, Y. Erdogdu, and I. H. Joe, “Molecular structure and vibrational spectra of 2, 6-bis (benzylidene) cyclohexanone: a density functional theoretical study,” *Spectrochim. Acta Part A Mol. Biomol. Spectrosc.*, vol. 78, no. 1, pp. 113–121, 2011.

[119] F. Ashrafi, V. Moeini, and F. A. Rostami, “Studying several physical and quantum properties of 1-hexyl-3-methylimidazoliumhexaflurorophosphate using density functional theory,” *J. Mol. Liq.*, vol. 229, pp. 27–30, 2017.

[120] C. R. Swartz, S. R. Parkin, J. E. Bullock, J. E. Anthony, A. C. Mayer, and G. G. Malliaras, "Synthesis and characterization of electron-deficient pentacenes," *Org. Lett.*, vol. 7, no. 15, pp. 3163–3166, 2005.

[121] D. H. Al-Amiedy, Z. A. Saleh, and R. K. Al-Yasari, "Calculating Structural, Electronics Structures, Electronic Properties and IR Spectra of Pentacene Molecule," *Int. J. Adv. Res. Phys. Sci. Vol.*, vol. 1, pp. 1–9, 2014.

[122] J. I. Gersten and F. W. Smith, *The physics and chemistry of materials*. Wiley New York, 2001.

[123] F. O. Essa, K. J. Kadhum, A. Abbas, and A. Drea, "Estimation of transition state and Synthesis of Barbituric Acid with their derivatives of 1, 3, 4-Thiadiazole," *J. Appl. Chem.*, vol. 1, no. 3, pp. 344–351, 2012.

[124] L. Shao, Lei Chen, Junsheng Wang, Chunxia Li, Ji-an Tang, Yumin Chen, Daijie Liu and Wen., "Characterization of a key aminoglycoside phosphotransferase in gentamicin biosynthesis," *Bioorg. Med. Chem. Lett.*, vol. 23, no. 5, pp. 1438–1441, 2013.

[125] S. Belaidi, R. Mazri, H. Belaidi, T. Lanez, and D. Bouzidi, "Electronic structure and physico-chemical property relationship for thiazole derivatives," *Asian J. Chem.*, vol. 25, no. 16, p. 9241, 2013.

[126] R. Singh, D. Kumar, Y. C. Goswami, and R. Sharma, "Synthesis, spectral studies and quantum-chemical investigations on S-benzyl β-N-(4-NN biscynodiethylaminophenylmethylene) dithiocarbazate," *Arab. J. Chem.*, vol. 12, no. 7, pp. 1537–1544, 2019.

[127] E. K. Kareem, S. M. Lateef, and A.-A. Drea, “Study of Preparation and Identification of some metals complexes of New Schiff Base Ligand type (NNO) Derived from Isatin,” *J. Multifunc mater. Photosci*, vol. 6, no. 1, pp. 1–10, 2015.

[128] H. T. Mohammed, A. Abbas, and A. Drea, “Prodrug Design by Computation Methods to Treat Parkinson’s Disease.”

[129] A. Mansoorinasab, A. Morsali, M. M. Heravi, and S. A. Beyramabadi, “Quantum mechanical study of carbon nanotubes functionalized with drug gentamicin,” *J. Struct. Chem.*, vol. 58, no. 3, pp. 462–470, 2017.

[130] L. H. Khdaim and A. A.-A. Draea, “Chemical Reactivity Study of Anew of Suggested Chemotherapy Agent Using DFT,” *Egypt. J. Chem.*, vol. 64, no. 10, pp. 3–4, 2021.

[131] J. Dhevaraj, M. Gopalakrishnan, and S. Pazhamalai, “Synthesis, characterization, molecular docking, ADME and biological evaluation of 3-(4-(tetrazol-1-yl) phenyl)-5-phenyl-1H-pyrazoles,” *J. Mol. Struct.*, vol. 1193, pp. 450–467, 2019.

[132] N. Süleymanoğlu, E. E. Demir, Ş. Direkel, and Y. Ünver, “Theoretical study and antimicrobial activities of New Schiff base derivatives with thiophene,” *J. Mol. Struct.*, vol. 1218, p. 128522, 2020.

[133] M. Frisch, M J ea Trucks, G W Schlegel, H B Scuseria, G E Robb, M A Cheeseman, J R Scalmani, G Barone, V Mennucci, B Petersson and G A., “gaussian 09, Revision d. 01, Gaussian,” *Inc., Wallingford CT*, vol. 201, 2009.

[134] C. Trindle and D. Shillady, *Electronic structure modeling: connections between theory and software*. CRC Press, 2008.

[135] R. M. Roat-Malone, *Bioinorganic chemistry: a short course*. John Wiley & Sons, 2007.

[136] S. C. Smith, "A Computational Study of Small Gold Clusters with H2S, Thiols, H2O, and Alcohols," 2014.

[137] M. L. Greenfield, "Molecular modelling and simulation of asphaltenes and bituminous materials," *Int. J. Pavement Eng.*, vol. 12, no. 4, pp. 325–341, 2011.

[138] HyperChem 8.0.2., "For windows molecular modeling system," *Hypercupe, Inc.*, 2011.

[139] A. Taylor, "Theoretical Investigations of Non-Covalent Interactions: From Small Water Clusters to Large DNA Quadruplexes," 2010.

[140] S. Chandra, "Electronic Structure Calculations of Some Organic Molecules Using Tools of Quantum Chemistry."

[141] B. S. Woods and P. H. Acioli, "Drag Assisted Simulated Annealing Method for Geometry Optimization of Molecules," *Procedia Comput. Sci.*, vol. 51, pp. 1878–1886, 2015.

[142] J. A. Pople, M. Head-Gordon, D. J. Fox, K. Raghavachari, and L. A. Curtiss, "Gaussian-1 theory: A general procedure for prediction of molecular energies," *J. Chem. Phys.*, vol. 90, no. 10, pp. 5622–5629, 1989.

[143] V. M. Ingman, A. J. Schaefer, L. R. Andreola, and S. E. Wheeler, "QChASM: Quantum chemistry automation and structure manipulation," *Wiley Interdiscip. Rev. Comput. Mol. Sci.*, vol. 11, no. 4, p. e1510, 2021.

[144] W. F. Polik and J. R. Schmidt, “WebMO: Web-based computational chemistry calculations in education and research,” *Wiley Interdiscip. Rev. Comput. Mol. Sci.*, p. e1554.

[145] N. Fey and J. M. Lynam, “Computational mechanistic study in organometallic catalysis: Why prediction is still a challenge,” *Wiley Interdiscip. Rev. Comput. Mol. Sci.*, p. e1590, 2021.

[146] K. B. Beć, J. Grabska, and C. W. Huck, “Biomolecular and bioanalytical applications of infrared spectroscopy–A review,” *Anal. Chim. Acta*, vol. 1133, pp. 150–177, 2020.

[147] N. Gholizadeh, Neda Pundavela, Jay Nagarajan, Rajakumar Dona, Anthony Quadrelli, Scott Biswas, Tapan Greer, Peter B Ramadan and Saadallah ., “Nuclear magnetic resonance spectroscopy of human body fluids and in vivo magnetic resonance spectroscopy: Potential role in the diagnosis and management of prostate cancer,” in *Urologic Oncology: Seminars and Original Investigations*, 2020, vol. 38, no. 4, pp. 150–173.

[148] V. Balachandran, T. Karthick, S. Perumal, and A. Nataraj, “Comparative theoretical studies on natural atomic orbitals, natural bond orbitals and simulated UV-visible spectra of N-(methyl) phthalimide and N-(2 bromoethyl) phthalimide,” 2013.

[149] J. Peter-Katalinic, “Life sciences and mass spectrometry: some personal reflections,” *Biol. Chem.*, vol. 402, no. 12, pp. 1603–1607, 2021.

[150] A. F. Jalbout, A. J. Hameed, and A. H. Essa, “Structural isomers of 2-(2, 3 and 4-substituted-phenyl)-1, 2-benzisoselenazol-3 (2H)-one: A Theoretical Study,” *J. Organomet. Chem.*, vol. 693, no. 12, pp. 2074–2078, 2008.

[151] F. Farzad, H. Farsi, and H. Raissi, “Quantum chemical studies on molecular conformations, energetic and intramolecular hydrogen bonding in ground and electronic excited state of (thioxosilyl) ethyleneselenol,” *J. Sulfur Chem.*, vol. 35, no. 2, pp. 152–163, 2014.

[152] S. Gunasekaran, R. A. Balaji, S. Kumeresan, G. Anand, and S. Srinivasan, “Experimental and theoretical investigations of spectroscopic properties of N-acetyl-5-methoxytryptamine,” *Can. J. Anal. Sci. Spectrosc*, vol. 53, no. 4, pp. 149–162, 2008.

[153] A. Abbas, A. Drea, and A. Salah, “Naman and Bhajat R-Jaffer," Theoretical Degradation Study of Methomyl,” *J. Appl. Chem.*, vol. 1, no. 1, pp. 125–136, 2012.

[154] M. Rahal, I. Bouimadaghene, R. D. El Bouzaidi, I. Bouabdallah, F. Malek, and A. El Hajbi, “Accessible approaches for vibrational zero point energy calculation of organoboron compounds,” *Vib. Spectrosc.*, vol. 110, p. 103131, 2020.

[155] L. F. Østergaard and S. Hammerum, “Secondary kinetic deuterium isotope effects on unimolecular cleavage reactions: Zero-point vibrational energy and qualitative RRKM theory,” *Mass Spectrom. Rev.*, 2021.

[156] F. Neese, “Orca 4.2. 1,” *Wiley Interdiscip. Rev. Comput. Mol. Sci.*, vol. 2, p. 73, 2012.

[157] S. Dheivamalar, L. Sugi, and K. Ambigai, “Density functional theory study of exohedral carbon atoms effect on electrophilicity of nicotine: comparative analysis,” *Comput. Chem.*, vol. 4, no. 1, pp. 17–31, 2016.

[158] B. Miehlich, “savin A, Stoll H, Preuss H,” *Chem. Phys. Lett*, vol. 157, pp. 200–206, 1989.

[159] H. P. Varbanov, M. A. Jakupec, A. Roller, F. Jensen, M. Galanski, and B. K. Keppler, “Theoretical investigations and density functional theory based quantitative structure–activity relationships model for novel cytotoxic platinum (IV) complexes,” *J. Med. Chem.*, vol. 56, no. 1, pp. 330–344, 2013.

[160] A. A. Balakit, Y. Sert, Ç. Çırak, K. Smith, B. M. Kariuki, and G. A. El-Hiti, “Synthesis, Vibrational Spectra, and DFT Simulations of 3-bromo-2-methyl-5-(4-nitrophenyl) thiophene,” *J. Appl. Spectrosc.*, vol. 84, no. 5, pp. 888–899, 2017.

[161] S. Riahi, S. Eynollahi, S. Soleimani, M. R. Ganjali, P. Norouzi, and H. M. Shiri, “Application of DFT method for determination of IR frequencies and electrochemical properties of 1, 4-dihydroxy-9, 10-anthraquinone-2-sulphonate,” *Int. J. Electrochem. Sci*, vol. 4, pp. 1407–1418, 2009.

[162] L. Sinha, O. Prasad, V. Narayan, and R. K. Srivastava, “Electronic structure, non-linear properties and vibrational analysis of Acenaphthene and its carbonyl derivative Acenaphthenequinone by density functional theory,” *J. Mol. Struct. THEOCHEM*, vol. 958, no. 1–3, pp. 33–40, 2010.

[163] F. H. Hannon, “Geometrical Optimization and Electronic Properties of Li on Xn Nanoclusters,” *Int. J. New Technol. Res.*, vol. 3, no. 2, 2017.

[164] A. Abbas, A. Drea, “Mechanism and Kinetic of Free Radical Reactions for Propane Using theoretical Calculations,” 2017.

[165] A. M. ELHORRI and M. Z. RABAH, “Dissociation of Basic Dyes by Advanced Oxidation: Theoretical Study by DFT Calculations,” *Chem. Sci.*, vol. 8, no. 3, pp. 388–404, 2019.

[166] P. S. Kalsi, *Spectroscopy of organic compounds*. New age international, 2007.

[167] A. Abbas, A. Drea, “INVESTIGATION STUDY OF TRANSITION STATE FOR SYNTHESIS NEW SCHIFF BASE LIGANDS OF ISATIN DERIVATIVES,” 2016.

[168] C. G. Tetsassi Feugmo, V. Liégeois, and B. Champagne, “Theoretical Investigation of Vibrational Sum-Frequency Generation Signatures of Functionalized H Si (111),” *J. Phys. Chem. C*, vol. 119, no. 6, pp. 3180–3191, 2015.

[169] Z. Liu, X. Zhang, Y. Zhang, and J. Jiang, “Theoretical investigation of the molecular, electronic structures and vibrational spectra of a series of first transition metal phthalocyanines,” *Spectrochim. Acta Part A Mol. Biomol. Spectrosc.*, vol. 67, no. 5, pp. 1232–1246, 2007.

[170] G. Shakila, H. Saleem, and N. Sundaraganesan, “FT-IR, FT-Raman, NMR and UV Spectral investigation: Computation of vibrational frequency, chemical shifts and electronic structure calculations of 1-bromo-4-nitrobenzene,” *World Sci. News*, vol. 61, no. 2, pp. 150–185, 2017.

[171] A. Akbari and Z. Alinia, “Comparative analysis of the Ni (II) complex of the N, N’-Bis-(4-hydroxysalicylidene)-1, 2-diaminoethane: combined experimental and theoretical study (DFT/PW91),” *Comput. Res*, vol. 1, pp. 19–26, 2013.

[172] L. Larabi, Y. Harek, A. Reguig, and M. M. Mostafa, “Synthesis, structural study and electrochemical properties of copper (II) complexes derived from benzene-and p-toluenesulphonylhydrazone,” *J. Serbian Chem. Soc.*, vol. 68, no. 2, pp. 85–96, 2003.

[173] M. Iovu and T. O. Nicolescu, *Chimie organică: metode experimentale*. Editura Universitară" Carol Davila, 2009.

[174] D. Muayad, S. A. Aowda and A. Abbas A. Drea, “Simulation Study of Oxidation for Oleic acid by KMnO4 Using Theoretical Calculations,” *J. Appl. Chem.*, vol. 2, no. 1, pp. 42–49, 2013.

[175] G. V Sukhodolskaya, V. M. Nikolayeva, S. M. Khomutov, and M. V Donova, “Steroid-1-dehydrogenase of Mycobacterium sp. VKM Ac-1817D strain producing 9α-hydroxy-androst-4-ene-3, 17-dione from sitosterol,” *Appl. Microbiol. Biotechnol.*, vol. 74, no. 4, pp. 867–873, 2007.

[176] X. Fu, C.-H. Tann, and T. K. Thiruvengadam, “Process improvements in the synthesis of corticosteroid 9, 11β-epoxides,” *Org. Process Res. Dev.*, vol. 5, no. 4, pp. 376–382, 2001.

[177] A. A. Drea, “Theoretical Study to Synthesis 1, 3, 5, Tri Glycerol Benzene Using Semi-Empirical and Ab-Intio Calculation Method,” *J. Nation. Chem*, vol. 37, no. 4, pp. 86–100, 2010.

[178] A. Mirza, R. Desai, and J. Reynisson, “Known drug space as a metric in exploring the boundaries of drug-like chemical space,” *Eur. J. Med. Chem.*, vol. 44, no. 12, pp. 5006–5011, 2009.

[179] J. Chen, M. A. Reed, A. M. Rawlett, and J. M. Tour, “Large on-off ratios and negative differential resistance in a molecular electronic device,” *Science (80-.).*, vol. 286, no. 5444, pp. 1550–1552, 1999.

[180] C. Majumder, H. Mizuseki, and Y. Kawazoe, “Effect of substituent groups on the electronic properties of a molecular device: an ab initio theoretical study,” *J. Mol. Struct. THEOCHEM*, vol. 681, no. 1–3, pp. 65–69, 2004.

[181] J.-S. Yang, K.-L. Liau, C.-M. Wang, and C.-Y. Hwang, “Substituent-dependent photoinduced intramolecular charge transfer in N-aryl-substituted trans-4-aminostilbenes,” *J. Am. Chem. Soc.*, vol. 126, no. 39, pp. 12325–12335, 2004.

[182] T. W. Schneider and A. M. Angeles-Boza, “Competitive 13C and 18O kinetic isotope effects on CO2 reduction catalyzed by Re (bpy)(CO) 3Cl,” *Dalt. Trans.*, vol. 44, no. 19, pp. 8784–8787, 2015.

[183] W. M. Campbell, Wayne M Jolley, Kenneth W Wagner, PawelWagner, Klaudi Walsh, Penny JGordon, Keith C Schmidt-Mende, Lukas Nazeeruddin, Mohammad K Wang, Qing Grätzel, Michael ., “Highly efficient porphyrin sensitizers for dye-sensitized solar cells,” *J. Phys. Chem. C*, vol. 111, no. 32, pp. 11760–11762, 2007.

[184] P. Politzer, J. S. Murray, W. M. Koppes, M. C. Concha, and P. Lane, “Computational Investigation of Amine Complexes of 2, 4, 6-Trinitrotoluene,” *Cent. Eur. J. Energ. Mater.*, vol. 6, no. 2, pp. 167–182, 2009.

[185] K. Eller, E. Henkes, R. Rossbacher, and H. Höke, “Amines,” *Aliphatic, Ullmann’s Encycl. Ind. Chem. Berlin, Ger.*, 2000.

[186] A. K. Ghose, V. N. Viswanadhan, and J. J. Wendoloski, “A knowledge-based approach in designing combinatorial or medicinal chemistry libraries for drug discovery. 1. A qualitative and quantitative characterization of known drug databases,” *J. Comb. Chem.*, vol. 1, no. 1, pp. 55–68, 1999.

[187] A. KERASSA, “Etude par la modélisation moléculaire des relations structures-propriétés de quelques séries hétérocycliques bioactives.” Université Mohamed Khider-Biskra, 2015.

[188] A. Kerassa, S. Belaidi, D. Harkati, T. Lanez, O. Prasad, and L. Sinha, “Investigations on Molecular Structure, Electronic Properties, NLO Properties and Comparison of Drug-Likeness of Triazolothiadiazole Derivatives by Quantum Methods and QSAR Analysis,” *Rev. Theor. Sci.*, vol. 4, no. 1, pp. 85–96, 2016.

[189] M. H. Obies, A. A. A. Drea, and F. H. Hussein, “Simulation Study of Photocatalytic Decolorization of Bismarck Brown-R Using Different Quantum Calculation Methods,” *Int. J. Chem. Sci.*, vol. 10, no. 1, pp. 63–79, 2012.

[190] E. G. Lewars, “Molecular mechanics,” in *Computational Chemistry*, Springer, 2016, pp. 51–99.

[191] S. N. Naman, B. R. J. Muhyedeen, and A. A. Drea, “Theoretical study for degradation of Captan in gas phase Using DFT,” *Iraqi Natl. J. Chem.*, vol. 44, p. 560, 2011.

[192] R. G. Parr, R. A. Donnelly, M. Levy, and W. E. Palke, “Electronegativity: the density functional viewpoint,” *J. Chem. Phys.*, vol. 68, no. 8, pp. 3801–3807, 1978.

[193] P. Udhayakala, “Density functional theory calculations on corrosion inhibitory action of five azlactones on mild steel,” *J Chem Pharm Res*, vol. 6, no. 7, pp. 117–127, 2014.

[194] J. V Burda, J. Šponer, and J. Leszczynski, “The interactions of square platinum (II) complexes with guanine and adenine: a quantum-chemical ab initio study of metalated tautomeric forms,” *JBIC J. Biol. Inorg. Chem.*, vol. 5, no. 2, pp. 178–188, 2000.

[195] Mohammad, M.A., “theoretical study of structural Properties of derivatives substituted thiophene using semiempercal calculation,” *Univ. of karbala*, 2013.

[196] D. C. Ghosh and J. Jana, “A study of correlation of the order of chemical reactivity of a sequence of binary compounds of nitrogen and oxygen in terms of frontier orbital theory,” *Curr. Sci.*, pp. 570–573, 1999.

[197] L. H. Mendoza-Huizar, “A theoretical study of chemical reactivity of tartrazine through DFT reactivity descriptors,” *J. Mex. Chem. Soc.*, vol. 58, no. 4, pp. 416–423, 2014.

Publication

Design Engineering

ISSN: 0011-9342 | Year 2021
Issue: 9 | Pages: 3358 - 3373

Structural Study of Betamethasone Drug by Using Theoretical Methods

Abbas Abdali Drea*, Frdous Samie Abdulameer**

University of Babylon, College of Science, Department of chemistry
Corresponding Author * abbasdrea@gmail.com
**samiferdoss21@gmail.com

Abstract

Structural and energetic properties of the Betamethasone drug has been studied using different calculation methods such as PM_3.semiempirical method and Density function theory(B_3LYP)at basis set(3-21G** and 6-31G**) that's implemented into Gaussian 09 program. Total energy, bandgap energy, bond lengths and bond angles are investigated through vacuumed optimization configuration of Betamethasone. Estimation of vibrational analysis spectra has been done and compared with practical spectra of Betamethasone drug. We found the geometry optimization structure of Betamethasone has -1331.652 a. u. units as total energy come out from the relaxation process with bandgap energy equal to 0.07945 e.v. units. The bond of C16-C17 with a length equal to 2.7693A^0 is more reactive bound due to their length than other chemical bonds to share in the important reaction. This bond is broken down at 0.77kCal/mol. The bond angle of C12-C17-C19 is equal to 133.5942 degree shows the lowest stability than others, which explain the effectiveness of Betamethasone at these bond to share in the various reaction. Theoretical vibration transitions are identical with experimental FT-IR spectrum for main bonds of Betamethasone as evidence about the reality of the theoretical calculation. Investigation shows the ability to drive some other derivative from this drag to maximize their activity toward inflammatory diseases.

Keywords: Betamethasone drug, Density functional theory, Molecular modelling methods, Gaussian 09 program, and Optimized structure.

Introduction

Betamethasone is one of the most used public drugs around the world due to its ability to treatment into many different diseases. It is used as an example, for skin diseases, allergic reactions, rheumatic disorders, Crohn's disease, and also for leukaemia[1]. In some drugs manufacturers, Betamethasone can be used to generate another drug, such as Clobetasol[2]. In general, Betamethasone has been listed according to the World Health Organization(WHO) model as an essential medicine for an anti-inflammatory and anti-pruritic drug[3].

In some countries, Betamethasone has different knowing names like Diprolene, Diprosone, Celestamine, Proctor (in Pakistan) and Betamethasone sodium phosphate is known as Bentelan

Appendix

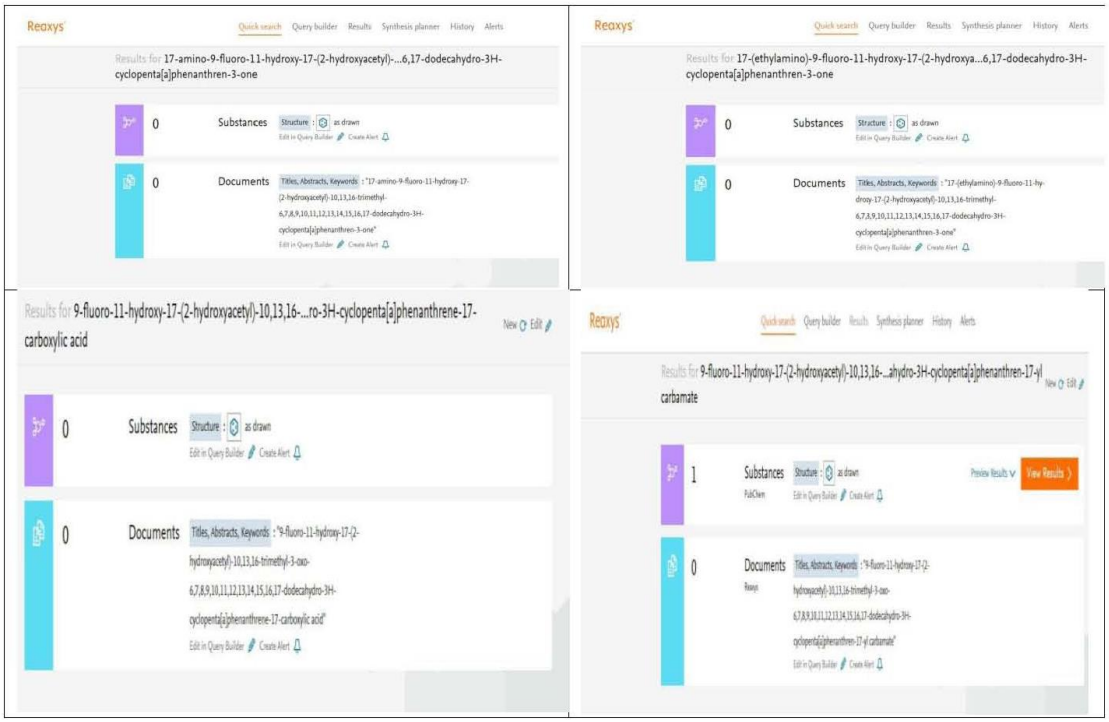
Reaxys
Quick search Query builder Results Synthesis planner History Alerts
Results for 17-amino-9-fluoro-11-hydroxy-17-(2-hydroxyacetyl)-...6,17-dodecahydro-3H-cyclopenta[a]phenanthren-3-one
0 Substances Structure : as drawn
0 Documents Titles, Abstracts, Keywords : "17-amino-9-fluoro-11-hydroxy-17-(2-hydroxyacetyl)-10,13,16-trimethyl-6,7,8,9,10,11,12,13,14,15,16,17-dodecahydro-3H-cyclopenta[a]phenanthren-3-one"
Reaxys
Quick search Query builder Results Synthesis planner History Alerts
Results for 17-(ethylamino)-9-fluoro-11-hydroxy-17-(2-hydroxya...6,17-dodecahydro-3H-cyclopenta[a]phenanthren-3-one
0 Substances Structure : as drawn
0 Documents Titles, Abstracts, Keywords : "17-(ethylamino)-9-fluoro-11-hydroxy-17-(2-hydroxyacetyl)-10,13,16-trimethyl-6,7,8,9,10,11,12,13,14,15,16,17-dodecahydro-3H-cyclopenta[a]phenanthren-3-one"
Results for 9-fluoro-11-hydroxy-17-(2-hydroxyacetyl)-10,13,16-...ro-3H-cyclopenta[a]phenanthrene-17-carboxylic acid
New Edit
0 Substances Structure : as drawn
Edit in Query Builder Create Alert
0 Documents Titles, Abstracts, Keywords : "9-fluoro-11-hydroxy-17-(2-hydroxyacetyl)-10,13,16-trimethyl-3-oxo-6,7,8,9,10,11,12,13,14,15,16,17-dodecahydro-3H-cyclopenta[a]phenanthrene-17-carboxylic acid"
Edit in Query Builder Create Alert
Reaxys
Quick search Query builder Results Synthesis planner History Alerts
Results for 9-fluoro-11-hydroxy-17-(2-hydroxyacetyl)-10,13,16-...ahydro-3H-cyclopenta[a]phenanthren-17-yl carbamate
New Edit
1 Substances Structure : as drawn
PubChem
Edit in Query Builder Create Alert
Preview Results View Results
0 Documents Titles, Abstracts, Keywords : "9-fluoro-11-hydroxy-17-(2-hydroxyacetyl)-10,13,16-trimethyl-3-oxo-6,7,8,9,10,11,12,13,14,15,16,17-dodecahydro-3H-cyclopenta[a]phenanthren-17-yl carbamate"
Reaxys
Edit in Query Builder Create Alert

Certificate of Participation

This is to certify that

FRDOES SAMEI

has participated with a paper entitled

Characterization and Identification of Betamethasone Drug Using Simulation Methods

at the 2'nd Postgraduate Students Annual Conference 2021(PSAC2021), which organized by unversity of Kufa, faculty of education for girls, department of chemistry, via the free conference call paltform on 18 April 2021

Ass.prof Alaa Naji Almawla
Dean of the faculty of education for girls

PSAC2

Ass.prof Safa Majeed Hameed
Head of department of chemistry

جامعة بابل - كلية العلوم - قسم الكيمياء

شهادة مشاركة

نؤيد مشاركة السيد\ة **فردوس سامي عبد الامير عمران**

في الندوة العلمية السابعة عشرة للدراسات العليا الافتراضية وتحت شعار

{الدراسات العليا سبيل النهوض بالبحث العلمي والمجتمع}

التي أقامها قسم الكيمياء – كلية العلوم – جامعة بابل يوم الأربعاء المصادف

2021\4\28

رئيس اللجنة التحضيرية	رئيس القسم	العميدة
أ.د. عباس نور الشريفي	أ.د. سعدون عبد الله عودة	أ.د. ايناس محمد الربيعي

5/16/2021

الخلاصة :-

إجريت دراسة المحاكاة لعقار البيتاميثازون بوساطة طرق حسابية مختلفة، مثل الطريقة شبه التجريبية (PM3) ونظرية دالة الكثافة (B_3LYP) عند مجموعة الأساس (3-21G و6-31G). استخدمت في هذه الدراسة برامج ميكانيك الكم النظرية مثل برنامج كاوسيين09 و هايبركم 8.02 لأجراء الحسابات النظرية اللازمة.

اجري التوصيف لدراسة المحاكاة النظرية بالاعتماد على التركيب الهندسي الامثل لجميع الأصناف الكيميائية في الحالة المستقرة، إضافة الى تقدير الخصائص الاخرى مثل الترتيب الفراغي للذرات في الجزيئة، معاملات الاواصر (اطول الاواصر وزوايا الاواصر) و الفعالية الكيميائية و طاقة جهد السطح و الاوربيتالات الجزيئية HOMO و LUMO و الجهد الكهروستاتيكي وطاقة نقطة الصفر التي تم تقديرها للحصول على رؤية واضحة حول النمذجة الكيميائية.

أجريت المحاكاة النظرية للطيف الجزيئي نسبة للانتقالات الإلكترونية والترددات الاهتزازية لعقار البيتاميثازون ومقارنتها مع الاطياف التجريبية العملية. تم تقدير الطيف الكتلي تجريبا لعقار البيتاميثازون للحصول على التركيب الكيميائي الفعلي لجزي العقار.

تم اختبار الحالات الانتقالية المقترحة للخطوة الضابطة لسرعة (الخطوة البطيئة) التفاعلات الكيميائية من خلال حساب التردد الخيالي السالب الاول وطاقة نقطة الصفر لاكتشاف الحالة الانتقالية التي تعطي خطوة المسار الفعلي للتفاعلات الكيميائية. تم حساب القيم الطاقية الدينيمية الحرارية وقيمة حاجز الطاقة لكل خطوة من التفاعل لتطبيق قانون هيس للكيمياء الحرارية لجميع التفاعلات الكيميائية.

تم اقتراح اربعة مشتقات جديدة للبيتاميثازون بوساطة تعويض مجاميع وظيفية في الموقع الفعال لجزي العقار وهي مجموعة الأمين ومجموعة الاثيل امين ومجموعة الكاربوكسيل ومجموعة الامايد. تم اجراء مقارنة ما بين الخصائص الطاقية لجزي العقار الاصلي والمشتقات الجديدة المقترحة والتي تعتمد على تكون الحالة الانتقالية للخطوة الضابطة لسرعة التفاعل ومحصلة خطوات تفاعل التكون الكيميائي للعقار و الفعالية الكيميائية ومؤشرات الفاعلية الكيميائية.

وجد ان

ان عقار البيتاميثازون يتمتع بطاقة كلية وطاقة فجوة مساوية الى 1331.653- كيلو سعرة للمول الواحد و 0.079 اليكترون فولت على التوالي. ابرز المواقع الفعالة في العقار يتمثل بالاصرة O5-H30 ذات الفاعلية الاعلى من بقية الاواصر الكيميائية والتي تكون قيمة طاقة تفكك مساوية الى 33.35كيلو سعرة للمول الواحد. ان التغير الكلي لانثالبي التفاعل المتسلسل لتكوين البيتاميثازون يساوي 452.406- كيلو سعرة للمول الواحد. المحاكاة النظرية اعطت اقتراح اربعة مشتقات جديدة للبيتاميثازون وهي AFHTDPO (Betamethasone.NH_2) ، EFHTDPO(Betamethasone.$NHCH_2CH_3$)، FHCPCC(Betamethasone. COOH) و FHACPC(Betamethasone.$CONH_2$). وجد ان

اثنان من المشتقات الجديدة المقترحة وهي AFHTDPO (Betamethasone.NH_2)، EFHTDPO(Betamethasone.$NHCH_2CH_3$) أكثر فعالية من الناحية الكيميائية من جزيئة البيتاميثازون الاصلية وفقا للحسابات النظرية بينما FHCPCC(Betamethasone. COOH) و

AFHTDPO المشتقان . كانت اقل فعالية كيميائية FHACPC(Betamethasone.$CONH_2$)
يمكن استخدام EFHTDPO(Betamethasone.$NHCH_2CH_3$)، (Betamethasone.NH_2)
كلاهما كمضاد للأدوية تجاه فيروس كورونا أو أي فيروسات أخرى بعد تحضيرها واجراء كافة الاختبارات أخرى للتطبيق.

وزارة التعليم العالي والبحث العلمي

جامعة بابل/ كلية العلوم

قسم الكيمياء

دراسة نظرية لمشتقات الكورتيكوستيرويدات الجديدة المعتمدة على دواء البيتاميثازون

تقدمت بها الطالبة

فردوس سامي عبد الامير عمران

الى مجلس كلية /جامعة بابل

وهي جزء من متطلبات نيل درجة الماجستير في العلوم

بكالوريوس علوم كيمياء 1997

بأشراف

ا.د. عباس عبد علي دريع الصالحي

1443هـ

2022 م

CHAPTER ONE

GENERAL INTRODUCTION

CHAPTER TWO

METHODOLOGY OF CALCULATION

CHAPTER THREE
RESULTS AND DISCUSSION

References